

**SKB P-25-08**

ISSN 1651-4416

ID 2078385

September 2025

# Shear properties of bentonite from the Prototype Repository field experiment

Robert J Cuss, Elliot J M Bird  
British Geological Survey

*Keywords:* Bentonite, MX-80, Direct shear, Äspö Hard Rock Laboratory, Prototype repository experiment

This report concerns a study which was conducted for Svensk Kärnbränslehantering AB (SKB). The conclusions and viewpoints presented in the report are those of the authors. SKB may draw modified conclusions, based on additional literature sources and/or expert opinions.

Data in SKB's database can be changed for different reasons. Minor changes in SKB's database will not necessarily result in a revised report. Data revisions may also be presented as supplements, available at [www.skb.se](http://www.skb.se).

This report is published on [www.skb.se](http://www.skb.se)

© 2025 Svensk Kärnbränslehantering AB

## Foreword

This report is the published product of a study by the British Geological Survey (BGS) conducted for Svensk Kärnbränslehantering AB of Sweden on the shear properties of cores from the Prototype Repository experiment conducted at the Äspö Hard Rock Laboratory in Sweden. The work was conducted within the Fracture Physics Laboratory as part of the Fluid Processes Laboratory facility.

## Acknowledgements

This study was undertaken by staff from the British Geological Survey (Radioactive Waste Team). Funding for the study was provided by SKB (Stockholm).

The authors would like to acknowledge the contribution of the staff of the National Geological Repository core preparation team, most notably Rob Bailey. Furthermore, the authors would like to acknowledge the expertise of the British Geological Survey's engineering workshops for the modifications made to the existing apparatus to facilitate the use of 47 mm diameter samples, most notably Humphrey Wallis and Wayne Leman.

We wish to thank the staff of the Äspö Hard Rock Laboratory for supplying the bentonite cores used in this study and Terese Bladström for clarifying aspects of the data supplied with the core.

## Summary

This report describes a study to determine the shear properties of pre-compacted MX-80 cores from the Prototype Repository (PRP) experiment under direct shear. A bespoke shear apparatus was used to conduct constant shear rate experiments that lasted approximately 2 hours each. A total of 23 experiments were conducted, including a repeatability test and a test conducted at half normal load to investigate the normal load dependence of MX-80 from the PRP test.



# Contents

<b>1</b>	<b>Introduction .....</b>	<b>5</b>
<b>2</b>	<b>Apparatus and sample preparation .....</b>	<b>6</b>
2.1	The Direct Shear Rig (DSR).....	6
2.2	Sample preparation .....	9
2.3	Calculation of geotechnical properties.....	12
2.4	Test procedure .....	17
2.5	Fracture surface analysis.....	18
<b>3</b>	<b>Test results.....</b>	<b>20</b>
3.1	Example Test FPR-24-274.....	20
3.2	Additional tests .....	24
3.3	Results for all tests .....	26
<b>4</b>	<b>Conclusions.....</b>	<b>35</b>
	<b>References.....</b>	<b>36</b>
	<b>Appendix – results for each shear test conducted .....</b>	<b>37</b>

# **1 Introduction**

BGS were commissioned by SKB to undertake direct shear tests of cored samples taken during decommissioning of the Prototype Repository (PRP) experiment, which was conducted at the Äspö Hard Rock Laboratory in Sweden. Cores were received at BGS Keyworth from the Äspö HRL and were tested between the 16<sup>th</sup> October and 1<sup>st</sup> November 2024. This report outlines the methodology used and the results gained from the study.

## 2 Apparatus and sample preparation

### 2.1 The Direct Shear Rig (DSR)

The experiments were performed using the bespoke Direct Shear Rig (DSR), a schematic is shown in Figure 2-1. This apparatus was designed to fracture intact, cylindrical cores with the added capability of being able to directly inject water or gas onto the fracture surface to observe the fracture transmissivity over time. The apparatus and experimental approach have been proven in several fracturing studies which have been applied to both radioactive waste disposal research and the field of carbon capture and storage (e.g. Cuss and Harrington, 2016; Cuss et al., 2024; 2022; 2019; 2018a,b; 2017; 2015; 2011; Harrington et al., 2017; Wiseall et al., 2018).

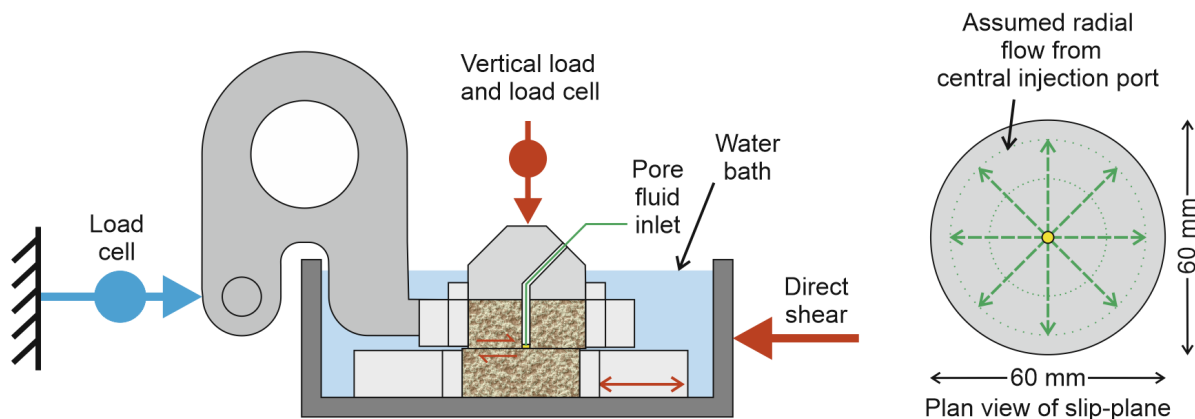


**Figure 2-1.** Schematic of the Direct Shear Rig (DSR). Note: Fluid injection was not used in the current study.

The custom-made Direct Shear Rig (Figure 2-1, Figure 2-2) comprises six main components:

Rigid steel frame that had been designed with a bulk modulus of compressibility and shear modulus approximately 2 orders of magnitude greater than the rock tested, resulting in minimal deformation of the apparatus compared to the test sample.

Vertical load system comprising an Enerpac hydraulic ram controlled by a Teledyne/ISCO 260D syringe pump, a rigid loading frame and an upper thrust block (up to 72 kN force). Vertical travel of the thrust block was measured by a high precision non-contact capacitance displacement transducer, which had a full range of  $\pm 0.5$  mm and an accuracy of  $0.06 \mu\text{m}$ .

Shear force actuator comprised of a modified and horizontally mounted Teledyne/ISCO 500D syringe pump designed to drive shear as slow as  $14 \mu\text{m}$  a day at a constant rate (equivalent to 1 mm in 69 days) or as fast as 0.5 mm per second along a low friction bearing. The movement of the bottom-block was measured using a linear variable differential transformer (LVDT), which had a full range of  $\pm 25$  mm and an accuracy of  $0.5 \mu\text{m}$ .

Pore pressure system comprising a Teledyne/ISCO 500D syringe pump that could deliver water or gas to a pressure of up to 25.8 MPa; note, not used in the current study.

A custom designed data acquisition system using National Instruments LabVIEW™ software facilitating the remote monitoring and control of all experimental parameters.

A sample assembly comprising two sample holders, where the bottom block was actively sheared, and the top block was connected through a linkage system to a force gauge measuring the shear stress along the slip plane. Vertical load was applied to the rock samples by means of a steel thrust block.

The apparatus was designed to take cylindrical samples of  $60 \pm 0.01$  mm diameter and  $53 \pm 1$  mm height (Figure 2-4). For the current study, the apparatus was modified (Figure 2-3) to accommodate 47 mm samples, as supplied by SKB. Inner rings were manufactured to allow the use of smaller samples. Samples were rigidly housed within two steel collars, with new inserts. The sample was loaded vertically by means of a hydraulic ram, which was actuated using an ISCO/Teledyne 260D syringe pump. The capacity of the pump and ram meant a maximum of 56.6 MPa could be achieved, although

in practice vertical stress was much lower. Load was measured by two Applied Measurements Limited load cells (DBBW-5T) with an accuracy of  $\pm 0.01$  MPa and vertical displacement by a MicroSense 4810/2810 induction sensor with a full range of  $\pm 0.5$  mm and an accuracy of  $\pm 0.06$   $\mu\text{m}$ . Horizontal stress was created by the Poisson's effect in response to vertical loading in a  $K_0$  geometry. The sample was sheared by means of a second (500D) syringe pump, which had been modified to directly shear the sample along a low-friction track. Shear stress transmitted through the sample/fracture was measured by a 50 kN rated load cell (28.7 MPa) with an accuracy of 0.01 MPa. Horizontal movement of the shear water bath was measured by a linear variable differential transformer (LVDT), which had a full range of  $\pm 25$  mm and an accuracy of 0.5  $\mu\text{m}$ . All three syringe pumps recorded pressure ( $\pm 0.003$  MPa), flow rate ( $\pm 0.25$   $\mu\text{l/h}$ ), and volume ( $\pm 1$   $\mu\text{l}$ ).



**Figure 2-2.** Components of the Direct Shear Rig. a) Photo of the complete apparatus; b) Loading frame with normal load cells at the bottom; c) normal load ram (yellow); d) sample assembly, shear load cell and Mitutoyo Digimatic Indicator (note the Mitutoyo device was replaced with a LVDT for this study).

The original DSR, as used during a previous study for SKB (Cuss et al., 2022) used square samples, meaning that as a sample sheared, the contact area between the top and bottom sample changed, and as a result normal stress increased if normal load was maintained constant. The use of a cubic arrangement meant that the change in contact area was simple, and experience showed that it was not necessary to correct if strain was limited to a maximum of 0.1 (10 %). Subsequent studies required the apparatus to be modified to accommodate cylindrical samples (Figure 2-4a). Holders were designed with two semi-circular collars that were bolted together to create a complete circular sample holder (Figure 2-4b). These were held in blocks that had been machined to hold the circular holders (Figure 2-4d). These were manufactured to give a close fit, with a grub screw securing the holders. This arrangement meant that samples could be stored between experimental stages and that batch testing could occur as multiple sets of collars were available.

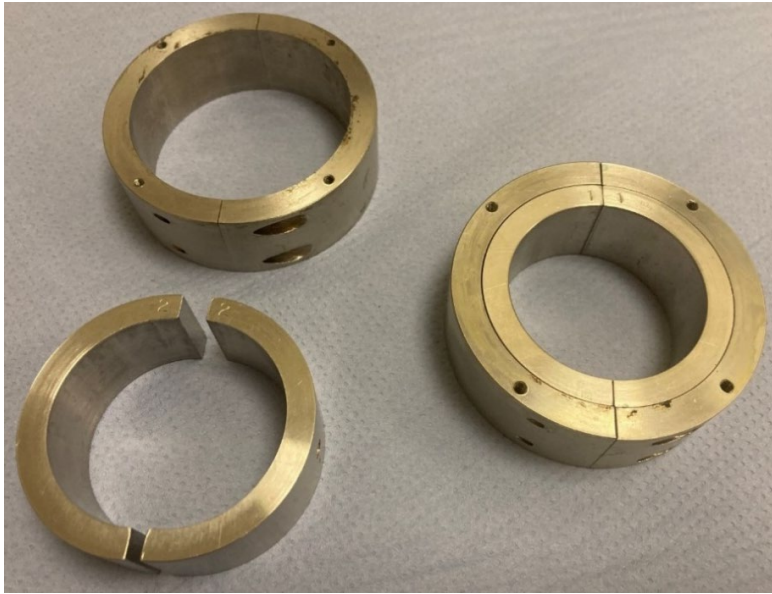


**Figure 2-3.** Modifications made to the sample rings so that 47mm diameter samples could be tested using the Direct Shear Rig. Inner rings were manufactured that held the samples well.

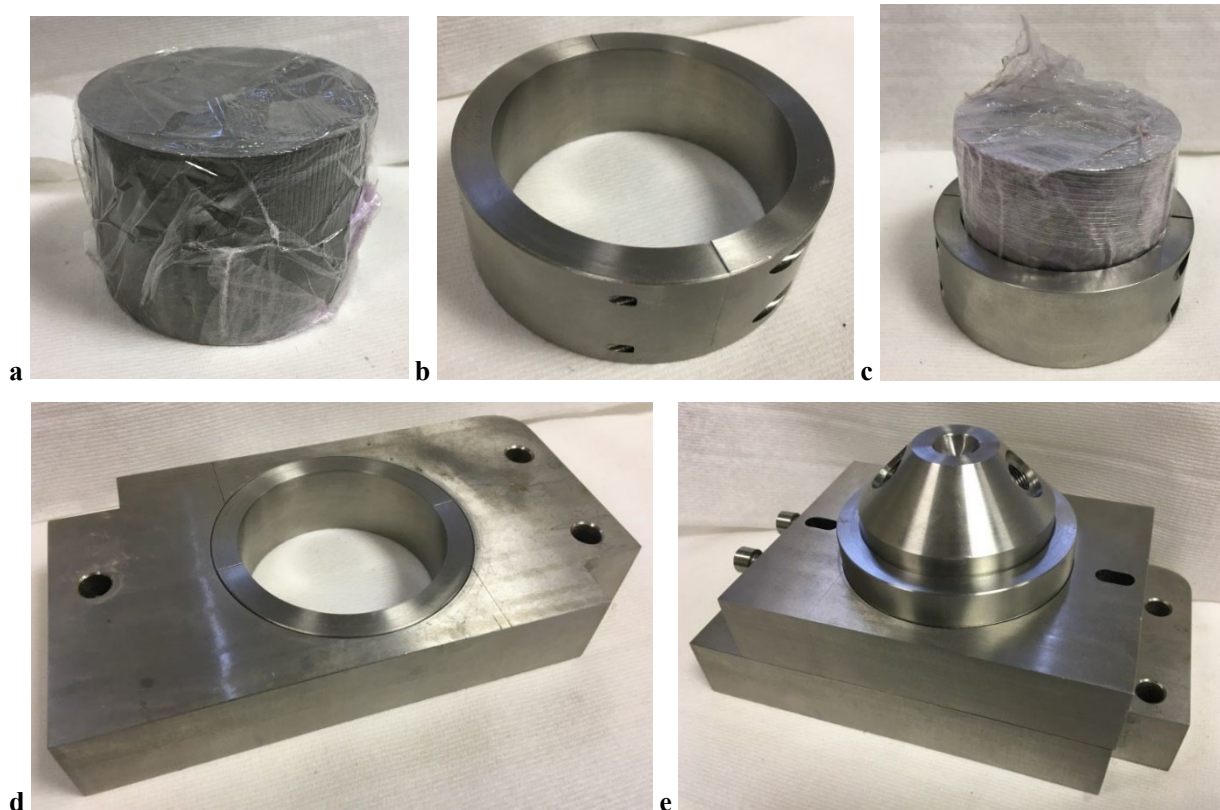


**Figure 2-4.** Sample holder arrangement. a) cylindrical sample; b) sample holder; c) sample holder and sample; d) sample holder and lower block arrangement; e) complete sample holder arrangement.



## 2.2 Sample preparation

Samples were received from SKB with the information listed in Table 2-1. The sample cores had originally been used by SKB to take samples for water content and dry density measurements and the shear properties were an added analysis to these samples. The samples were examined in their protective plastic bags and it was apparent that three were broken, as shown in Figure 2-5. Samples DH3:R9:200:825-BGS (Figure 2-5a) and DH4:R6:290:825-BGS (Figure 2-5c) had lengthwise splits that meant that samples could not be made. This type of lengthwise split can occur in samples taken at the interface between blocks and pellets, and they must have separated as the samples had dried somewhat. Sample DH4:R2:290:725-BGS (Figure 2-5b) had broken perpendicular to the long axis of the core. A single sample was still able to be made from this core.

Each core was cut using a dry diamond tipped saw to create two samples of approximately 70 mm height. Each sample was then lathed to a nominal height of 52 mm with parallel faces. Immediately after sample manufacturing, the samples were vacuum packed in foil bags to minimise moisture loss.

Figure 2-6 shows the different stages of sample manufacture. From each core supplied, four sub-samples were created; 2 test samples, a small offcut for geotechnics, and the remaining core material. Each of these were assigned a BGS identified in the FPR-24-xxx series, as summarised in Table 2-2. As multiple samples were made from each SKB core, results are reported giving the BGS identifier. The diameter, height, and colour of the samples were measured twelve and six times respectively, and one weight measurement taken.

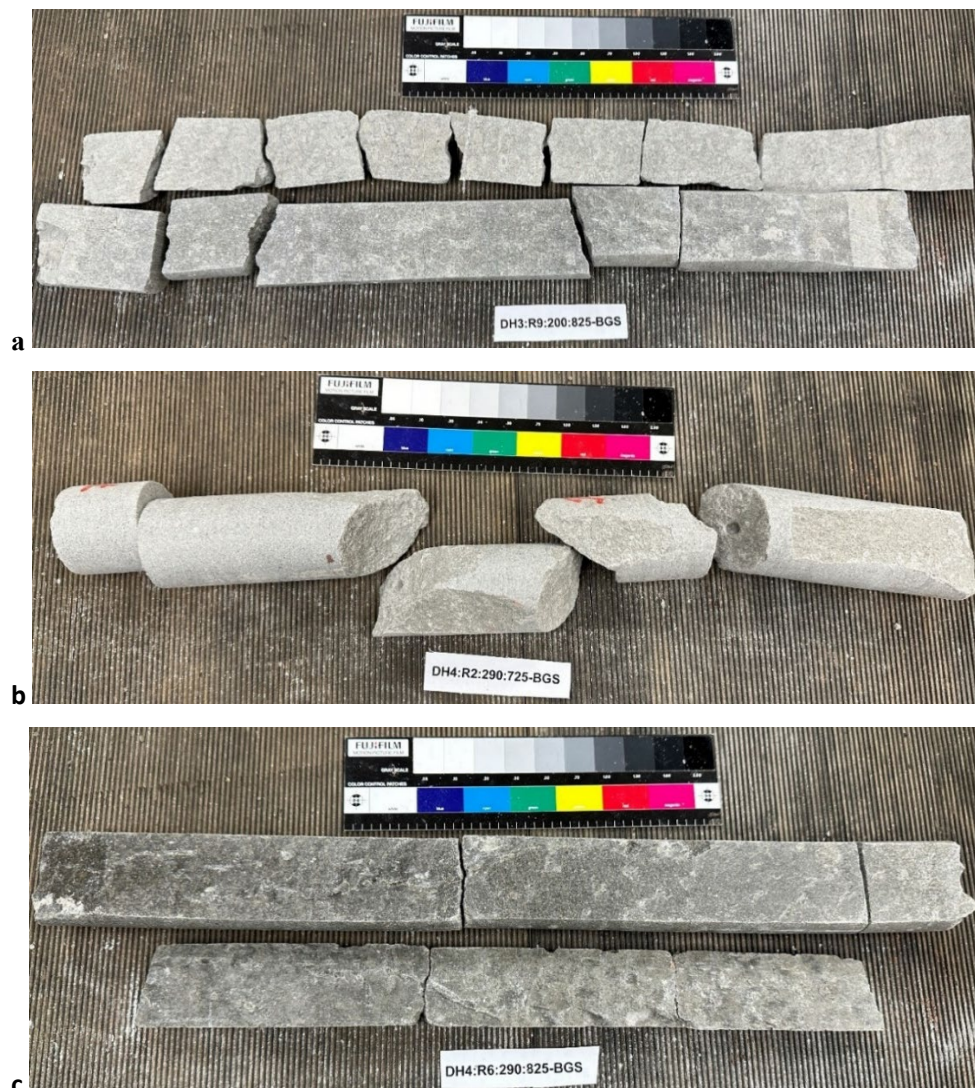


**Figure 2-5.** Problematic cores. a) DH3:R9:200:825; b) DH4:R2:290:725-BGS; c) DH4:R6:290:825-BGS.

**Table 2-1. Supplied information from SKB on the supplied core sample. Note samples coloured red could not be tested**

SKB Id-nr	Date sampling	Material	Sample type	Amount	Comment	BGS comment
DH3:R9:200:575-BGS	6/11/2023	MX-80	Drill core	Approx. 1.6 kg		
DH3:R9:200:625-BGS	6/11/2023	MX-80	Drill core	Approx. 1.6 kg	Not to be analysed, reserve sample	
DH3:R9:200:675-BGS	6/11/2023	MX-80	Drill core	Approx. 1.6 kg		
DH3:R9:200:725-BGS	6/11/2023	MX-80	Drill core	Approx. 1.6 kg		
DH3:R9:200:775-BGS	6/11/2023	MX-80	Drill core	Approx. 1.6 kg	Not to be analysed, reserve sample	
DH3:R9:200:825-BGS	6/11/2023	MX-80	Drill core	Approx. 1.6 kg		No sample, core split length ways. See Figure 2-5a
DH2:R9:200:575-BGS	3/4/2024	MX-80	Drill core	Approx. 1.6 kg		
DH2:R9:200:625-BGS	3/4/2024	MX-80	Drill core	Approx. 1.6 kg		
DH2:R9:200:675-BGS	3/4/2024	MX-80	Drill core	Approx. 1.6 kg		
DH2:R9:200:725-BGS	3/4/2024	MX-80	Drill core	Approx. 1.6 kg		
DH2:R9:200:775-BGS	3/4/2024	MX-80	Drill core	Approx. 1.6 kg	Not to be analysed, reserve sample	
DH2:R9:200:825-BGS	3/4/2024	MX-80	Drill core	Approx. 1.6 kg		
DH4:R2:290:575-BGS	9/8/2023	MX-80	Drill core	Approx. 1.6 kg		
DH4:R2:290:625-BGS	9/8/2023	MX-80	Drill core	Approx. 1.6 kg		
DH4:R2:290:675-BGS	9/8/2023	MX-80	Drill core	Approx. 1.6 kg		
DH4:R2:290:725-BGS	9/8/2023	MX-80	Drill core	Approx. 1.6 kg		Core split (disked), only one sample made. See Figure 2-5b
DH4:R2:290:775-BGS	9/8/2023	MX-80	Drill core	Approx. 1.6 kg		
DH4:R2:290:825-BGS	9/8/2023	MX-80	Drill core		Sample not available	
DH4:R6:290:575-BGS	26/6/2023	MX-80	Drill core	Approx. 1.6 kg		
DH4:R6:290:625-BGS	26/6/2023	MX-80	Drill core	Approx. 1.6 kg		
DH4:R6:290:675-BGS	26/6/2023	MX-80	Drill core	Approx. 1.6 kg		
DH4:R6:290:725-BGS	26/6/2023	MX-80	Drill core	Approx. 1.6 kg		
DH4:R6:290:775-BGS	26/6/2023	MX-80	Drill core	Approx. 1.6 kg		
DH4:R6:290:825-BGS	26/6/2023	MX-80	Drill core	Approx. 1.6 kg		No sample, core split length wise. See Figure 2-5c



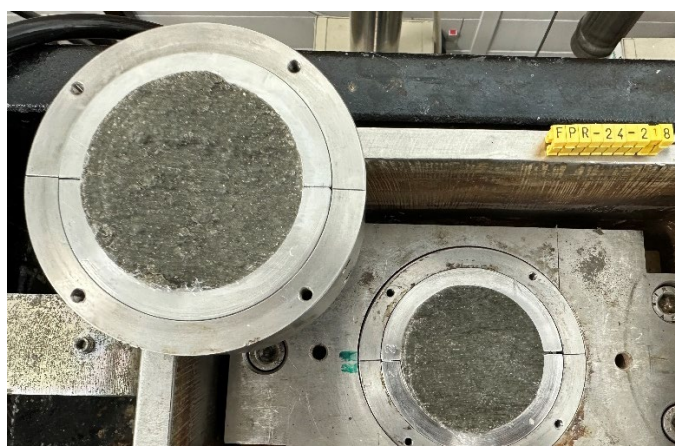
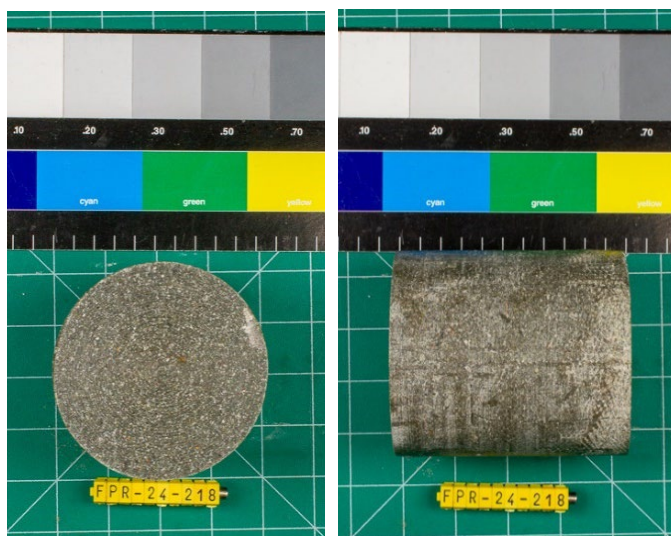


**Figure 2-6.** Sample manufacture showing a complete core for FPR-24-218 / DH2\_R9\_200\_575-BGS, one of the samples made from this core, and the fracture created by shear testing.



**Table 2-2. Assignment of parent and child sample identification**

Parent	Subsample 1	Subsample 2	Offcut 1	Offcut 2
DH2:R9:200:575-BGS	FPR-24-218	FPR-24-219	FPR-24-220	FPR-24-221
DH2:R9:200:625-BGS	FPR-24-222	FPR-24-223	FPR-24-224	FPR-24-225
DH2:R9:200:675-BGS	FPR-24-226	FPR-24-227	FPR-24-228	FPR-24-229
DH2:R9:200:725-BGS	FPR-24-230	FPR-24-231	FPR-24-232	FPR-24-233
DH2:R9:200:775-BGS	FPR-24-234	FPR-24-235	FPR-24-236	FPR-24-237
DH2:R9:200:825-BGS	FPR-24-238	FPR-24-239	FPR-24-240	FPR-24-241
DH3:R9:200:575-BGS	FPR-24-242	FPR-24-243	FPR-24-244	FPR-24-245
DH3:R9:200:625-BGS	FPR-24-246	FPR-24-247	FPR-24-248	FPR-24-249
DH3:R9:200:675-BGS	FPR-24-250	FPR-24-251	FPR-24-252	FPR-24-253
DH3:R9:200:725-BGS	FPR-24-254	FPR-24-255	FPR-24-256	FPR-24-257
DH3:R9:200:775-BGS	FPR-24-258	FPR-24-259	FPR-24-260	FPR-24-261
DH4:R2:290:575-BGS	FPR-24-262	FPR-24-263	FPR-24-264	FPR-24-265
DH4:R2:290:625-BGS	FPR-24-266	FPR-24-267	FPR-24-268	FPR-24-269
DH4:R2:290:675-BGS	FPR-24-270	FPR-24-271	FPR-24-272	FPR-24-273
DH4:R2:290:725-BGS	FPR-24-274	-	FPR-24-275	FPR-24-276
DH4:R2:290:775-BGS	FPR-24-277	FPR-24-278	FPR-24-279	FPR-24-280
DH4:R6:290:575-BGS	FPR-24-281	FPR-24-282	FPR-24-283	FPR-24-284
DH4:R6:290:625-BGS	FPR-24-285	FPR-24-286	FPR-24-287	FPR-24-288
DH4:R6:290:675-BGS	FPR-24-289	FPR-24-290	FPR-24-291	FPR-24-292
DH4:R6:290:725-BGS	FPR-24-293	FPR-24-294	FPR-24-295	FPR-24-296
DH4:R6:290:775-BGS	FPR-24-297	FPR-24-298	FPR-24-299	FPR-24-300

## 2.3 Calculation of geotechnical properties

Table 2-3 shows the dimensions, weight, and calculated bulk density for all the test samples manufactured. All shear samples and offcuts made for geotechnics were oven dried at 105 °C for at least 24 hours to determine water content, as shown in Table 2-4.

Water content can be expressed in one of two ways:

$$W = \frac{m_w}{m_s} \times 100$$

$$WC = \frac{m_w}{m} \times 100$$

where  $m$  = mass of sample (pre-drying),  $m_s$  = mass of solid (post drying weight),  $m_w$  = mass of water ( $m - m_s$ ). The two expressions for water content describe water relative to the total weight (WC) or the weight of solids (dry weight, W). From water content, it is possible to calculate void ratio and saturation using:

$$e = \frac{\text{volume of voids}}{\text{volume of solids}} = 1 - \frac{\rho_d}{\rho_g}$$

$$S = \frac{\text{volume of water}}{\text{volume of voids}} = \frac{WC}{100} \times \frac{\rho_g}{e}$$

where  $e$  = void ratio,  $\rho_d$  = dry density, and  $\rho_g$  = grain density = 2.78 g/cm<sup>3</sup> for MX-80 bentonite.

Water content and bulk density as measured at BGS is compared with the supplied values from SKB in Table 2-5.

Values are shown for  $W$  and  $WC$ . Some water loss had occurred, with a maximum of 15.9 % water loss and a minimum of 1.7 %. However, the calculated density had not altered much. also includes calculated values for void ratio ( $e$ ) and saturation ( $S$ ). Where more than one measure of WC had been made, average values have been used in the calculation for each sample.

Measuring the colour of samples has become a routine operation at BGS as a way of assessing moisture loss through the full life cycle of test samples. Colour was measured using a digital colorimeter manufactured by Beley. This device has an illuminating lamp that measures the colour through an 8 mm hole at the base of the device. A simple single button operation quickly takes a reading and supplied data in the CIELAB colour space. It expresses colour as three values; L for perceptual lightness and a and b for the four unique colours of human vision: red, green, blue, and yellow. Colour was measured four times prior to testing, and the final fracture surface was also measured four times. The results are shown in Table 2-6.

**Table 2-3. Sample dimensions and weight as measured for all manufactured test sample**

FPR Number	SKB Core ID	Height (mm)	Diameter	Weight (g)	Volume (cm <sup>3</sup> )	Bulk density (g/cm <sup>3</sup> )	Dry density (g/cm <sup>3</sup> )
FPR-24-218	DH2:R9:200:575-BGS	52.84±0.03	47.04±0.10	182.70	91.86	1.99	1.58
FPR-24-219	DH2:R9:200:575-BGS	52.16±0.01	47.27±0.09	181.00	91.37	1.98	1.57
FPR-24-222	DH2:R9:200:625-BGS	52.88±0.01	47.12±0.10	183.75	92.10	2.00	1.58
FPR-24-223	DH2:R9:200:625-BGS	53.22±0.02	47.06±0.14	184.75	92.51	2.00	1.58
FPR-24-226	DH2:R9:200:675-BGS	51.44±0.03	47.03±0.12	178.61	89.37	2.00	1.58
FPR-24-227	DH2:R9:200:675-BGS	51.85±0.02	47.11±0.10	180.57	90.61	1.99	1.58
FPR-24-230	DH2:R9:200:725-BGS	53.23±0.01	47.01±0.12	184.69	92.87	1.99	1.57
FPR-24-231	DH2:R9:200:725-BGS	53.32±0.01	46.99±0.13	184.51	92.74	1.99	1.57
FPR-24-234	DH2:R9:200:775-BGS	52.84±0.01	46.92±0.11	182.57	91.47	2.00	1.57
FPR-24-235	DH2:R9:200:775-BGS	53.21±0.02	47.01±0.07	183.80	92.42	1.99	1.57
FPR-24-238	DH2:R9:200:825-BGS	52.69±0.03	47.00±0.08	181.40	91.52	1.98	1.56
FPR-24-239	DH2:R9:200:825-BGS	53.00±0.05	46.77±0.12	181.00	89.46	2.02	1.59
FPR-24-242	DH3:R9:200:575-BGS	51.85±0.07	47.15±0.12	184.49	90.90	2.03	1.64
FPR-24-243	DH3:R9:200:575-BGS	52.08±0.02	47.12±0.14	185.30	90.97	2.04	1.65
FPR-24-246	DH3:R9:200:625-BGS	52.52±0.00	47.22±0.09	188.19	92.01	2.05	1.65
FPR-24-247	DH3:R9:200:625-BGS	52.56±0.01	47.22±0.10	188.27	91.93	2.05	1.65
FPR-24-250	DH3:R9:200:675-BGS	52.30±0.03	47.24±0.08	187.13	91.73	2.04	1.65
FPR-24-251	DH3:R9:200:675-BGS	52.80±0.00	47.30±0.08	189.43	92.70	2.04	1.65
FPR-24-254	DH3:R9:200:725-BGS	53.28±0.02	47.15±0.06	190.41	92.98	2.05	1.66
FPR-24-255	DH3:R9:200:725-BGS	53.18±0.04	47.19±0.07	189.69	93.11	2.04	1.65
FPR-24-258	DH3:R9:200:775-BGS	53.38±0.01	47.06±0.03	189.84	92.64	2.05	1.66
FPR-24-259	DH3:R9:200:775-BGS	52.38±0.01	47.13±0.04	186.72	91.23	2.05	1.66
FPR-24-262	DH4:R2:290:575-BGS	53.10±0.02	47.25±0.02	194.11	93.14	2.08	1.82
FPR-24-263	DH4:R2:290:575-BGS	52.71±0.02	47.23±0.04	191.78	92.55	2.07	1.81
FPR-24-266	DH4:R2:290:625-BGS	52.88±0.01	47.24±0.02	193.45	92.69	2.09	1.81
FPR-24-267	DH4:R2:290:625-BGS	52.82±0.03	47.27±0.02	192.91	92.71	2.08	1.81
FPR-24-270	DH4:R2:290:675-BGS	53.18±0.02	47.21±0.02	195.26	93.14	2.10	1.82
FPR-24-271	DH4:R2:290:675-BGS	49.96±0.03	47.18±0.01	182.59	87.39	2.09	1.81
FPR-24-274	DH4:R2:290:725-BGS	52.74±0.05	47.21±0.01	193.40	92.38	2.09	1.81
FPR-24-277	DH4:R2:290:775-BGS	53.14±0.01	47.23±0.01	195.24	93.01	2.10	1.81
FPR-24-278	DH4:R2:290:775-BGS	51.90±0.01	47.23±0.01	190.56	90.91	2.10	1.81
FPR-24-281	DH4:R6:290:575-BGS	52.76±0.03	47.04±0.10	189.69	91.68	2.07	1.72
FPR-24-282	DH4:R6:290:575-BGS	53.24±0.04	47.04±0.10	192.28	92.73	2.07	1.73
FPR-24-285	DH4:R6:290:625-BGS	51.90±0.02	47.11±0.09	187.46	90.62	2.07	1.71
FPR-24-286	DH4:R6:290:625-BGS	53.44±0.01	47.05±0.09	191.70	92.57	2.07	1.71
FPR-24-289	DH4:R6:290:675-BGS	52.88±0.01	47.03±0.07	190.20	91.91	2.07	1.71
FPR-24-290	DH4:R6:290:675-BGS	53.17±0.01	47.07±0.07	191.73	92.47	2.07	1.71
FPR-24-293	DH4:R6:290:725-BGS	52.89±0.01	46.99±0.05	190.84	91.75	2.08	1.73
FPR-24-294	DH4:R6:290:725-BGS	52.91±0.01	46.97±0.05	191.23	91.78	2.08	1.73
FPR-24-297	DH4:R6:290:775-BGS	52.81±0.01	46.89±0.06	189.18	91.17	2.08	1.71
FPR-24-298	DH4:R6:290:775-BGS	53.22±0.01	46.89±0.06	190.60	91.98	2.07	1.71

**Table 2-4. Calculation of moisture content of tested samples and offcuts**

FPR number	SKB Core ID	Sample	Pre-drying sample weight (g)	Post-drying sample weight (g)	Moisture content (%)	Moisture content (%)
					W	WC
FPR-24-218	DH2:R9:200:575-BGS	Subsample	93.185	73.7878	26.3	20.8
FPR-24-220	DH2:R9:200:575-BGS	Offcut	14.194	11.280	25.8	20.5
FPR-24-222	DH2:R9:200:625-BGS	Subsample	95.592	75.730	26.2	20.8
FPR-24-224	DH2:R9:200:625-BGS	Offcut	18.858	15.005	25.7	20.4
FPR-24-226	DH2:R9:200:675-BGS	Subsample	94.887	75.062	26.4	20.9
FPR-24-228	DH2:R9:200:675-BGS	Offcut	14.616	11.613	25.9	20.5
FPR-24-231	DH2:R9:200:725-BGS	Subsample	95.867	75.783	26.5	20.9
FPR-24-232	DH2:R9:200:725-BGS	Offcut	31.130	24.658	26.2	20.8
FPR-24-234	DH2:R9:200:775-BGS	Subsample	93.111	73.338	27.0	21.2
FPR-24-235	DH2:R9:200:775-BGS	Subsample	93.489	73.567	27.1	21.3
FPR-24-236	DH2:R9:200:775-BGS	Offcut	25.923	20.474	26.6	21.0
FPR-24-238	DH2:R9:200:825-BGS	Subsample	92.768	72.824	27.4	21.5
FPR-24-240	DH2:R9:200:825-BGS	Offcut	31.340	24.794	26.4	20.9
FPR-24-242	DH3:R9:200:575-BGS	Subsample	93.352	75.472	23.7	19.2
FPR-24-244	DH3:R9:200:575-BGS	Offcut	20.823	16.854	23.5	19.1
FPR-24-246	DH3:R9:200:625-BGS	Subsample	102.080	82.451	23.8	19.2
FPR-24-248	DH3:R9:200:625-BGS	Offcut	27.104	21.927	23.6	19.1
FPR-24-250	DH3:R9:200:675-BGS	Subsample	94.239	76.109	23.8	19.2
FPR-24-251	DH3:R9:200:675-BGS	Subsample	97.963	79.078	23.9	19.3
FPR-24-252	DH3:R9:200:675-BGS	Offcut	18.922	15.301	23.7	19.1
FPR-24-254	DH3:R9:200:725-BGS	Subsample	93.659	75.864	23.5	19.0
FPR-24-256	DH3:R9:200:725-BGS	Offcut	30.528	24.755	23.3	18.9
FPR-24-258	DH3:R9:200:775-BGS	Subsample	97.009	78.795	23.1	18.8
FPR-24-260	DH3:R9:200:775-BGS	Offcut	26.997	21.968	22.9	18.6
FPR-24-262	DH4:R2:290:575-BGS	Subsample	100.925	87.924	14.8	12.9
FPR-24-264	DH4:R2:290:575-BGS	Offcut	31.747	27.627	14.9	13.0
FPR-24-266	DH4:R2:290:625-BGS	Subsample	96.473	83.839	15.1	13.1
FPR-24-267	DH4:R2:290:625-BGS	Subsample	95.157	82.749	15.0	13.0
FPR-24-268	DH4:R2:290:625-BGS	Offcut	18.045	15.677	15.1	13.1
FPR-24-271	DH4:R2:290:675-BGS	Subsample	93.577	81.197	15.2	13.2
FPR-24-272	DH4:R2:290:675-BGS	Offcut	20.545	17.806	15.4	13.3
FPR-24-274	DH4:R2:290:725-BGS	Subsample	97.152	83.951	15.7	13.6
FPR-24-275	DH4:R2:290:725-BGS	Offcut	26.669	23.039	15.8	13.6
FPR-24-277	DH4:R2:290:775-BGS	Subsample	97.306	83.932	15.9	13.7
FPR-24-279	DH4:R2:290:775-BGS	Offcut	27.779	23.952	16.0	13.8
FPR-24-282	DH4:R6:290:575-BGS	Subsample	97.340	81.042	20.1	16.7
FPR-24-283	DH4:R6:290:575-BGS	Offcut	35.961	29.775	20.8	17.2
FPR-24-285	DH4:R6:290:625-BGS	Subsample	98.464	81.305	21.1	17.4
FPR-24-287	DH4:R6:290:625-BGS	Offcut	21.612	17.950	20.4	16.9
FPR-24-290	DH4:R6:290:675-BGS	Subsample	96.422	79.628	21.1	17.4
FPR-24-291	DH4:R6:290:675-BGS	Offcut	15.480	12.823	20.7	17.2
FPR-24-294	DH4:R6:290:725-BGS	Subsample	94.246	78.393	20.2	16.8
FPR-24-295	DH4:R6:290:725-BGS	Offcut	26.177	21.734	20.4	17.0
FPR-24-297	DH4:R6:290:775-BGS	Subsample	97.282	80.201	21.3	17.6
FPR-24-299	DH4:R6:290:775-BGS	Offcut	27.942	23.067	21.1	17.4

**Table 2-5. Comparing calculated moisture content with data supplied by SKB to assess moisture loss during storage**

Core ID	Moisture content W (%)			Density (g/cm <sup>3</sup> )			Dry density (g/cm <sup>3</sup> )			Void ratio			Saturation		
	SKB	BGS	Loss	SKB	BGS	Difference	SKB	BGS	Difference	SKB	BGS	Difference	SKB	BGS	Difference
DH2:R9:200:575-BGS	28.7	26.3	8.5	1.982	1.985	0.3%	1.540	1.575	3.5%	0.446	0.433	-1.3%	0.991	0.955	-3.6%
DH2:R9:200:625-BGS	28.4	26.2	7.6	1.985	1.996	1.1%	1.546	1.581	3.5%	0.444	0.431	-1.3%	0.989	0.960	-2.9%
DH2:R9:200:675-BGS	28.4	26.4	7.0	1.985	1.996	1.1%	1.546	1.581	3.5%	0.444	0.431	-1.3%	0.989	0.968	-2.1%
DH2:R9:200:725-BGS	28.6	26.5	7.3	1.983	1.989	0.6%	1.542	1.573	3.1%	0.445	0.434	-1.1%	0.991	0.960	-3.1%
DH2:R9:200:775-BGS	28.9	27.0	6.7	1.979	1.992	1.3%	1.535	1.569	3.4%	0.448	0.436	-1.2%	0.991	0.974	-1.7%
DH2:R9:200:825-BGS	29.7	27.4	7.8	1.957	1.982	2.5%	1.509	1.556	4.7%	0.457	0.440	-1.7%	0.980	0.968	-1.2%
DH3:R9:200:575-BGS	26.5	23.7	10.6	2.021	2.033	1.2%	1.598	1.641	4.3%	0.425	0.410	-1.5%	0.995	0.949	-4.6%
DH3:R9:200:625-BGS	26.5	23.8	10.2	2.023	2.047	2.4%	1.599	1.652	5.3%	0.425	0.406	-1.9%	0.997	0.969	-2.8%
DH3:R9:200:675-BGS	26.8	23.8	10.9	2.019	2.042	2.3%	1.592	1.649	5.7%	0.427	0.407	-2.0%	0.999	0.967	-3.2%
DH3:R9:200:725-BGS	26.8	23.5	12.5	2.019	2.043	2.4%	1.592	1.659	6.7%	0.427	0.403	-2.4%	0.998	0.965	-3.3%
DH3:R9:200:775-BGS	27.5	23.1	15.9	2.010	2.048	3.8%	1.576	1.664	8.8%	0.433	0.401	-3.2%	1.002	0.959	-4.3%
DH4:R2:290:575-BGS	16	14.8	7.6	2.087	2.078	-0.9%	1.799	1.816	1.7%	0.353	0.347	-0.6%	0.816	0.774	-4.2%
DH4:R2:290:625-BGS	16	15.1	5.8	2.093	2.084	-0.9%	1.804	1.812	0.8%	0.351	0.348	-0.3%	0.822	0.781	-4.1%
DH4:R2:290:675-BGS	16	15.2	4.7	2.096	2.093	-0.3%	1.807	1.813	0.6%	0.350	0.348	-0.2%	0.826	0.795	-3.1%
DH4:R2:290:725-BGS	16	15.7	1.7	2.103	2.094	-0.9%	1.813	1.809	-0.4%	0.348	0.349	0.1%	0.834	0.815	-1.9%
DH4:R2:290:775-BGS	17	15.9	6.3	2.104	2.098	-0.6%	1.798	1.811	1.3%	0.353	0.349	-0.4%	0.866	0.827	-3.9%
DH4:R6:290:575-BGS	23	20.1	12.6	2.061	2.071	1.0%	1.676	1.726	5.0%	0.397	0.379	-1.8%	0.970	0.916	-5.4%
DH4:R6:290:625-BGS	24	21.1	12.1	2.060	2.070	1.0%	1.661	1.708	4.7%	0.402	0.386	-1.6%	0.991	0.935	-5.6%
DH4:R6:290:675-BGS	23	21.1	8.3	2.064	2.072	0.8%	1.678	1.712	3.4%	0.396	0.384	-1.2%	0.973	0.940	-3.3%
DH4:R6:290:725-BGS	24	20.2	15.7	2.061	2.082	2.1%	1.662	1.733	7.1%	0.402	0.377	-2.5%	0.992	0.931	-6.1%
DH4:R6:290:775-BGS	24	21.3	11.3	2.058	2.074	1.6%	1.660	1.711	5.1%	0.403	0.385	-1.8%	0.989	0.947	-4.2%
<b>Average</b>			<b>9.1%</b>			<b>1%</b>			<b>3.9%</b>			<b>-1.4%</b>			<b>-3.6%</b>

**Table 2-6. The measurement of colour for pre- and post-test samples**

FPR Number	SKB Core ID	Pre-test			Slip-surface		
		L	a	b	L	a	b
FPR-24-218	DH2:R9:200:575-BGS	46.98	-5.74	7.94	39.26	-6.87	7.88
FPR-24-219	DH2:R9:200:575-BGS	46.36	-6.02	7.30			
FPR-24-222	DH2:R9:200:625-BGS	46.88	-5.81	7.60	37.38	-7.05	7.34
FPR-24-223	DH2:R9:200:625-BGS	47.42	-5.65	7.62			
FPR-24-226	DH2:R9:200:675-BGS	46.56	-5.87	8.05	36.85	-6.15	7.99
FPR-24-227	DH2:R9:200:675-BGS	47.38	-5.79	7.70			
FPR-24-230	DH2:R9:200:725-BGS	45.73	-6.01	7.77			
FPR-24-231	DH2:R9:200:725-BGS	46.21	-5.91	7.96	35.62	-6.10	7.76
FPR-24-234	DH2:R9:200:775-BGS	45.97	-6.21	7.67	34.44	-6.50	7.37
FPR-24-235	DH2:R9:200:775-BGS	44.71	-6.30	7.99	33.56	-6.08	7.67
FPR-24-238	DH2:R9:200:825-BGS	44.08	-6.42	7.42	37.40	-6.15	7.84
FPR-24-239	DH2:R9:200:825-BGS	45.02	-6.60	7.47			
FPR-24-242	DH3:R9:200:575-BGS	49.64	-5.42	7.93	40.58	-5.02	8.14
FPR-24-243	DH3:R9:200:575-BGS	49.59	-5.54	7.73			
FPR-24-246	DH3:R9:200:625-BGS	48.32	-5.81	7.79	37.76	-5.48	8.08
FPR-24-247	DH3:R9:200:625-BGS	48.27	-5.79	7.74			
FPR-24-250	DH3:R9:200:675-BGS	48.80	-5.79	7.53	36.38	-5.55	7.70
FPR-24-251	DH3:R9:200:675-BGS	49.03	-5.55	7.70	39.17	-5.54	8.40
FPR-24-254	DH3:R9:200:725-BGS	48.01	-5.77	7.66	41.95	-5.42	8.34
FPR-24-255	DH3:R9:200:725-BGS	48.85	-5.53	7.93			
FPR-24-258	DH3:R9:200:775-BGS	50.76	-5.47	7.81	39.60	-5.32	7.92
FPR-24-259	DH3:R9:200:775-BGS	49.65	-5.52	7.87			
FPR-24-262	DH4:R2:290:575-BGS	67.41	-5.73	6.51	68.07	-4.72	7.25
FPR-24-263	DH4:R2:290:575-BGS	68.37	-5.74	6.74			
FPR-24-266	DH4:R2:290:625-BGS	67.12	-5.56	7.08	61.69	-4.69	7.30
FPR-24-267	DH4:R2:290:625-BGS	67.41	-5.76	6.58	60.22	-4.66	6.80
FPR-24-270	DH4:R2:290:675-BGS	65.81	-5.41	6.86			
FPR-24-271	DH4:R2:290:675-BGS	65.91	-5.62	6.90	57.36	-5.11	7.12
FPR-24-274	DH4:R2:290:725-BGS	63.76	-5.54	7.04	59.96	-4.37	7.63
FPR-24-277	DH4:R2:290:775-BGS	64.49	-5.52	7.14	61.44	-4.63	7.79
FPR-24-278	DH4:R2:290:775-BGS	64.17	-5.53	7.54			
FPR-24-281	DH4:R6:290:575-BGS	56.80	-5.15	7.97			
FPR-24-282	DH4:R6:290:575-BGS	56.42	-5.22	7.57	49.73	-4.56	8.37
FPR-24-285	DH4:R6:290:625-BGS	55.91	-5.23	8.04	48.24	-4.07	9.39
FPR-24-286	DH4:R6:290:625-BGS	57.15	-5.25	7.82			
FPR-24-289	DH4:R6:290:675-BGS	54.39	-5.32	8.01			
FPR-24-290	DH4:R6:290:675-BGS	53.19	-5.35	8.10	47.08	-4.41	9.12
FPR-24-293	DH4:R6:290:725-BGS	54.11	-4.98	8.21			
FPR-24-294	DH4:R6:290:725-BGS	55.32	-5.14	8.08	49.43	-4.39	8.83
FPR-24-297	DH4:R6:290:775-BGS	53.16	-5.48	7.65	45.81	-4.66	6.80
FPR-24-298	DH4:R6:290:775-BGS	54.26	-5.13	7.64			

## 2.4 Test procedure

All tests were conducted in a near-identical manner. Cuss et al., (2022) showed minimal sensitivity for MX-80 to both normal stress and strain rate, with the latter only being sensitive when tests were conducted for prolonged times. Communication with SKB suggested that total stress in the PRP experiment had ranged between 1 and 8 MPa. Given the lack of sensitivity of pre-compacted MX-80 to normal load, it was decided to perform the experiments at the same normal load as the previous study (Cuss et al., 2022) for direct comparison of results. A normal stress of 4.7 MPa was therefore used with shear experiments each lasting a maximum of 2 hours.

All tests were conducted with identical protocols. The vacuum-packed samples were removed from their packing. The sample was then wrapped in fresh cling-film. The samples were loaded into the shear sample collars, which itself was loaded into the shear rig. At this point data logging was started and normal load was placed on the sample in steps. Once the pump of the load system had settled (usually within a minute) the shear actuator was started. The data were then logged until the full range of shear occurred (approximately 6 mm or 12 % strain). The data logger was then stopped, and normal stress was reduced in steps. The sample assembly was carefully dismantled, the fracture surface was photographed and laser scanned to determine the surface characteristics of the fracture. The lower fracture sample was weighed and oven dried for geotechnical properties and the top sample was vacuum packed for storage.

## 2.5 Fracture surface analysis

Understanding the topography of fracture surfaces (fracture roughness) is important in estimating the hydro-mechanical behaviour of discontinuities within a rock mass or along interfaces. Flow properties and mechanical strength will be affected by the spatial distribution of contact areas, which in turn affect the stress distribution and ensuing asperity damage during normal and shear loading.

Fracture surfaces were measured using laser triangulation, whereby the fracture surfaces were scanned to produce a 3D mesh model of the fracture surface. A Revopoint MINI 3D Scanner was used (*Figure 2-7*). The Revopoint MINI had an accuracy of  $\pm 20 \mu\text{m}$ . The output surface data were processed using TrueMap 5.0 surface topography software.



*Figure 2-7. Laser scanning of fracture surfaces using a Revopoint MINI 3D Scanner.*

### 2.5.1 Fracture Roughness Measurements

In the present study, laser triangulation method was adopted, whereby the fracture surfaces were scanned using a RevoPoint MINI 3D scanner. This produced a 3D mesh model of the fracture surface accurate within an error of  $\pm 20 \mu\text{m}$ . Algorithms inbuilt within the data acquisition RevoScan software produced clean surface data, which were used in subsequent empirical and statistical analysis.

The measured surface data was composed of three components: form, waviness, and roughness. The form corresponds to the underlying shape and tilt of the surfaces with respect to the measuring platform. A “corrected” profile obtained by removing form from the surface data can be used to obtain a 2-D profile that describes the surface texture. This profile after removal of form is usually referred to as the “primary profile”. The stages are depicted in Figure 2-8.

From the primary profile, the waviness profile is removed by applying a band-pass filter. In theory, difference between the primary and waviness profile gives the roughness profile. However, in the present study no band-pass filters were applied due to lack of uniform waviness in the dataset. Hence, surface roughness calculations were performed on “primary profile” datasets spanning the entire fracture surface.



All the data processing and surface parameter calculations were performed in TrueMap 5.0 surface topography software. This software package was able to calculate surface or profile parameters using SI methods. Table 2-7 lists the common parameters calculated for describing the fracture surfaces, with data reported for average roughness ( $s_a$ ), root mean squared (RMS) roughness ( $s_q$ ), and peak to valley height ( $s_t$ ).

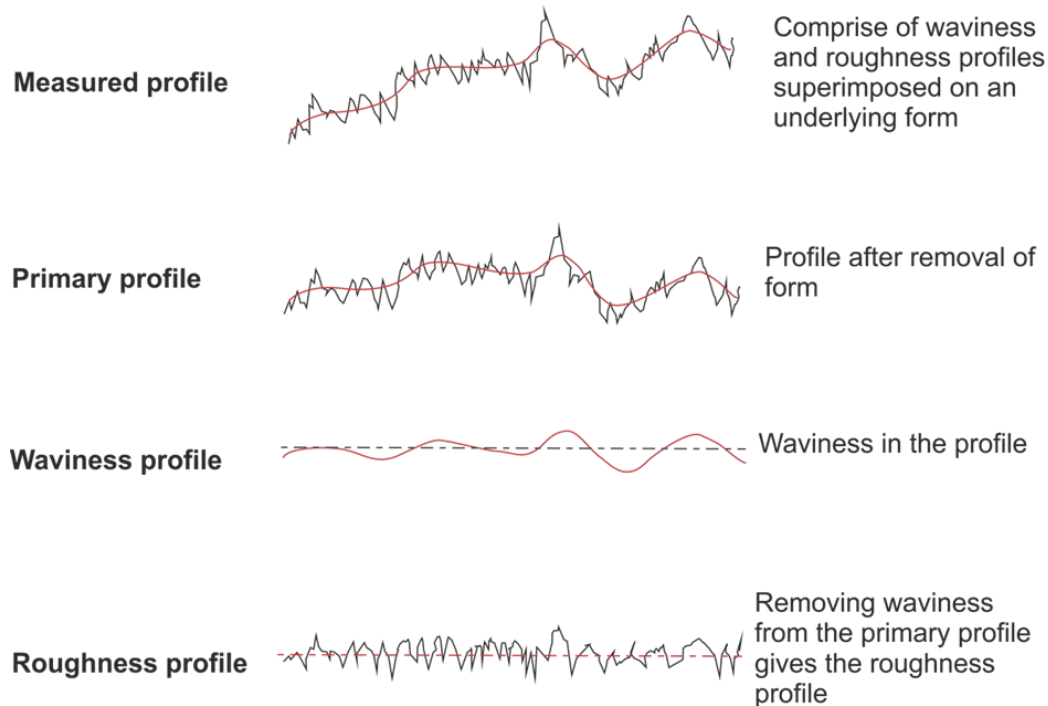


**Figure 2-8.** Summary of stages involved in analysis of measured profile to obtain a roughness profile (From ASTM standard, 2009).

**Table 2-7. List of parameters calculated to describe surface characteristics of a test fracture**

Parameter	Symbol	Description
Roughness average	$R_a$ ; $S_a$	Arithmetic mean of the absolute distances of the surface points from the mean plane/profile
Root Mean Square (RMS) Roughness	$R_q$ ; $S_q$	Square root of average squared absolute height values of the surface profile from the mean line
Peak Height	$R_p$ ; $S_p$	Maximum height above the mean line/plane
Valley Depth	$R_v$ ; $S_v$	Maximum depth below the mean line/plane
Peak to Valley Height	$R_t$ ; $S_t$	Maximum peak to valley distance
Kurtosis	$R_{ku}$ ; $S_{ku}$	Measure of the sharpness of the surface/profile
Skewness	$R_{sk}$ ; $S_{sk}$	Measures the symmetry of the variation of a profile/surface about its mean line/plane
Texture Direction	$S_{td}$	Direction of the texture of a surface with respect to the y axis
Texture Direction Index	$S_{tdi}$	Measure of how dominant the predominant direction is relative to the rest of the surface



### 3 Test results

Table 2-1 shows the supplied core samples from SKB, with three samples listed as “Not to be analysed, reserve sample.” Please note that in error all three of these were tested. Two of the core samples were not tested for the reasons stated above. All test results are shown in Appendix. One test will be described for completeness.

#### 3.1 Example Test FPR-24-274

Figure 3-1 and Table 3-1 show the results from test FPR-24-274 on core DH4:R2:290:725-BGS.

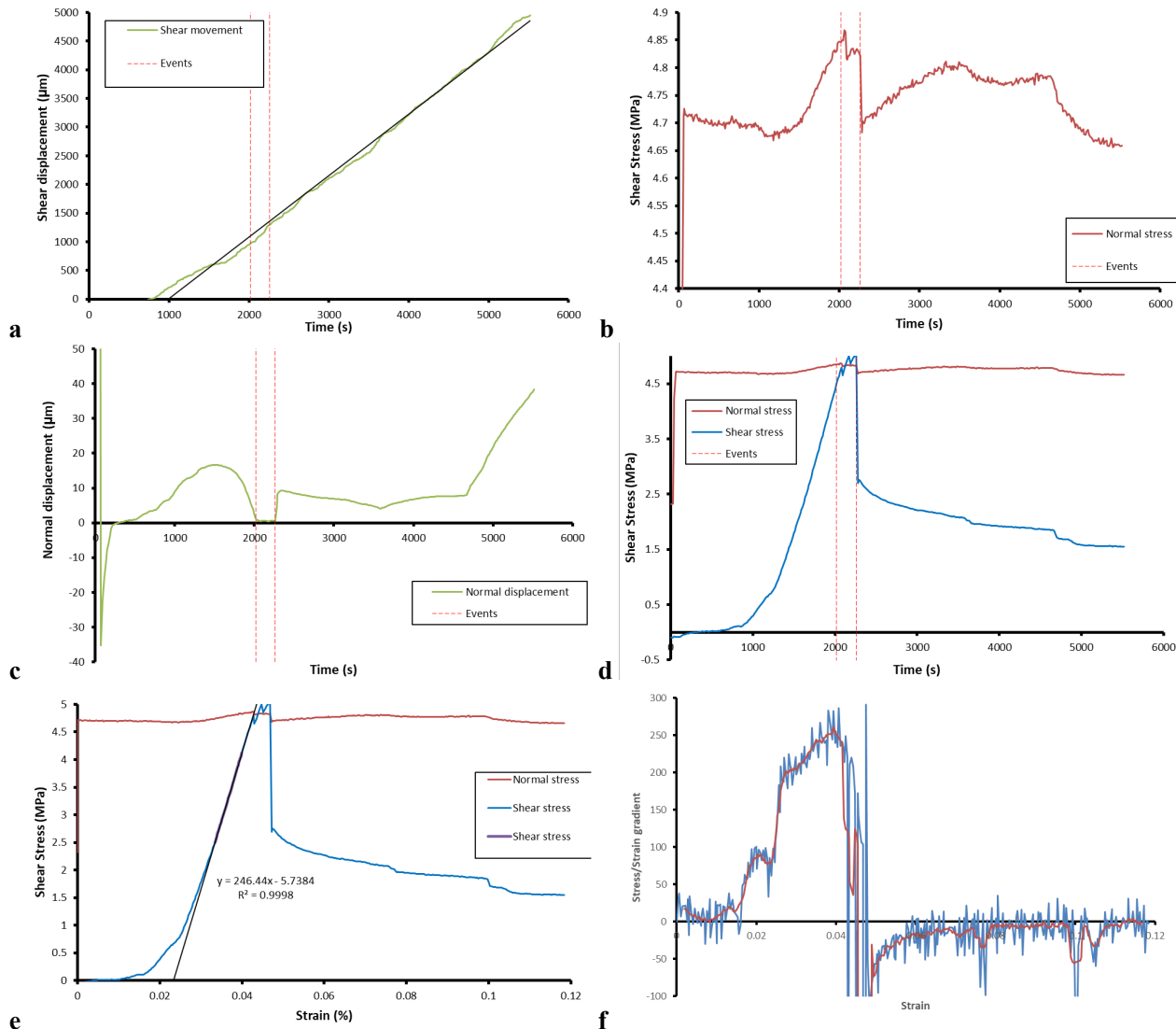


**Figure 3-1.** Shear results for test FPR-24-274 (DH4:R2:290:725-BGS). a) Displacement with time; b) Normal load with time; c) Normal displacement with time; d) Normal and shear stress with time; e) Stress vs strain; f) Gradient of stress/strain (shear modulus).

Figure 3-1a shows the displacement during the experiment. As shown, the LVDT attached to the apparatus gave noisy results, but displacement was linear once the backlash in the drive-system had been taken up. Calibration of the apparatus showed that the low friction bearing resulted in minor twisting of the shear assembly, meaning that measurement from only one side of the assembly gives non-linear results. Calibration experiments with two LVDTs showed that the complete assembly moved in a near perfect linear manner. Therefore, the LVDT result was used to ascertain proper execution of the test, but linear movement was calculated from calibration data to account for assembly twisting. Please note that the twisting would not impact the shear experiment.

Figure 3-1b shows the normal load for the test. The Teledyne/ISCO pump maintained constant pressure in the axial ram. However, the normal load cells record small variations in normal load as shear stress built up in the test sample. This is normal for the shear apparatus. Figure 3-1c shows the normal displacement on the sample. As shear stress built up in the sample the sample contracted up until a time of ~1500 seconds, when the sample started to dilate. Dilation continued until ~2000 seconds, when no dilation/contraction occurred. This time corresponds with yield, as shown by the first event line. The sample contracted at the time of the second event line, which corresponds to the shear stress drop. Following this, the sample dilated a few microns, before starting to contract around 3700 seconds.

**Table 3-1. Results for test FPR-24-274 (DH4:R2:290:725-BGS)**

Parameter	Value	±	Units
SKB Sample name	DH4:R2:290:725-BGS		
BGS Sample name	FPR-24-274		
Normal load	4.771	0.003	MPa
Peak shear stress	5.047		MPa
Yield shear stress	4.495		MPa
Residual shear stress	1.756		MPa
Shear modulus	260.5		MPa
Displacement at peak	2198		µm
Maximum displacement	5563		µm
Displacement rate	1.032		µm/s
Sample diameter	47.21	0.01	mm
Sample height	52.74	0.05	mm
Sample weight	193.40		g
Bulk density	2.09		g/cm <sup>3</sup>
Sample colour	63.76,-5.54,7.04		L, a, b
Colour of bottom slip plane	59.96,-4.37,7.63		L, a, b
Weight of bottom sample	97.152		g
Weight after drying	83.951		g
Moisture content	13.6		%
Bottom: Raw: $s_a$	0.62		mm
Bottom: Raw: $s_q$	0.804		mm
Bottom: Raw: $s_t$	5.403		mm
Top: Raw: $s_a$	0.814		mm
Top: Raw: $s_q$	1.023		mm
Top: Raw: $s_t$	5.284		mm
Bottom: Surf: $s_a$	0.464		mm
Bottom: Surf: $s_q$	0.577		mm
Bottom: Surf: $s_t$	3.832		mm
Top: Surf: $s_a$	0.431		mm
Top: Surf: $s_q$	0.532		mm
Top: Surf: $s_t$	3.855		mm

Figure 3-1d shows the shear stress plotted against time, while Figure 3-1e shows shear stress plotted against strain. A linear relationship was established after early non-linearity, which is normal in direct shear testing. The linear relationship in stress/strain gives the shear modulus of the sample. The deviation from the linear signifies the onset of yield. In the example test, yield stress was close to normal stress. Shear stress continued to increase after yield, with a couple of small reduction events before peak stress was established. Each of the small reductions signify the development of a shear plane and small lateral movements of the sample. The second event line at 2260 seconds shows a reduction in shear stress of nearly 2 MPa and signifies the creation of the shear fracture and separation of the top and bottom halves of the sample. Following this, shear stress reduced as the two halves of the sample sheared. Figure 3-1f shows stress/strain throughout the test. This was used to identify the maximum shear modulus during the linear region of the stress/strain response, giving a shear modulus of 260.5 MPa.

Table 3-1 shows the results for test FPR-24-274. Peak shear stress was 5.047 MPa, with yield occurring at 4.495 MPa. A residual strength of 1.756 MPa was recorded, although it should be noted that a clear plateau had not occurred by the limit of shear imposed.

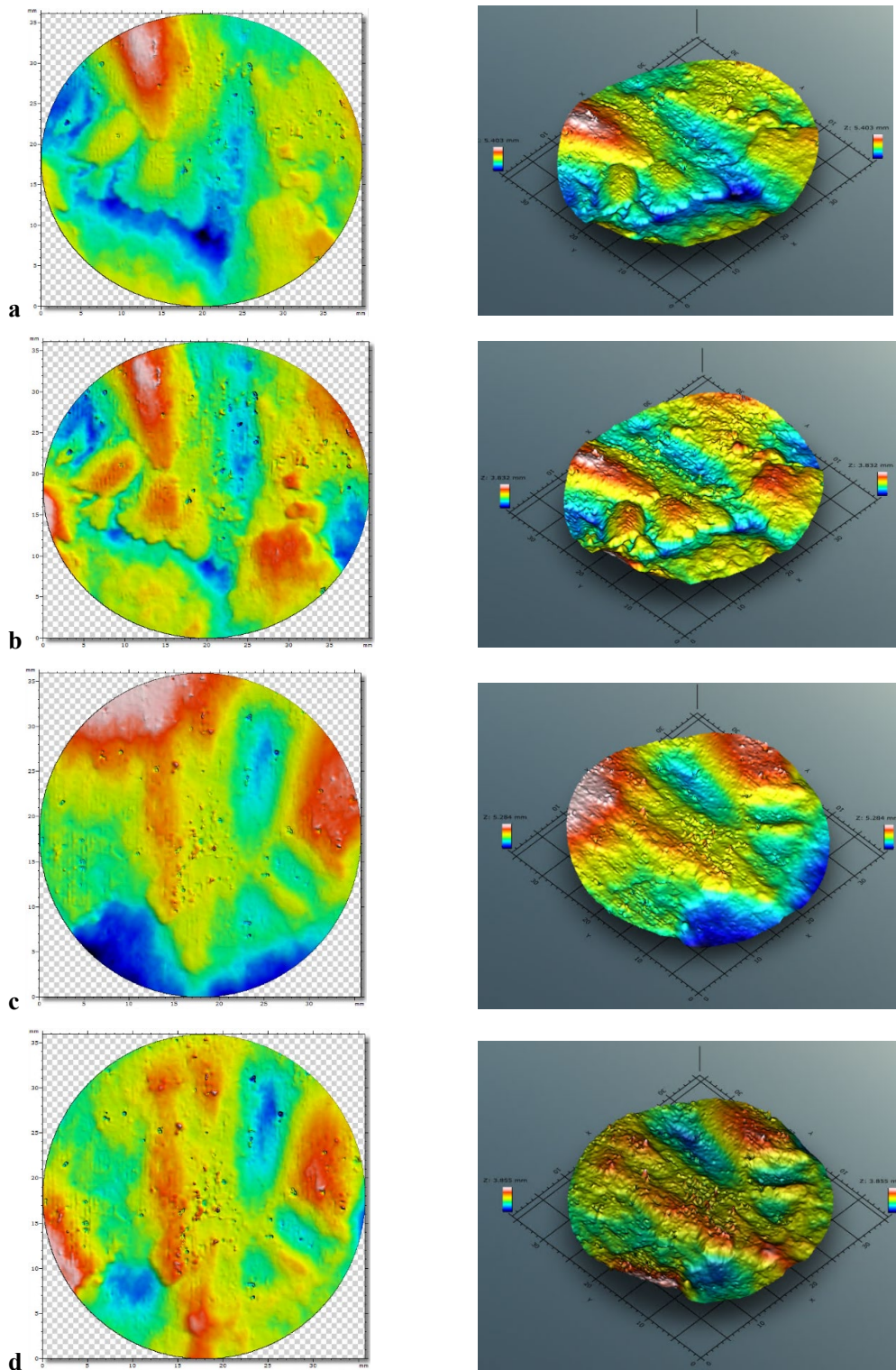


**Figure 3-2.** Laser scan of shear fracture FPR-24-274 (DH4:R2:290:725-BGS). *a)* Bottom surface raw scan; *b)* Bottom surface with form removed; *c)* Top surface raw scan; *d)* Top surface with form removed. Shear direction is parallel with Y-axis, i.e. top-to-bottom in left.



Figure 3-3 shows the fracture surface created during the direct shear test. The fracture surfaces were scanned, as shown in Figure 3-2. Figure 3-2ac show the raw shear surface, while Figure 3-2bd show the surfaces after the removal of a polynomial surface to extract roughness without form. The results of the surface analysis are shown in Table 3-1, with a roughness of ~0.45 mm.

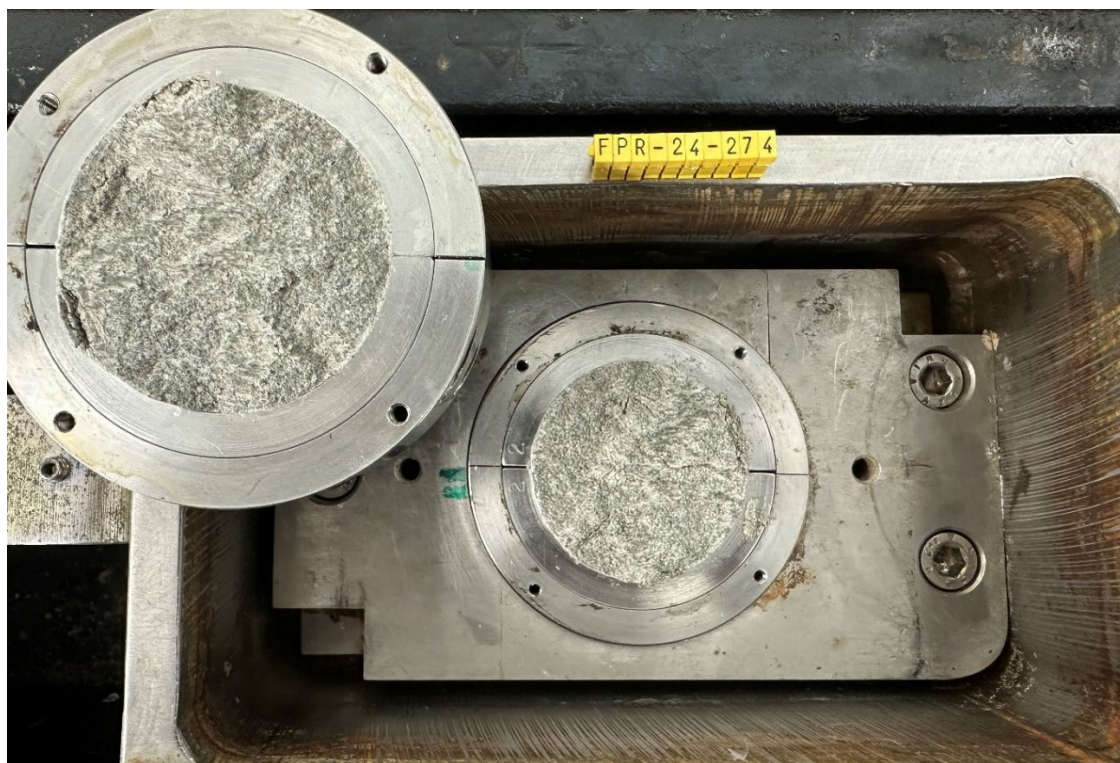


**Figure 3-3.** Fracture surface created in sample FPR-24-274 (DH4:R2:290:725-BGS) during direct shear experiment.

## 3.2 Additional tests

Two additional tests were conducted to add confidence to the results, as summarised in Table 3-2. A repeat test was performed on core DH4:R2:290:625-BGS to examine the repeatability of direct shear experiments (test FPR-24-267). A test was also performed at half the normal load to ensure that the shear properties were not normal load dependent (test FPR-24-251).

**Table 3-2. Additional tests conducted in the current study**

BGS Id	SKB Id	Reason for additional test
FPR-24-267	DH4:R2:290:625-BGS	Repeat test to examine repeatability of direct shear tests
FPR-24-251	DH3:R9:200:675-BGS	Conducted at half normal load to see influence of load

### 3.2.1 Repeatability test

Figure 3-4a and Table 3-3 show the results of the repeatability study for tests FPR-24-266 and FPR-24-267 on core DH4:R2:290:625-BGS. As seen, repeatability was very good, giving similar shear modulus of 214 and 230 MPa, and peak shear stress of 4.53 and 4.63 MPa. Variation is seen in yield modulus but as this parameter is difficult to determine this is not unexpected. Repeatability is therefore seen to be good.

### 3.2.2 Normal load study

Figure 3-4b and Table 3-3 show the results of the normal load study for tests FPR-24-250 and FPR-24-251 on core DH3:R9:200:675-BGS. Test FPR-24-250 was conducted at the usual normal load of 4.68 MPa, while test FPR-24-251 was conducted at 2.26 MPa, approximately half the normal load (labelled HL in Figure 3-4b). Repeatability was very good, giving similar shear modulus of 118 and 129 MPa, and peak shear stress of 2.15 and 2.19 MPa. Differences are seen post peak stress, but this does not significantly alter the dataset as similar residual strengths are achieved of 0.86 and 0.71 MPa. These tests show that MX-80 samples from the PRP are not significantly sensitive to normal load and therefore the use of a relatively high 4.68 MPa will not have affected the results.

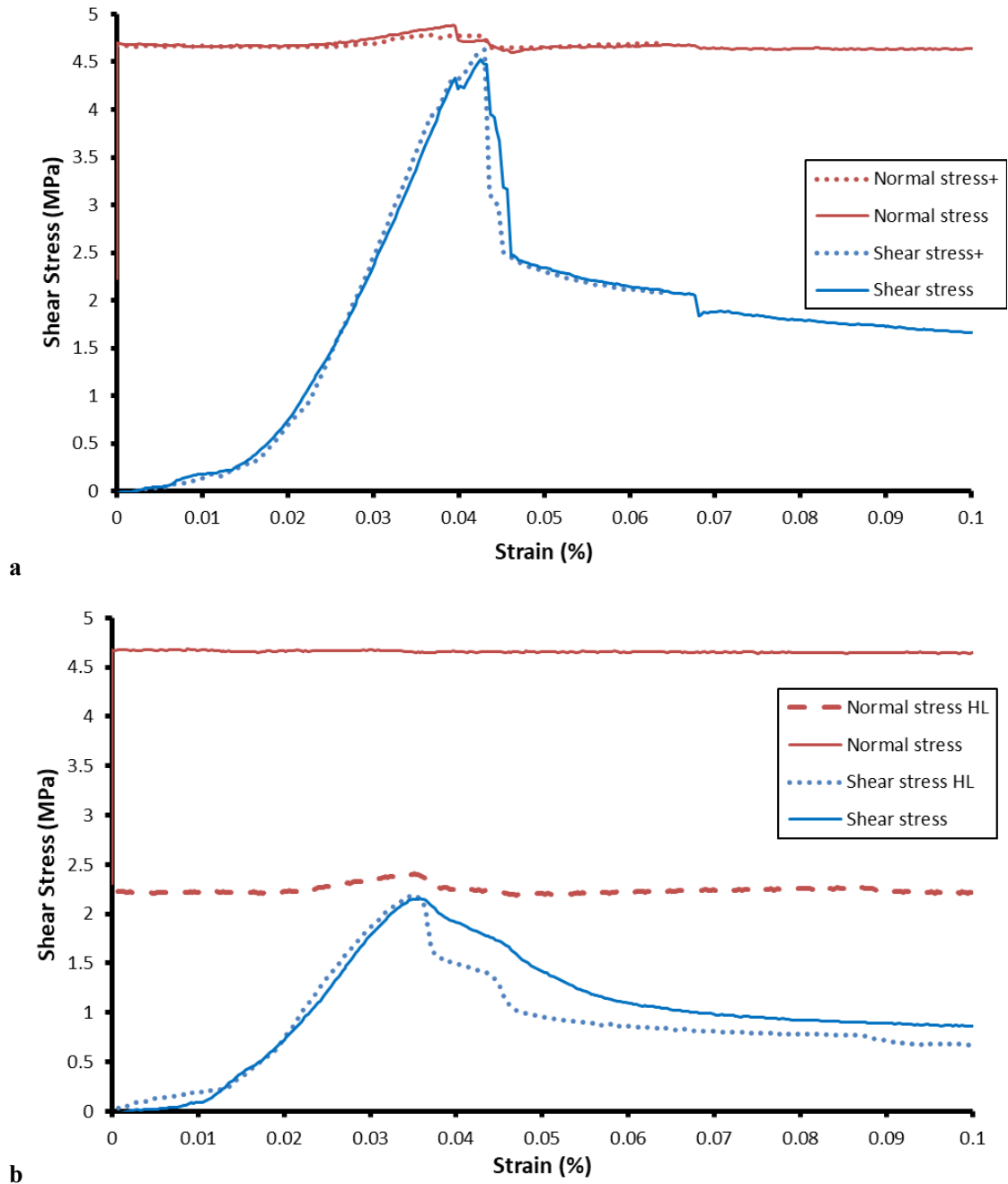


**Figure 3-4.** Additional tests conducted. a) Repeatability study; b) Influence of normal load. Note HL denotes half (normal) load.

**Table 3-3. Results of the additional tests conducted**

BGS Sample name	SKB Sample name	Normal load (MPa)	$\mu$	Peak shear stress (MPa)	Yield shear stress (MPa)	Residual shear stress (MPa)	Shear modulus (MPa)	Displacement at peak ( $\mu$ m)	Maximum displacement ( $\mu$ m)
FPR-24-250	DH3:R9:200:675-BGS	4.684	0.001	2.153	1.320	0.859	118.3	1682	5594
FPR-24-251	DH3:R9:200:675-BGS	2.255	0.002	2.192	1.011	0.712	128.6	2131	5587
FPR-24-266	DH4:R2:290:625-BGS	4.695	0.003	4.530	4.116	1.660	214.7	2002	5573
FPR-24-267	DH4:R2:290:625-BGS	4.711	0.003	4.629	3.644	2.082	230.0	2162	3147

### 3.3 Results for all tests

Appendix shows the results for all shear tests (Figure A-1 to Figure A-46 and Table A-1 to A-23). The mechanical shear results are shown in Table 3-4 and graphically in Figure 3-5 and Figure 3-7. Peak stress is seen to have a strong dependence on the group that the test samples originated (Figure 3-5a). Samples from DH2:R9 show a relatively weak behaviour with peak stress of 1.32 MPa, compared with DH4:R2, which had a peak stress of 4.61 MPa. The results show that the sample strength was ordered DH4:R2 > DH4:R6 > DH3:R9 > DH2:R9. Therefore peak shear strength varied by a factor of 3.5. A similar trend is seen for yield strength (Figure 3-5b) and residual strength (Figure 3-5c). Greater variation is seen in each grouping for yield and residual strengths, especially for group 2 (DH3:R9) and group 3 (DH4:R2). Figure 3-6a shows the data for peak, yield, and residual strength together. This highlights that group 3 (DH4:R2) showed considerable strength drop from peak to residual strength conditions. In group 3 samples, the stress-strain response is that of classic elastic-brittle behaviour (see Figure 3-4a). For group 1 and group 2, the behaviour was more elastic – strain softening, as seen in Figure 3-4b. Therefore, not only did the shear properties of the groupings change, the overall mechanical behaviour changed. Figure 3-6b shows that the shear modulus of the groupings also changed, with shear modulus ordered DH4:R2 > DH4:R6 > DH3:R9 > DH2:R9. Group 3 (DH4:R2) had a relatively high shear modulus of 232 MPa, while group 1 had a much lower shear modulus of 69 MPa. Therefore shear modulus varied by a factor of 3.4. Figure 3-6c shows that no systematic variation was seen in the displacement at peak stress.

Figure 3-7a shows peak and residual strength plotted against dry density irrespective of the groupings of the samples (note: yield strength is not shown for clarity). This shows that peak strength had a clear linear dependence on dry density, with higher dry densities being much stronger. This is also seen in residual strength, with a clear linear response  $1/3^{\text{rd}}$  of that seen for peak strength. Figure 3-7b shows that shear strength also displays a linear increase with dry density, although with greater scatter. These two plots suggest that dry density is the primary control on strength. However, Figure 3-7c shows shear strength plotted against under-saturation. The data have been plotted this way so that a logarithmic relationship can be fitted to the data, with under-saturation being  $1 - \text{saturation}$ . This plot shows that saturation also plays a role in determining strength, with a reduction in saturation resulting in an increase in strength. This would be seen as the sample becoming more brittle in mechanical behaviour. Figure 3-7 therefore shows that mechanical shear strength is dependent primarily on dry density of the bentonite blocks, but secondary the saturation of the sample influences strength. The data of Figure 3-7c shows that the drying of the samples by an average of 9.1 % (Table 2-5) seen between the measurements of SKB and the current study could be corrected.

Figure 3-8, Figure 3-9, and Table 3-5 summarise the fracture topology data for all tests. Figure 3-8a shows the results for fracture roughness after removal of a polynomial surface. Variation is seen for each group, with group 1 (DH2:R9) and group 2 (DH3:R9) giving similar results, with averages of 0.22 mm. Group 3 (DH4:R2) shows the greatest roughness of 0.39 mm, while group 4 (DH4:R6) showed intermediate roughness of 0.28 mm.

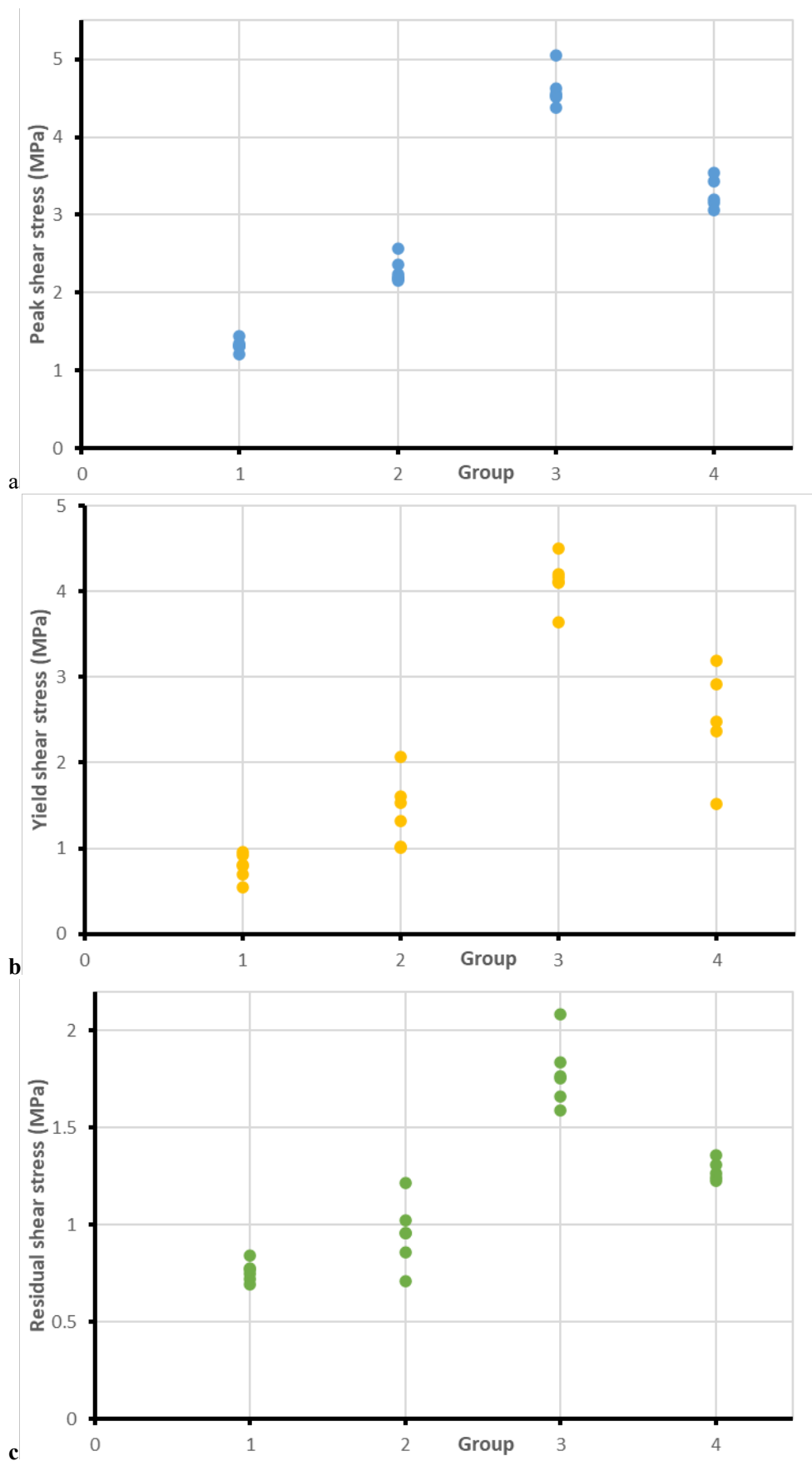
Similar results are seen for both RMS roughness (Figure 3-8b) and peak-to-valley height (Figure 3-8c). Therefore, the groupings of samples show distinctly different fracture characteristics. Figure 3-9 shows that fracture characteristics is dependent on dry density, with roughness (Figure 3-9a) and peak-to-valley height (Figure 3-9b) both increasing linearly for increasing dry density, albeit with scatter from the general trend. This shows that not only are higher dry-density samples mechanically stronger and stiffer in shear, they result in more rough shear fractures.

Figure 3-10a shows the results for lightness (*L*) versus dry density, as measured by the colorimeter. This shows that higher dry density results in higher *L* and that once sheared, lightness reduces. Water content has a linear influence on lightness, with increasing water content reducing lightness (Figure 3-10b). Figure 3-10c shows that a logarithmic relationship is seen between lightness and moisture content. Therefore, this suggests that lightness is both influenced by dry density (amount of clay) and moisture content (amount of water).

**Table 3-4. Mechanical results of all tests conducted**

BGS Sample name	SKB Sample name	Normal load (MPa)	$\pm$	Peak shear stress (MPa)	Yield shear stress (MPa)	Residual shear stress (MPa)	Shear modulus (MPa)	Displacement at peak ( $\mu\text{m}$ )	Maximum displacement ( $\mu\text{m}$ )
FPR-24-218	DH2:R9:200:575-BGS	4.560	0.001	1.438	0.915	0.844	65.5	2260	5573
FPR-24-222	DH2:R9:200:625-BGS	4.656	0.001	1.319	0.955	0.719	57.6	2012	6316
FPR-24-226	DH2:R9:200:675-BGS	4.676	0.001	1.301	0.547	0.748	77.2	2198	5624
FPR-24-231	DH2:R9:200:725-BGS	4.700	0.001	1.317	0.793	0.770	70.6	2064	5397
FPR-24-234	DH2:R9:200:775-BGS	4.667	0.001	1.347	0.700	0.774	80.4	1868	4974
FPR-24-238	DH2:R9:200:825-BGS	4.684	0.001	1.204	0.808	0.695	64.2	1548	5573
FPR-24-242	DH3:R9:200:575-BGS	4.681	0.000	2.234	2.064	0.959	74.2	1940	6481
FPR-24-246	DH3:R9:200:625-BGS	4.677	0.001	2.176	1.024	0.959	143.4	1785	5955
FPR-24-250	DH3:R9:200:675-BGS	4.684	0.001	2.153	1.320	0.859	118.3	1682	5594
FPR-24-251	DH3:R9:200:675-BGS	2.255	0.002	2.192	1.011	0.712	128.6	2131	5587
FPR-24-254	DH3:R9:200:725-BGS	4.657	0.001	2.361	1.602	1.024	141.9	1754	5563
FPR-24-258	DH3:R9:200:775-BGS	4.656	0.001	2.572	1.530	1.213	133.7	2116	5594
FPR-24-262	DH4:R2:290:575-BGS	4.704	0.004	4.553	4.165	1.591	229.6	1517	5532
FPR-24-266	DH4:R2:290:625-BGS	4.695	0.003	4.530	4.116	1.660	214.7	2002	5573
FPR-24-267	DH4:R2:290:625-BGS	4.711	0.003	4.629	3.644	2.082	230.0	2162	3147
FPR-24-271	DH4:R2:290:675-BGS	4.809	0.008	4.382	4.105	1.838	217.8	1892	5659
FPR-24-274	DH4:R2:290:725-BGS	4.771	0.003	5.047	4.495	1.756	260.5	2198	5563
FPR-24-277	DH4:R2:290:775-BGS	4.695	0.003	4.510	4.206	1.762	240.9	2095	5913
FPR-24-282	DH4:R6:290:575-BGS	4.686	0.005	3.431	3.189	1.244	132.0	2405	5552
FPR-24-285	DH4:R6:290:625-BGS	4.700	0.002	3.200	2.918	1.266	133.6	2023	7038
FPR-24-290	DH4:R6:290:675-BGS	4.673	0.003	3.152	1.513	1.224	171.0	2353	5563
FPR-24-294	DH4:R6:290:725-BGS	4.682	0.004	3.540	2.362	1.357	142.7	2663	5614
FPR-24-297	DH4:R6:290:775-BGS	4.686	0.002	3.067	2.480	1.308	126.8	2436	5170





**Figure 3-5.** Shear results for all tests conducted. Group 1 = DH2:R9; Group 2 = DH3:R9; Group 3 = DH4:R2; Group 4 = DH4:R6. a) Peak shear stress; b) Yield shear stress; c) Residual shear stress.

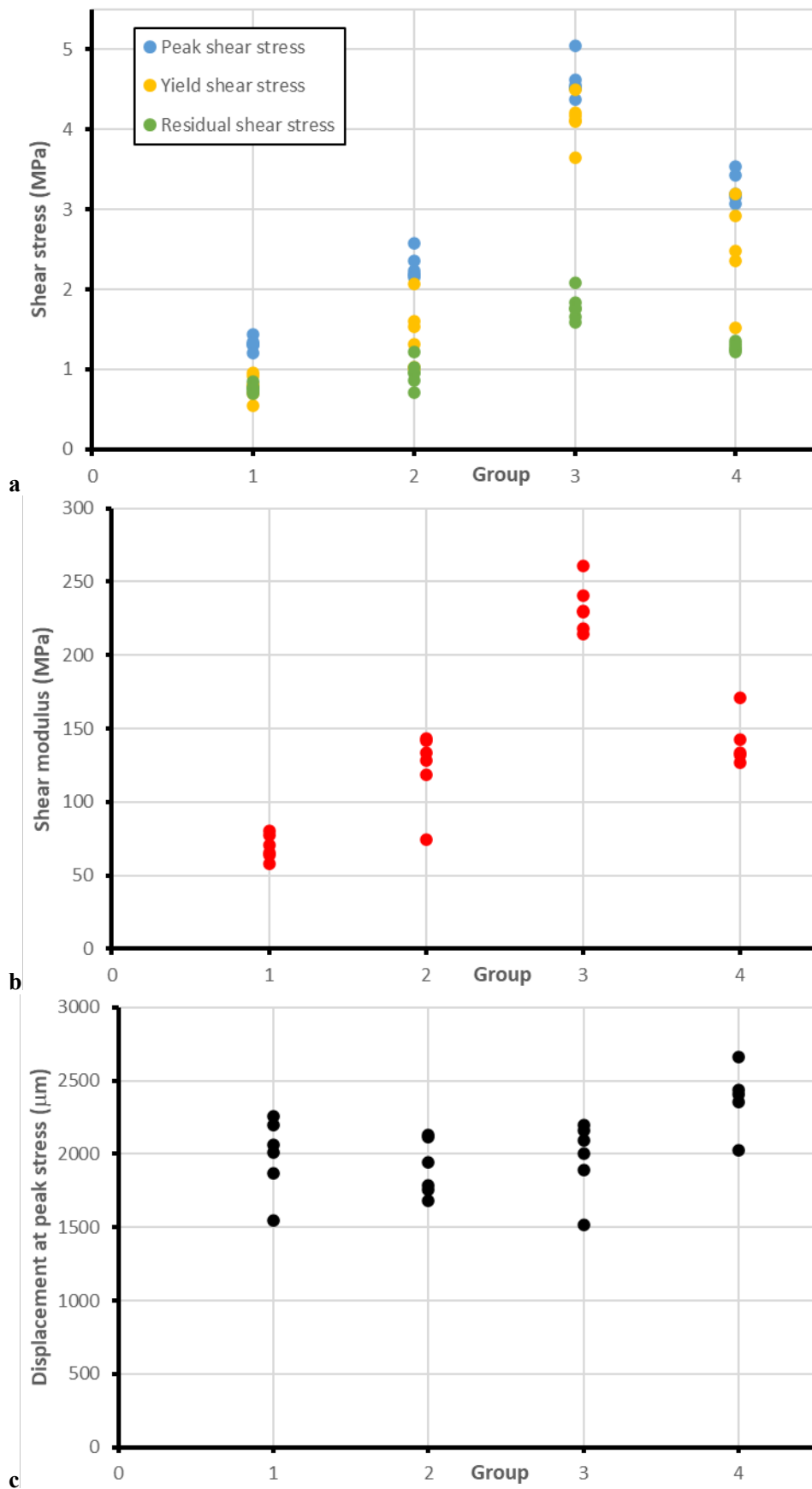


**Figure 3-6.** Shear results for all tests conducted. Group 1 = DH2:R9; Group 2 = DH3:R9; Group 3 = DH4:R2; Group 4 = DH4:R6. a) Shear stress; b) Shear modulus; c) Displacement at peak stress.

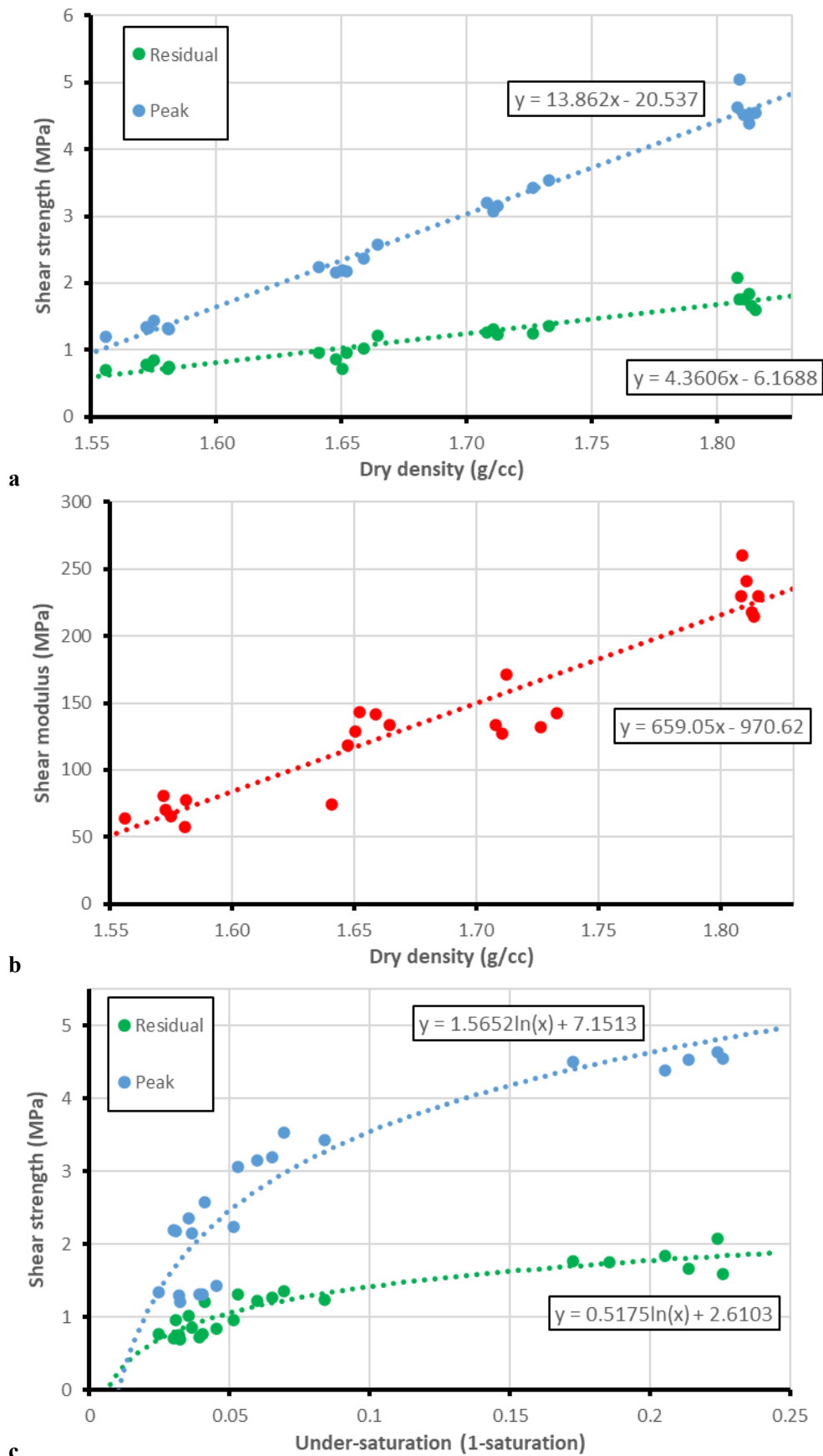


**Figure 3-7.** Shear results for all tests conducted plotted versus dry density or under-saturation. a) Shear strength versus dry density; b) Shear modulus versus dry density; c) Shear strength versus under-saturation (1-saturation).

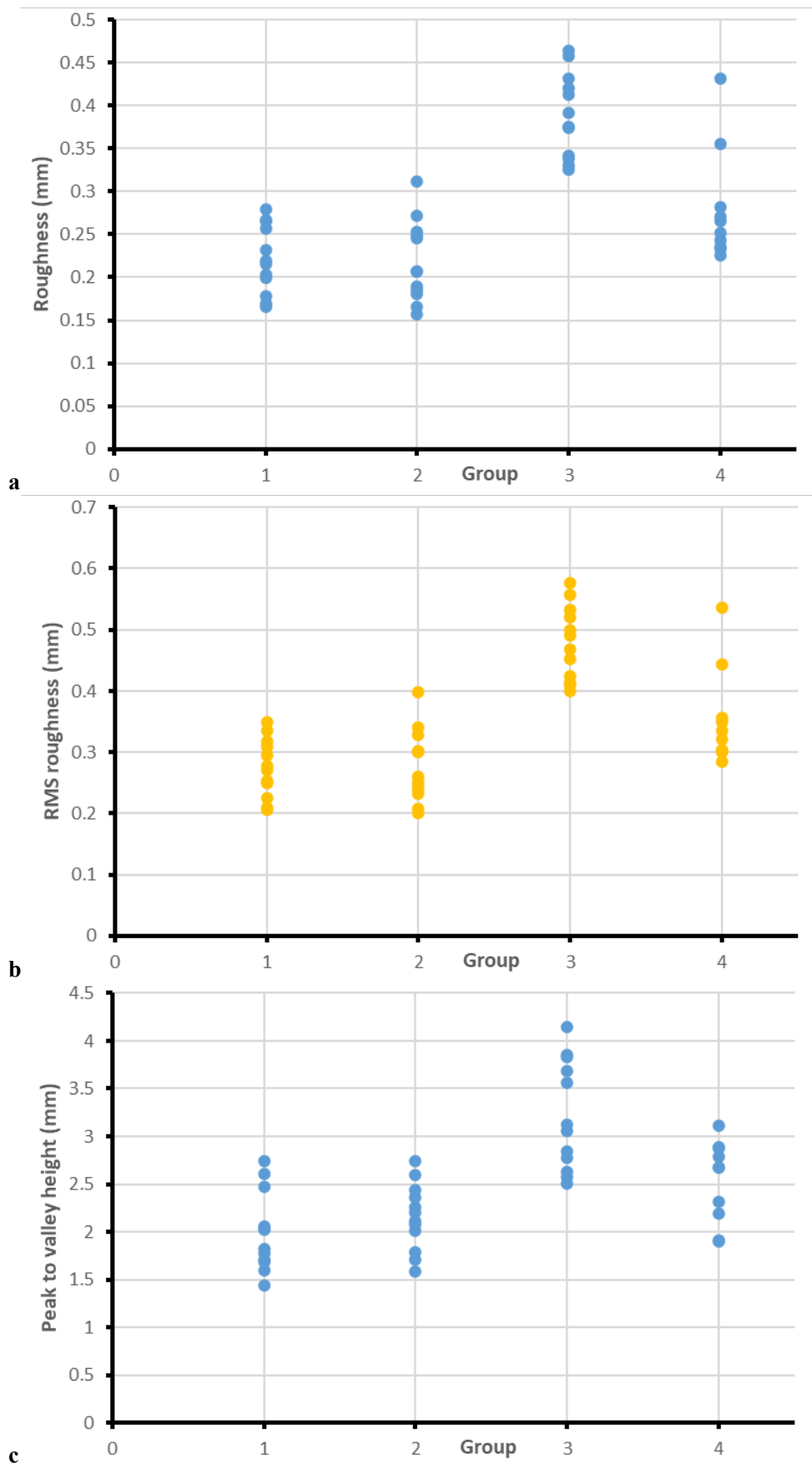
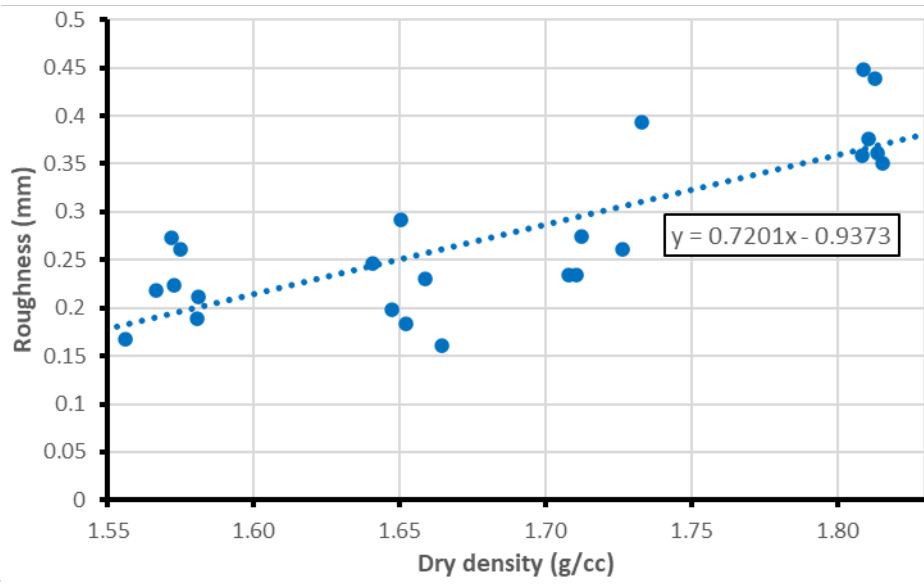
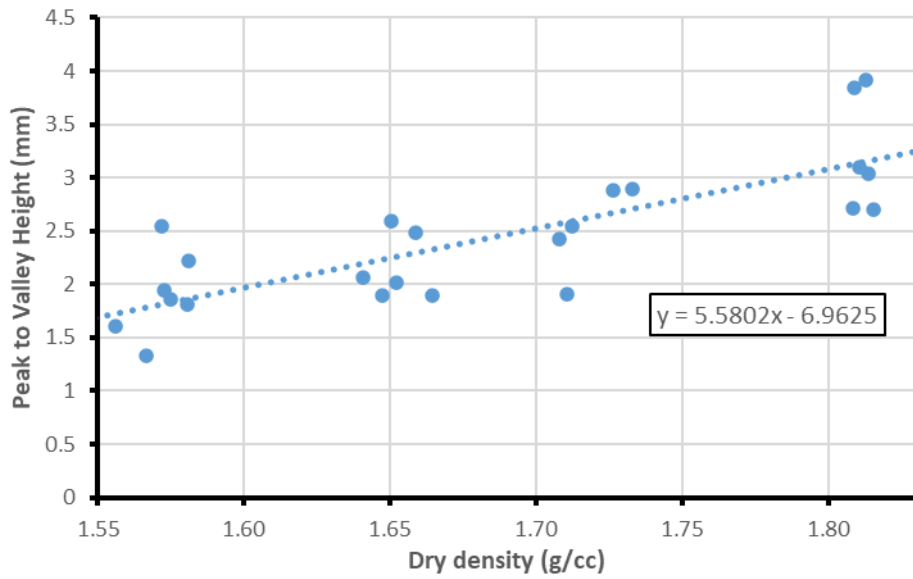


**Figure 3-8.** Fracture surface characteristics for all tests conducted. Group 1 = DH2:R9; Group 2 = DH3:R9; Group 3 = DH4:R2; Group 4 = DH4:R6. a) Fracture roughness; b) RMS roughness; c) Peak-to-valley height.



a



b

**Figure 3-9.** Fracture surface characteristics for all tests conducted plotted versus dry density. a) Roughness; b) Peak to Valley Height.

**Table 3-5. Fracture surface analysis. Note: RAW refers to analysis on scan data as taken; SURF refers to analysis after a polynomial surface has been removed;  $s_a$  is roughness average,  $s_q$  is RMS roughness, and  $s_t$  is peak to valley height**

BGS NO.	FRACTURE SURFACE	SKB SAMPLE NO.	RAW			SURF		
			$s_a$	$s_q$	$s_t$	$s_a$	$s_q$	$s_t$
FPR-24-218	Bottom	DH2:R9:200: 575-BGS	1.039	1.207	5.115	0.257	0.309	2.025
	Top		1.845	2.13	7.398	0.265	0.317	1.689
FPR-24-222	Bottom	DH2:R9:200: 625-BGS	0.465	0.57	3.421	0.199	0.253	2.034
	Top		1.127	1.323	5.51	0.178	0.225	1.594
FPR-24-226	Bottom	DH2:R9:200: 675-BGS	0.343	0.427	2.403	0.203	0.25	2.736
	Top		0.393	0.486	2.985	0.219	0.271	1.703
FPR-24-231	Bottom	DH2:R9:200: 725-BGS	0.553	0.683	3.691	0.232	0.295	1.818
	Top		0.571	0.701	4.015	0.215	0.277	2.058
FPR-24-234	Bottom	DH2:R9:200: 775-BGS	0.656	0.774	3.516	0.267	0.335	2.612
	Top		0.638	0.759	4.007	0.279	0.35	2.477
FPR-24-238	Bottom	DH2:R9:200: 825-BGS	0.493	0.59	2.976	0.166	0.206	1.44
	Top		1.087	1.291	5.51	0.169	0.209	1.774
FPR-24-242	Bottom	DH3:R9:200: 575-BGS	0.399	0.521	3.423	0.245	0.3	2.117
	Top		1.12	1.32	5.438	0.248	0.302	2.015
FPR-24-246	Bottom	DH3:R9:200: 625-BGS	0.746	0.898	4.348	0.18	0.24	2.253
	Top		0.842	1.053	5.351	0.186	0.247	1.783
FPR-24-250	Bottom	DH3:R9:200: 675-BGS	0.53	0.685	4.177	0.207	0.252	2.208
	Top		0.892	1.038	4.626	0.189	0.232	1.581
FPR-24-251	Bottom	DH3:R9:200: 675-BGS	0.824	1.041	5.222	0.312	0.398	2.745
	Top		0.693	0.866	4.527	0.272	0.341	2.443
FPR-24-254	Bottom	DH3:R9:200: 725-BGS	0.626	0.758	3.726	0.253	0.328	2.599
	Top		1.067	1.251	5.611	0.207	0.26	2.361
FPR-24-258	Bottom	DH3:R9:200: 775-BGS	1.059	1.242	5.347	0.157	0.2	2.079
	Top		0.866	1.035	4.402	0.165	0.207	1.703
FPR-24-262	Bottom	DH4:R2:290: 575-BGS	1.075	1.314	5.188	0.325	0.4	2.773
	Top		1.344	1.551	6.056	0.375	0.452	2.633
FPR-24-266	Bottom	DH4:R2:290: 625-BGS	0.814	0.967	4.775	0.392	0.49	3.565
	Top		1.516	1.751	7.53	0.33	0.411	2.511
FPR-24-267	Bottom	DH4:R2:290: 625-BGS	0.715	0.91	5.047	0.374	0.468	2.847
	Top		0.6	0.743	4.349	0.342	0.424	2.57
FPR-24-271	Bottom	DH4:R2:290: 675-BGS	1.438	1.671	8.109	0.42	0.52	4.146
	Top		1.178	1.37	6.287	0.458	0.557	3.686
FPR-24-274	Bottom	DH4:R2:290: 725-BGS	0.62	0.804	5.403	0.464	0.577	3.832
	Top		0.814	1.023	5.284	0.431	0.532	3.855
FPR-24-277	Bottom	DH4:R2:290: 775-BGS	1.138	1.434	6.217	0.413	0.5	3.061
	Top		0.741	0.924	4.575	0.338	0.414	3.129
FPR-24-282	Bottom	DH4:R6:290: 575-BGS	0.992	1.239	5.407	0.271	0.35	2.89
	Top		1.241	1.409	5.536	0.252	0.321	2.877
FPR-24-285	Bottom	DH4:R6:290: 625-BGS	1.632	1.793	6.097	0.243	0.303	2.672
	Top		1.082	1.276	5.074	0.226	0.285	2.188
FPR-24-290	Bottom	DH4:R6:290: 675-BGS	0.667	0.799	3.99	0.282	0.357	2.787
	Top		0.481	0.591	3.445	0.266	0.336	2.314
FPR-24-294	Bottom	DH4:R6:290: 725-BGS	0.952	1.164	5.375	0.432	0.537	3.111
	Top		0.651	0.789	3.348	0.355	0.444	2.679
FPR-24-297	Bottom	DH4:R6:290: 775-BGS	0.667	0.803	3.835	0.236	0.302	1.915
	Top		0.695	0.842	4.087	0.233	0.3	1.898

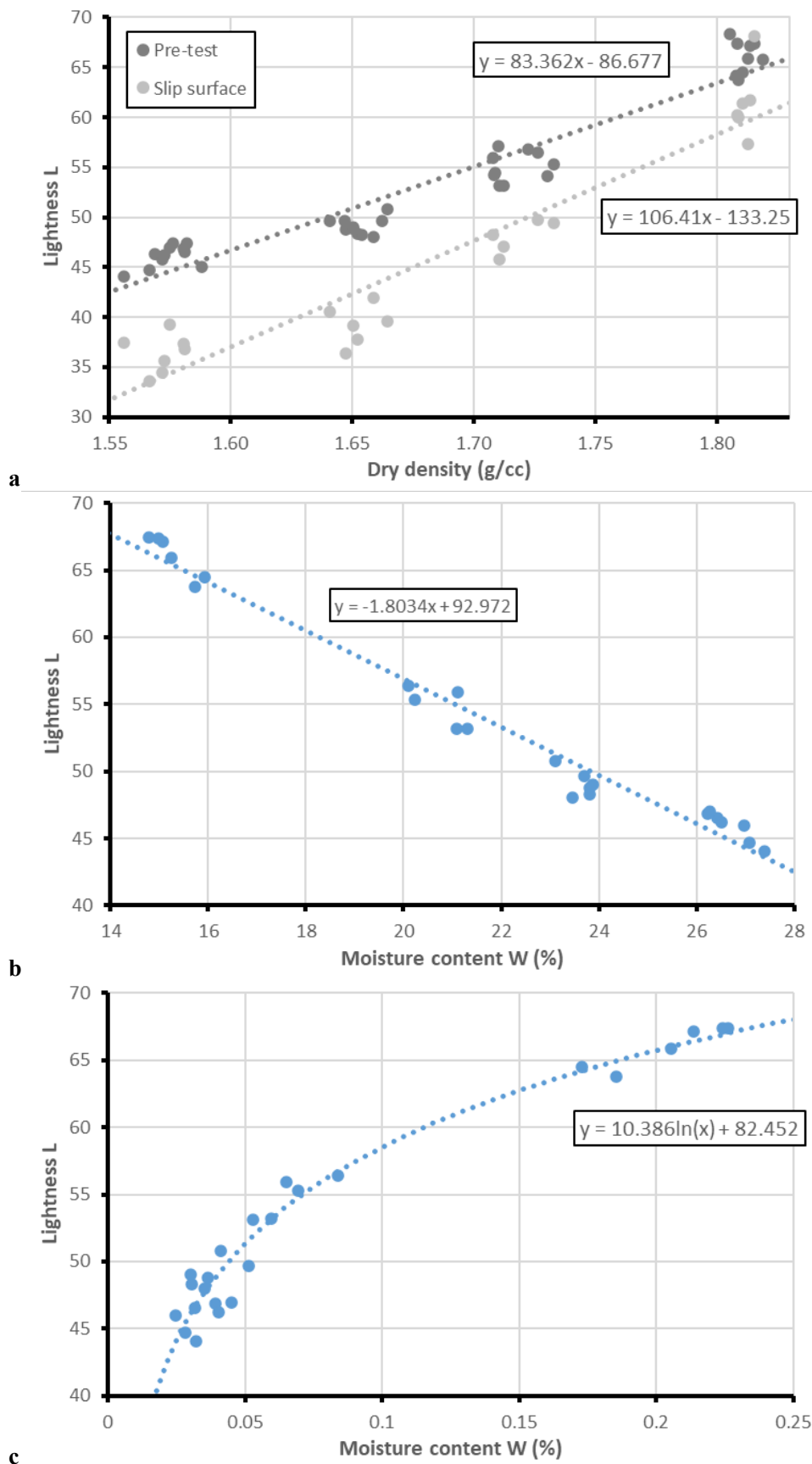


**Figure 3-10.** Lightness of the sample versus dry density for the starting material and the slip surface post-shear testing. a) Comparison of relationship of lightness with dry density for starting and sheared samples; b) Lightness versus moisture content; c) Lightness versus moisture content.

## 4 Conclusions

A study has been conducted to determine the shear properties of pre-compacted MX-80 cores from the Prototype Repository (PRP) experiment under direct shear. A bespoke shear apparatus was used to conduct constant shear rate experiments that lasted approximately 2 hours each. A total of 23 experiments were conducted, including a repeatability test and a test conducted at half normal load to investigate the normal load dependence of MX-80 from the PRP test. The samples provided were members of four groups. Considerable differences were seen between the dry density and moisture contents of the four groups. However, examining shear properties as a function of dry density showed that strength and stiffness increased linearly with dry density. In addition, a secondary control on shear properties was found related to the saturation of the samples. An average reduction of 9.1 % of moisture content was seen in the samples between coring the PRP experiment and arrival at BGS Keyworth. This will have resulted in the increase in shear strength and stiffness, as a dried sample is more brittle than a fully saturated one. The relationship found between saturation and shear properties means that data from this study could be corrected for loss of moisture. In general, the drying of the samples will not have significantly altered the findings of this report.



## References

- ASTM Standard, 2009.** Standard guide for assessment of surface texture of non-porous biomaterials in two dimensions. F2791-09.
- Cuss R J, Harrington J F, 2016.** An experimental study of the potential for fault reactivation during changes in gas and porewater pressure. *International Journal of Greenhouse Gas Control*, 53, pp.41-55. DOI: 10.1016/j.ijggc.2016.07.028
- Cuss R J, Milodowski A, Harrington J F, 2011.** Fracture transmissivity as a function of normal and shear stress: first results in Opalinus clay. *Physics and Chemistry of the Earth*. 36, pp.1960-1971. DOI: 10.1016/j.pce.2011.07.080
- Cuss R J, Harrington J F, Sathar S, Norris S, 2015.** An experimental study of the flow of gas along faults of varying orientation to the stress-field; Implications for performance assessment of radioactive waste disposal. *Journal of Geophysical Research – Solid Earth*. 120, pp.3932-3945, doi:10.1002/2014JB011333
- Cuss R J, Harrington J F, Sathar S, Norris S, Talandier J, 2017.** The role of the stress-path and importance of stress history on the flow of water along faults; an experimental study. *Applied Clay Science*, 150, pp.282-292, <https://dx.doi.org/10.1016/j.clay.2017.09.029>
- Cuss R J, Wiseall A C, Dobbs M R, Parkes D, Harrington J F, Talandier J, Bourbon X, 2018a.** Experiments on interface processes at the cement/Callovo-Oxfordian Claystone interface and the impact on physical properties; Mechanical and flow properties of fresh interfaces. Proceedings of the 3<sup>rd</sup> Annual Workshop of the CEBAMA Project, Nantes, France, 17<sup>th</sup>-18<sup>th</sup> April, 2018. 10pp.
- Cuss R J, Wiseall A C, Tamayo-Mas E, Harrington J F 2018b.** An experimental study of the influence of stress history on fault slip during injection of supercritical CO<sub>2</sub>. *Journal of Structural Geology*, 109, pp.86-98. <https://doi.org/10.1016/j.jsg.2018.01.006>
- Cuss R J, Wiseall A C, Harrington J F, Talandier J, Bourbon X, 2019.** Experiments on interface processes at the cement/Callovo-Oxfordian claystone interface and the impact on physical properties; mechanical results from the Callovo-Oxfordian claystone. In *Proceedings of the Second Workshop of the HORIZON 2020 CEBAMA Project (KIT Scientific Reports; 7752)* (Vol. 7752, p. 41). KIT Scientific Publishing.
- Cuss R J, Wiseall A C, Holyoake S, Harrington J F, Sellin P, 2022.** The strength of pre-compacted MX-80 bentonite in direct shear. British Geological Survey Commissioned Report, CR/23/061. 97pp.
- Cuss R J, Wiseall A C, Harrington J F, 2024.** Self-sealing potential of fractures as a result of hydration, shear, and temperature. 9th International Conference on Clays in Natural and Engineered Barriers for Radioactive Waste Confinement, Hannover, Germany.
- Harrington J F, Cuss R J, Wiseall A C, Daniels K A, Graham C C, Tamayo-Mas E, 2017.** Scoping study examining the behaviour of Boom Clay at disposal depths investigated in OPERA. OPERA-PU-BGS523&616.
- Wiseall A C, Cuss R J, Hough E, Kemp S J, 2018.** The role of fault gouge properties on fault reactivation during hydraulic stimulation; an experimental study using analogue faults. *Journal of Natural Gas Science and Engineering*, 59, pp.21-34 <https://doi.org/10.1016/j.jngse.2018.08.021>

# Appendix – results for each shear test conducted

FPR-24-218

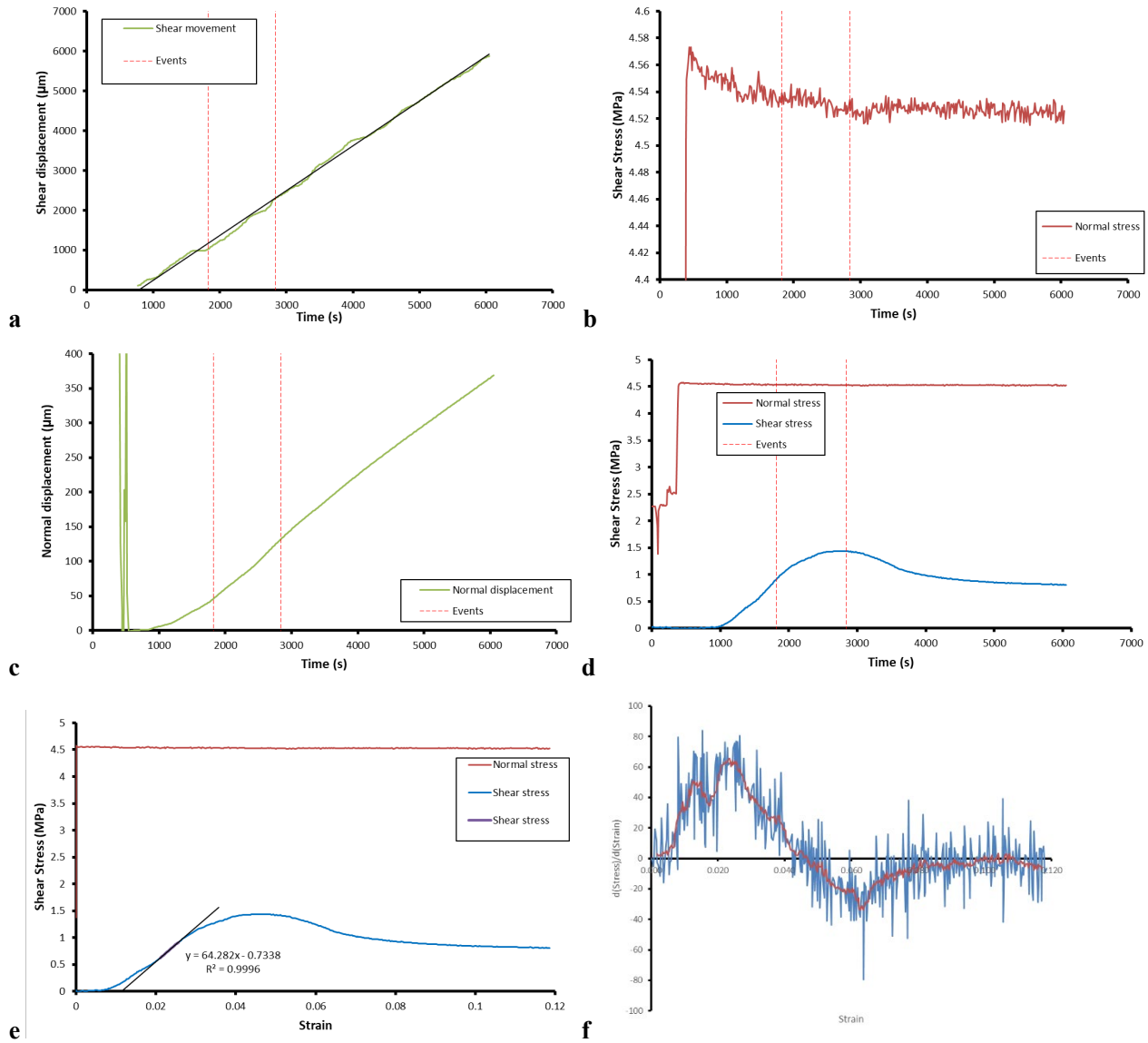


**Figure A-1.** Shear results for test FPR-24-218 (DH2:R9:200:575-BGS). a) Displacement with time; b) Normal load with time; c) Normal displacement with time; d) Normal and shear stress with time; e) Stress vs strain; f) Gradient of stress/strain (shear modulus).

**FPR-24-218**

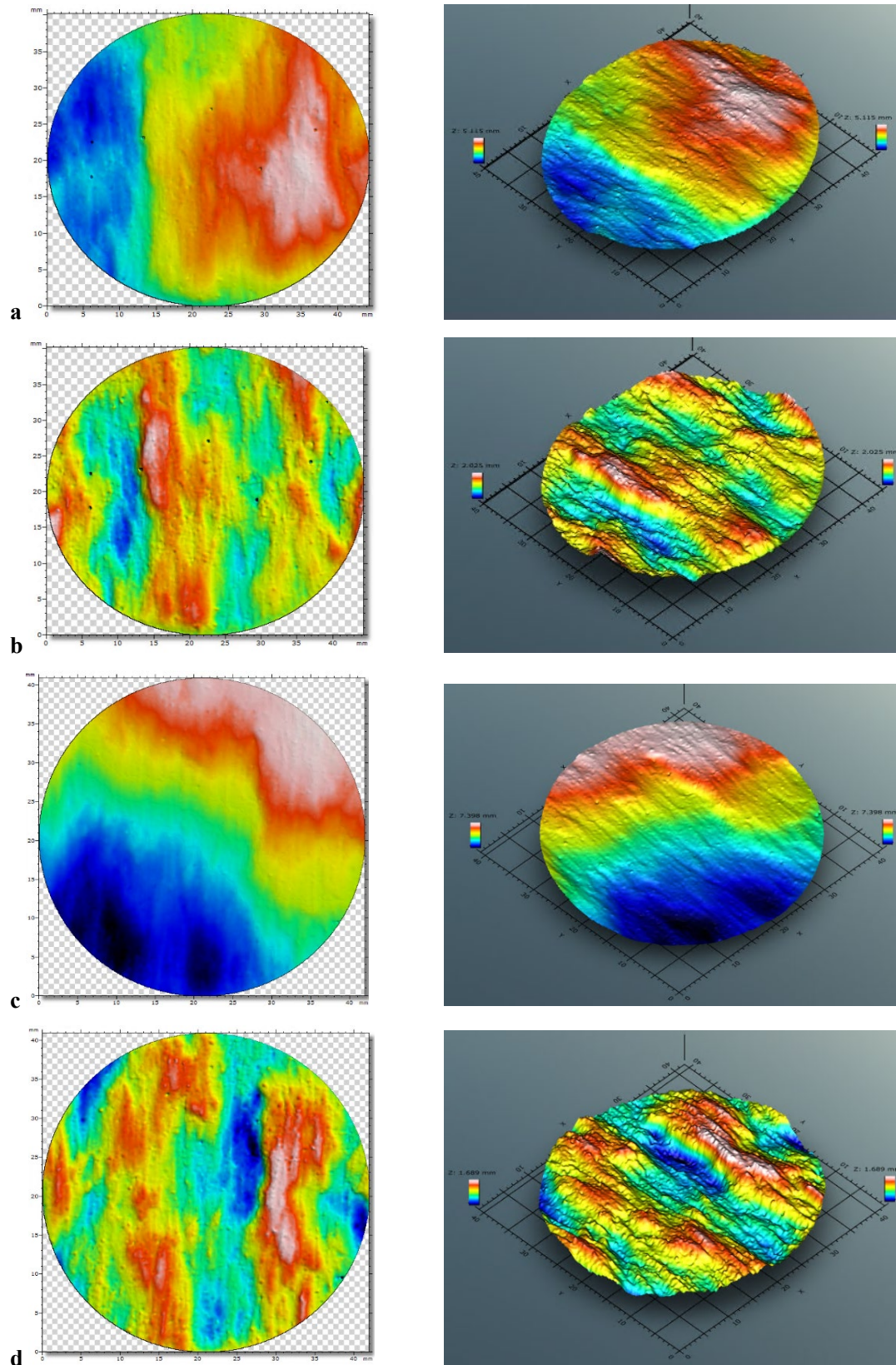


**Figure A-2.** Laser scan of shear fracture FPR-24-218 (DH2:R9:200:575-BGS). *a)* Bottom surface raw scan; *b)* Bottom surface with form removed; *c)* Top surface raw scan; *d)* Top surface with form removed. Shear direction is parallel with Y-axis, i.e. top-to-bottom in left.

**FPR-24-218****Table A-1. Results for test FPR-24-218 (DH2:R9:200:575-BGS)**

Parameter	Value	±	Units
SKB Sample name	DH2:R9:200:575-BGS		
BGS Sample name	FPR-24-218		
Normal load	4.560	0.001	MPa
Peak shear stress	1.438		MPa
Yield shear stress	0.915		MPa
Residual shear stress	0.844		MPa
Shear modulus	65.5		MPa
Displacement at peak	2260		µm
Maximum displacement	5573		µm
Displacement rate	1.032		µm/s
Sample diameter	47.04	0.10	mm
Sample height	52.84	0.03	mm
Sample weight	182.59		g
Bulk density	2.09		g/cm <sup>3</sup>
Sample colour	65.91,-5.62,6.90		L, a, b
Colour of bottom slip plane	57.36,-5.11,7.12		L, a, b
Weight of bottom sample	93.577		g
Weight after drying	81.197		g
Moisture content	13.2		%
Bottom: Raw: $s_a$	1.039		mm
Bottom: Raw: $s_q$	1.207		mm
Bottom: Raw: $s_t$	5.115		mm
Top: Raw: $s_a$	1.845		mm
Top: Raw: $s_q$	2.13		mm
Top: Raw: $s_t$	7.398		mm
Bottom: Surf: $s_a$	0.257		mm
Bottom: Surf: $s_q$	0.309		mm
Bottom: Surf: $s_t$	2.025		mm
Top: Surf: $s_a$	0.265		mm
Top: Surf: $s_q$	0.317		mm
Top: Surf: $s_t$	1.689		mm

# FPR-24-222

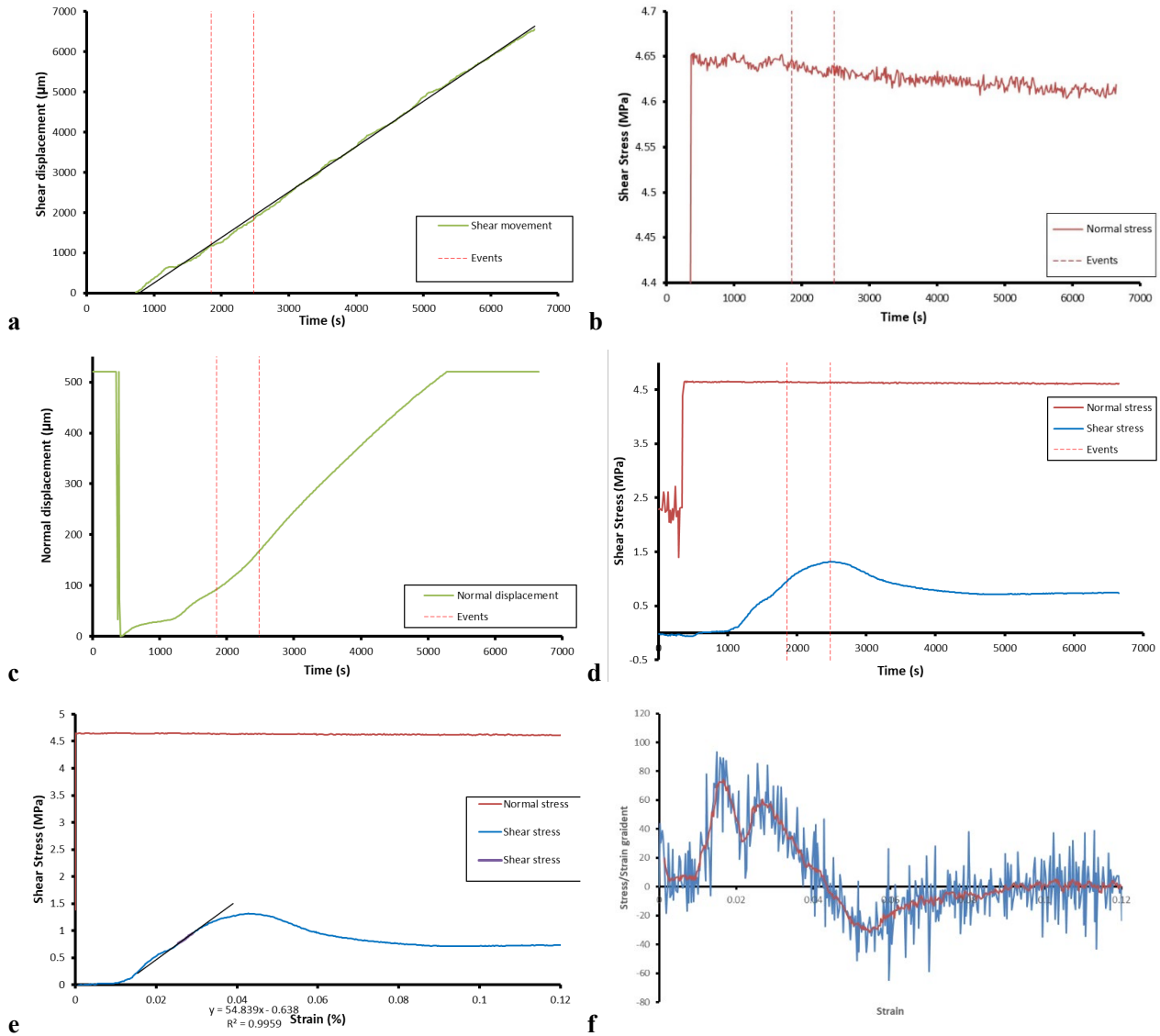


**Figure A-3.** Shear results for test FPR-24-222 (DH2:R9:200:625-BGS). a) Displacement with time; b) Normal load with time; c) Normal displacement with time; d) Normal and shear stress with time; e) Stress vs strain; f) Gradient of stress/strain (shear modulus).



# **FPR-24-222**

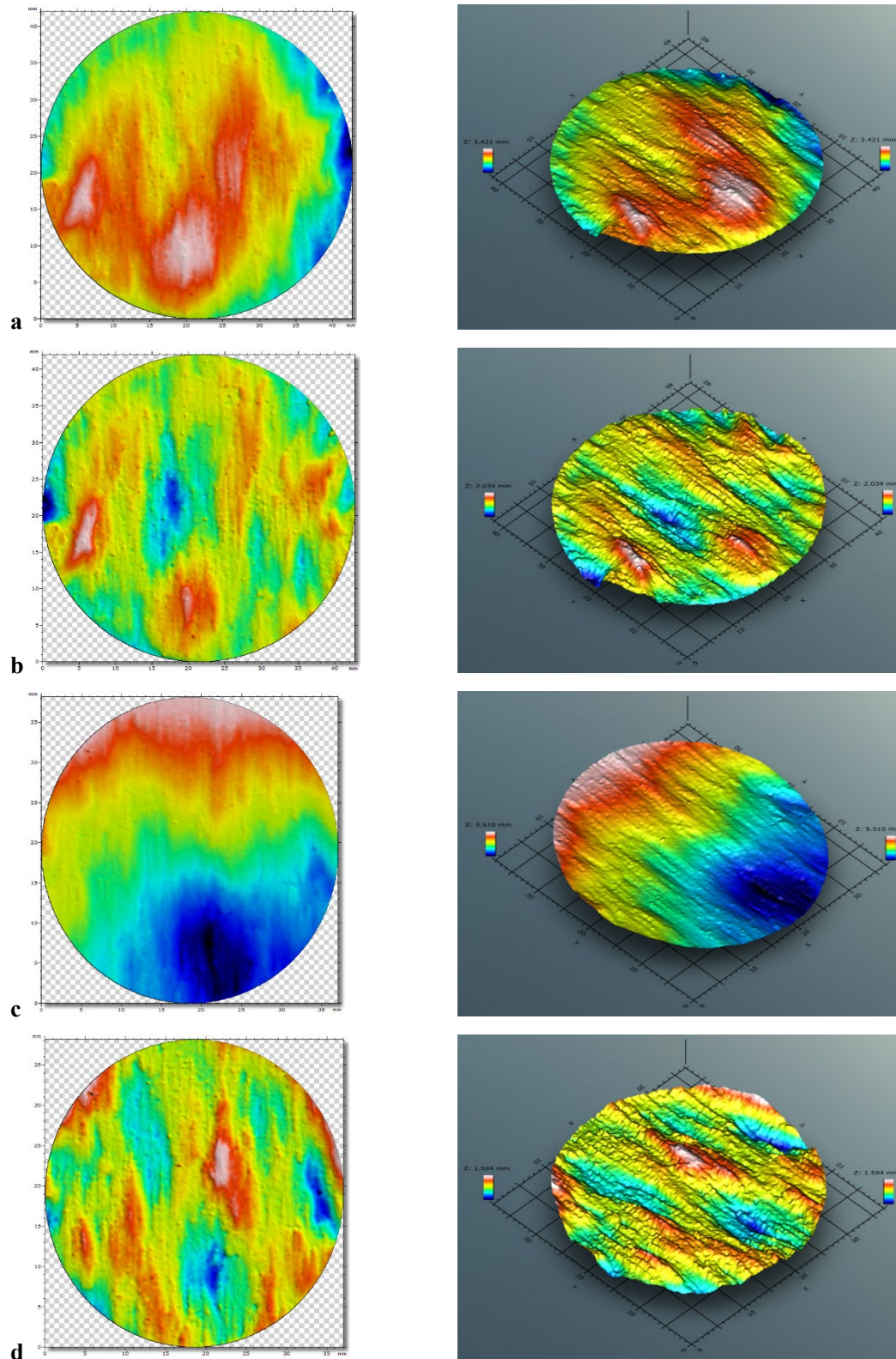


**Figure A-4.** Laser scan of shear fracture FPR-24-222 (DH2:R9:200:625-BGS). a) Bottom surface raw scan; b) Bottom surface with form removed; c) Top surface raw scan; d) Top surface with form removed. Shear direction is parallel with Y-axis, i.e. top-to-bottom in left.

**FPR-24-222****Table A-2. Results for test FPR-24-222 (DH2:R9:200:625-BGS)**

Parameter	Value	±	Units
SKB Sample name	DH2:R9:200:625-BGS		
BGS Sample name	FPR-24-222		
Normal load	4.656	0.001	MPa
Peak shear stress	1.319		MPa
Yield shear stress	0.955		MPa
Residual shear stress	0.719		MPa
Shear modulus	57.6		MPa
Displacement at peak	2012		µm
Maximum displacement	6316		µm
Displacement rate	1.032		µm/s
Sample diameter	47.12	0.10	mm
Sample height	52.88	0.01	mm
Sample weight	183.75		g
Bulk density	2.00		g/cm <sup>3</sup>
Sample colour	46.88,-5.81,7.60		L, a, b
Colour of bottom slip plane	37.38,-7.05,7.34		L, a, b
Weight of bottom sample	95.592		g
Weight after drying	75.730		g
Moisture content	20.8		%
Bottom: Raw: $s_a$	0.465		mm
Bottom: Raw: $s_q$	0.57		mm
Bottom: Raw: $s_t$	3.421		mm
Top: Raw: $s_a$	1.127		mm
Top: Raw: $s_q$	1.323		mm
Top: Raw: $s_t$	5.51		mm
Bottom: Surf: $s_a$	0.199		mm
Bottom: Surf: $s_q$	0.253		mm
Bottom: Surf: $s_t$	2.034		mm
Top: Surf: $s_a$	0.178		mm
Top: Surf: $s_q$	0.225		mm
Top: Surf: $s_t$	1.594		mm



# **FPR-24-226**

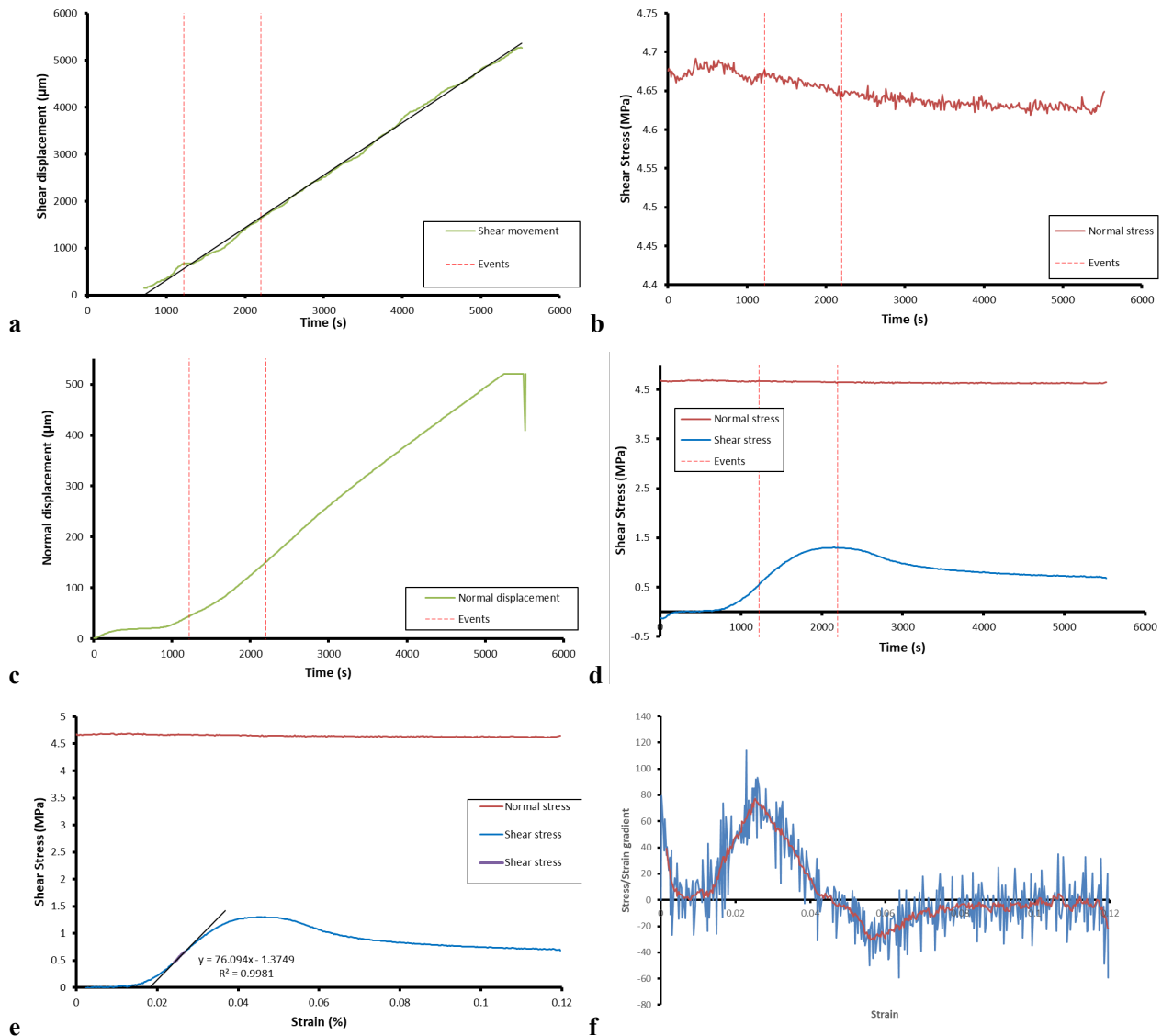


**Figure A-5.** Shear results for test FPR-24-226 (DH2:R9:200:675-BGS). a) Displacement with time; b) Normal load with time; c) Normal displacement with time; d) Normal and shear stress with time; e) Stress vs strain; f) Gradient of stress/strain (shear modulus).

# **FPR-24-226**

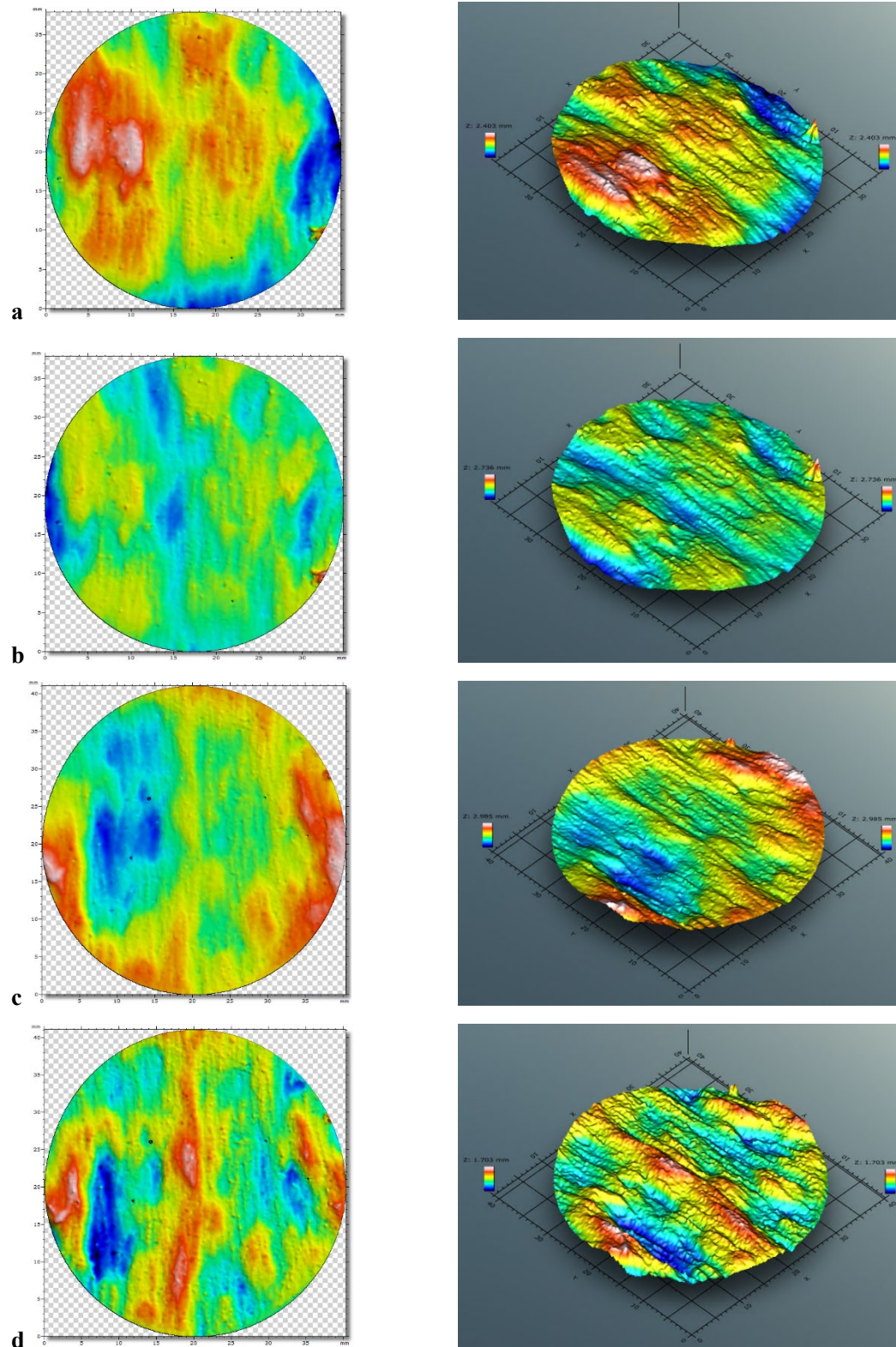


**Figure A-6.** Laser scan of shear fracture FPR-24-226 (DH2:R9:200:675-BGS). *a)* Bottom surface raw scan; *b)* Bottom surface with form removed; *c)* Top surface raw scan; *d)* Top surface with form removed. Shear direction is parallel with Y-axis, i.e. top-to-bottom in left.

**FPR-24-226****Table A-3. Results for test FPR-24-226 (DH2:R9:200:675-BGS)**

Parameter	Value	±	Units
SKB Sample name	DH2:R9:200:675-BGS		
BGS Sample name	FPR-24-226		
Normal load	4.676	0.001	MPa
Peak shear stress	1.301		MPa
Yield shear stress	0.547		MPa
Residual shear stress	0.748		MPa
Shear modulus	77.2		MPa
Displacement at peak	2198		µm
Maximum displacement	5624		µm
Displacement rate	1.032		µm/s
Sample diameter	47.03	0.12	mm
Sample height	51.44	0.03	mm
Sample weight	178.61		g
Bulk density	2.00		g/cm <sup>3</sup>
Sample colour	46.56,-5.87,8.05		L, a, b
Colour of bottom slip plane	36.85,-6.15,7.99		L, a, b
Weight of bottom sample	94.887		g
Weight after drying	75.062		g
Moisture content	20.9		%
Bottom: Raw: $s_a$	0.343		mm
Bottom: Raw: $s_q$	0.427		mm
Bottom: Raw: $s_t$	2.403		mm
Top: Raw: $s_a$	0.393		mm
Top: Raw: $s_q$	0.486		mm
Top: Raw: $s_t$	2.985		mm
Bottom: Surf: $s_a$	0.203		mm
Bottom: Surf: $s_q$	0.25		mm
Bottom: Surf: $s_t$	2.736		mm
Top: Surf: $s_a$	0.219		mm
Top: Surf: $s_q$	0.271		mm
Top: Surf: $s_t$	1.703		mm

# **FPR-24-231**

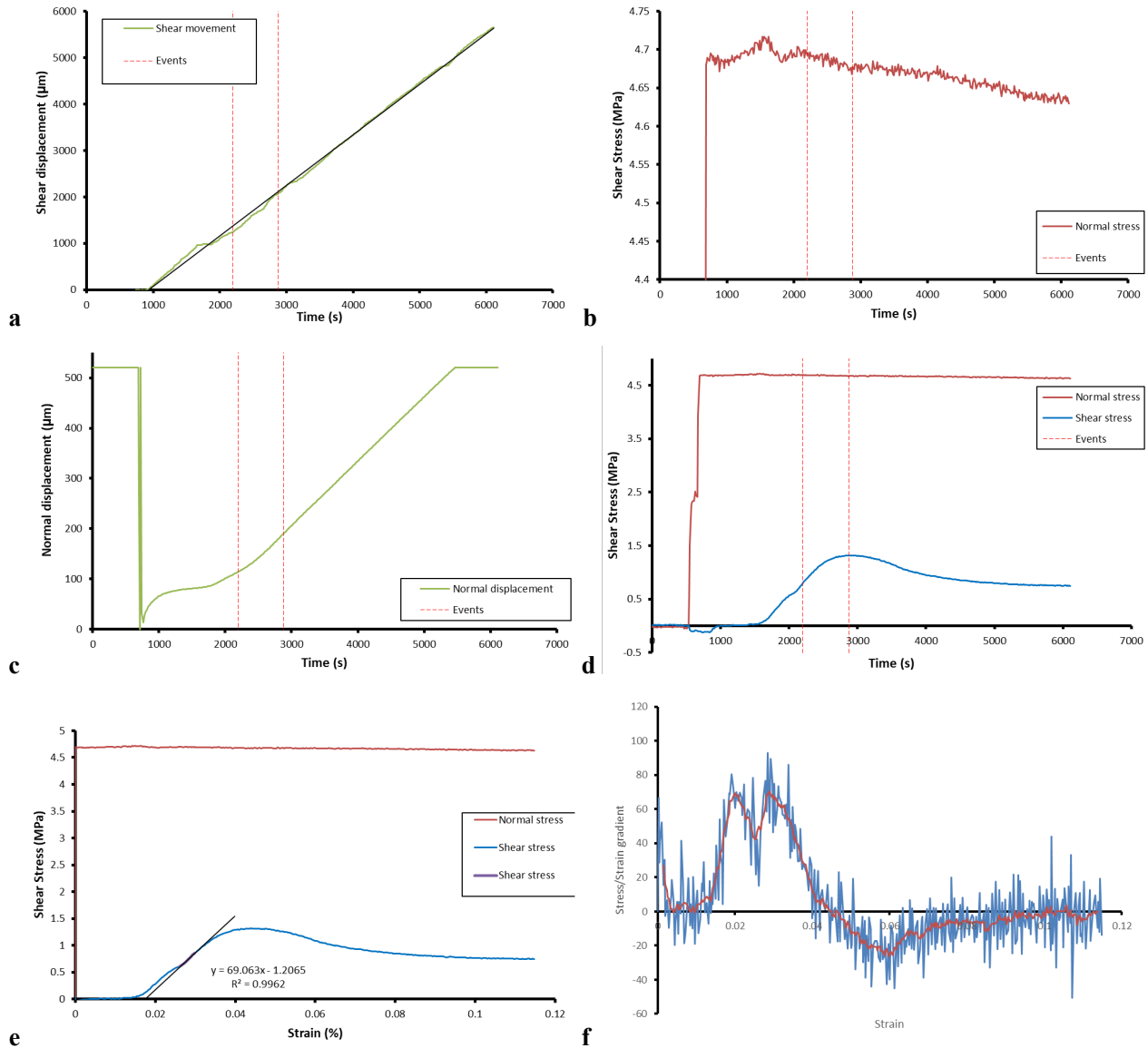


**Figure A-7.** Shear results for test FPR-24-231 (DH2:R9:200:725-BGS). a) Displacement with time; b) Normal load with time; c) Normal displacement with time; d) Normal and shear stress with time; e) Stress vs strain; f) Gradient of stress/strain (shear modulus).



# **FPR-24-231**

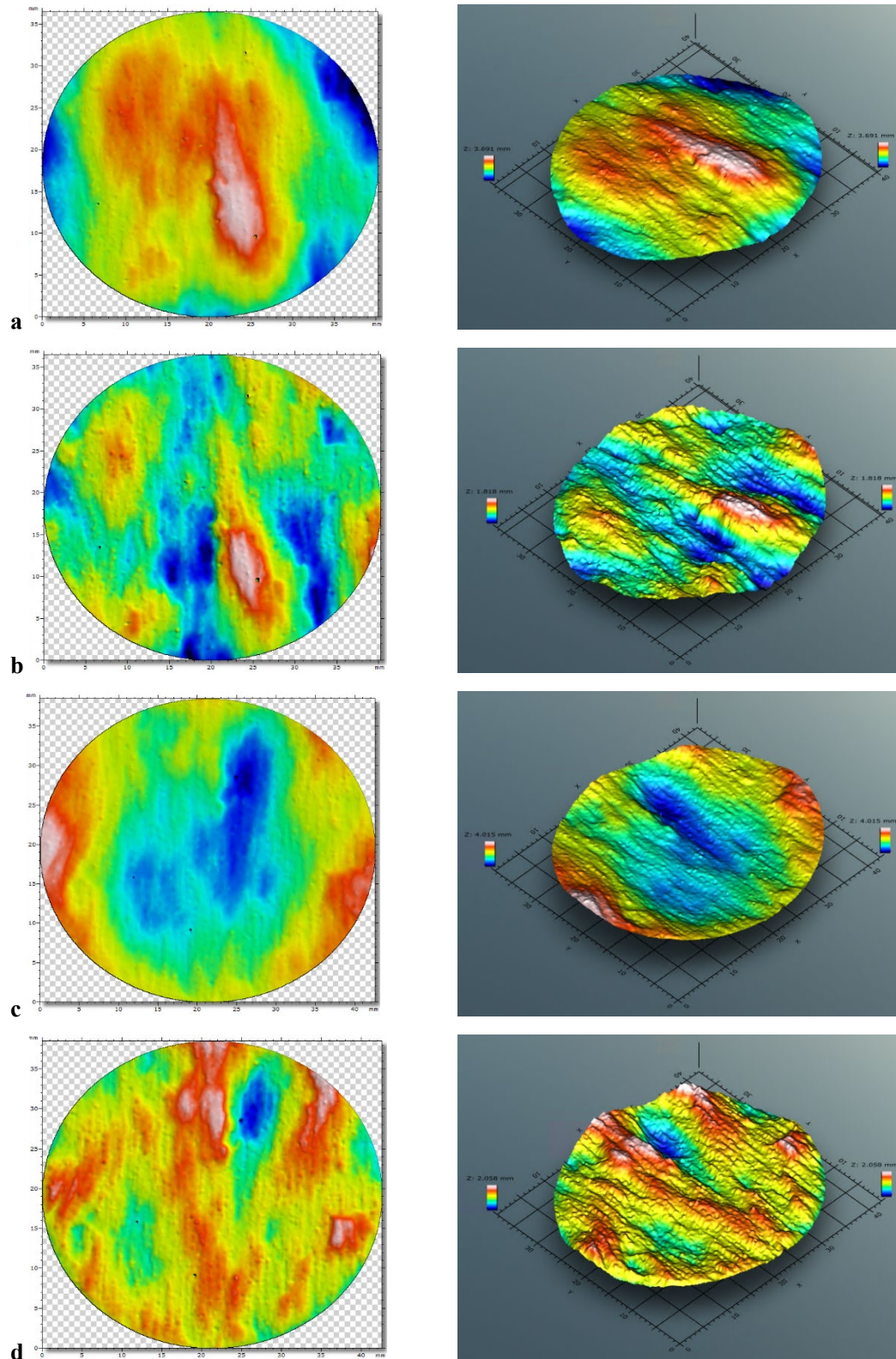


**Figure A-8.** Laser scan of shear fracture FPR-24-231 (DH2:R9:200:725-BGS). *a)* Bottom surface raw scan; *b)* Bottom surface with form removed; *c)* Top surface raw scan; *d)* Top surface with form removed. Shear direction is parallel with Y-axis, i.e. top-to-bottom in left.

**FPR-24-231****Table A-4. Results for test FPR-24-231 (DH2:R9:200:725-BGS)**

Parameter	Value	±	Units
SKB Sample name	DH2:R9:200:725-BGS		
BGS Sample name	FPR-24-231		
Normal load	4.700	0.001	MPa
Peak shear stress	1.317		MPa
Yield shear stress	0.793		MPa
Residual shear stress	0.770		MPa
Shear modulus	70.6		MPa
Displacement at peak	2064		µm
Maximum displacement	5397		µm
Displacement rate	1.032		µm/s
Sample diameter	46.99	0.13	mm
Sample height	53.32	0.01	mm
Sample weight	184.51		g
Bulk density	1.99		g/cm <sup>3</sup>
Sample colour	46.21,-5.91,7.96		L, a, b
Colour of bottom slip plane	35.62,-6.10,7.76		L, a, b
Weight of bottom sample	95.867		g
Weight after drying	75.783		g
Moisture content	20.9		%
Bottom: Raw: $s_a$	0.553		mm
Bottom: Raw: $s_q$	0.683		mm
Bottom: Raw: $s_t$	3.691		mm
Top: Raw: $s_a$	0.571		mm
Top: Raw: $s_q$	0.701		mm
Top: Raw: $s_t$	4.015		mm
Bottom: Surf: $s_a$	0.232		mm
Bottom: Surf: $s_q$	0.295		mm
Bottom: Surf: $s_t$	1.818		mm
Top: Surf: $s_a$	0.215		mm
Top: Surf: $s_q$	0.277		mm
Top: Surf: $s_t$	2.058		mm

# **FPR-24-234**

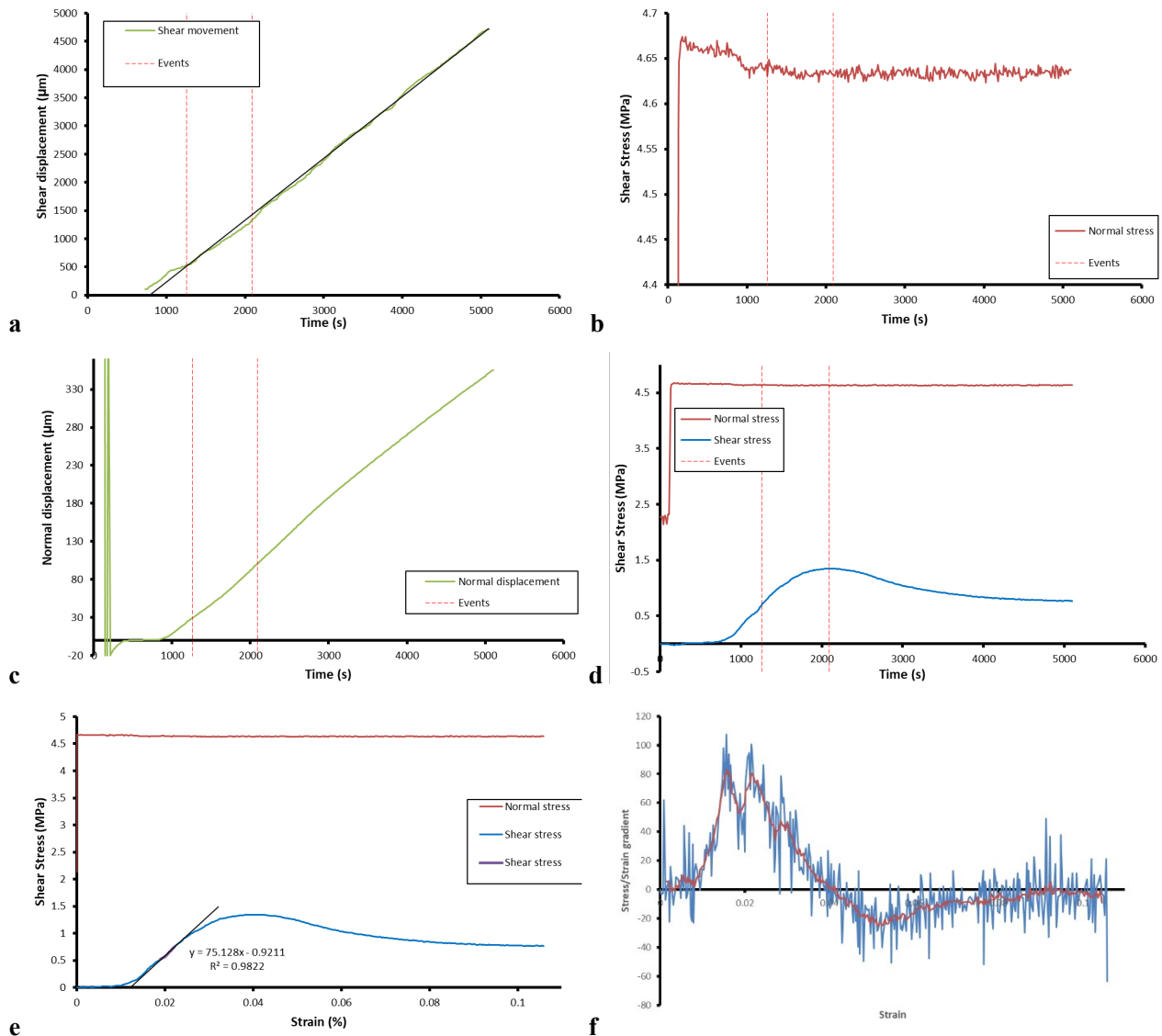


**Figure A-9.** Shear results for test FPR-24-234 (DH2:R9:200:775-BGS). a) Displacement with time; b) Normal load with time; c) Normal displacement with time; d) Normal and shear stress with time; e) Stress vs strain; f) Gradient of stress/strain (shear modulus).



# **FPR-24-234**

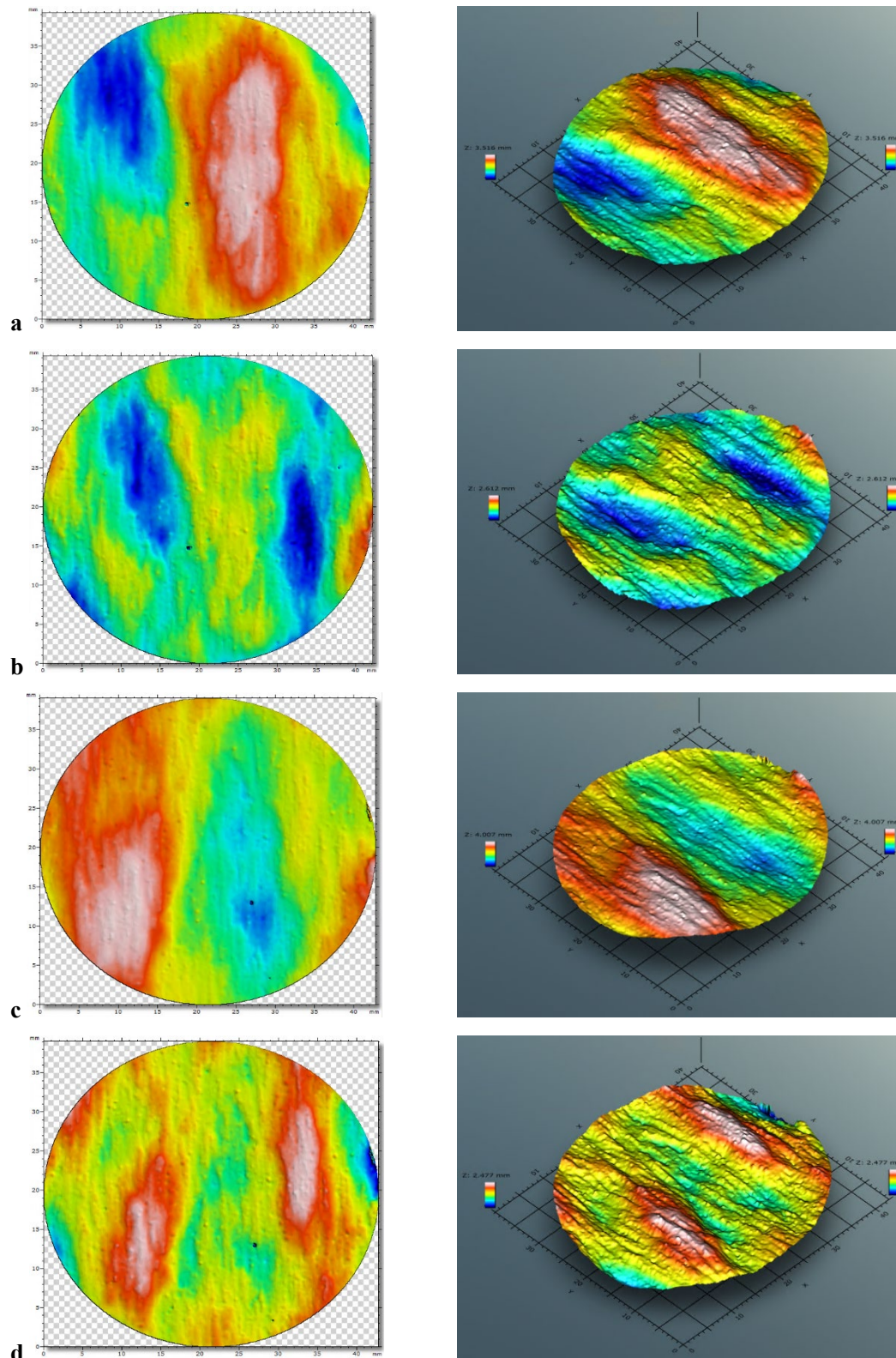


**Figure A-10.** Laser scan of shear fracture FPR-24-234 (DH2:R9:200:775-BGS). a) Bottom surface raw scan; b) Bottom surface with form removed; c) Top surface raw scan; d) Top surface with form removed. Shear direction is parallel with Y-axis, i.e. top-to-bottom in left.

**FPR-24-234****Table A-5. Results for test FPR-24-234 (DH2:R9:200:775-BGS)**

Parameter	Value	±	Units
SKB Sample name	DH2:R9:200:775-BGS		
BGS Sample name	FPR-24-234		
Normal load	4.667	0.001	MPa
Peak shear stress	1.347		MPa
Yield shear stress	0.700		MPa
Residual shear stress	0.774		MPa
Shear modulus	80.4		MPa
Displacement at peak	1868		µm
Maximum displacement	4974		µm
Displacement rate	1.032		µm/s
Sample diameter	46.92	0.11	mm
Sample height	52.84	0.01	mm
Sample weight	182.57		g
Bulk density	2.00		g/cm <sup>3</sup>
Sample colour	45.97,-6.21,7.67		L, a, b
Colour of bottom slip plane	34.44,-6.50,7.37		L, a, b
Weight of bottom sample	93.111		g
Weight after drying	73.338		g
Moisture content	21.2		%
Bottom: Raw: $s_a$	0.656		mm
Bottom: Raw: $s_q$	0.774		mm
Bottom: Raw: $s_t$	3.516		mm
Top: Raw: $s_a$	0.638		mm
Top: Raw: $s_q$	0.759		mm
Top: Raw: $s_t$	4.007		mm
Bottom: Surf: $s_a$	0.267		mm
Bottom: Surf: $s_q$	0.335		mm
Bottom: Surf: $s_t$	2.612		mm
Top: Surf: $s_a$	0.279		mm
Top: Surf: $s_q$	0.35		mm
Top: Surf: $s_t$	2.477		mm

# **FPR-24-238**

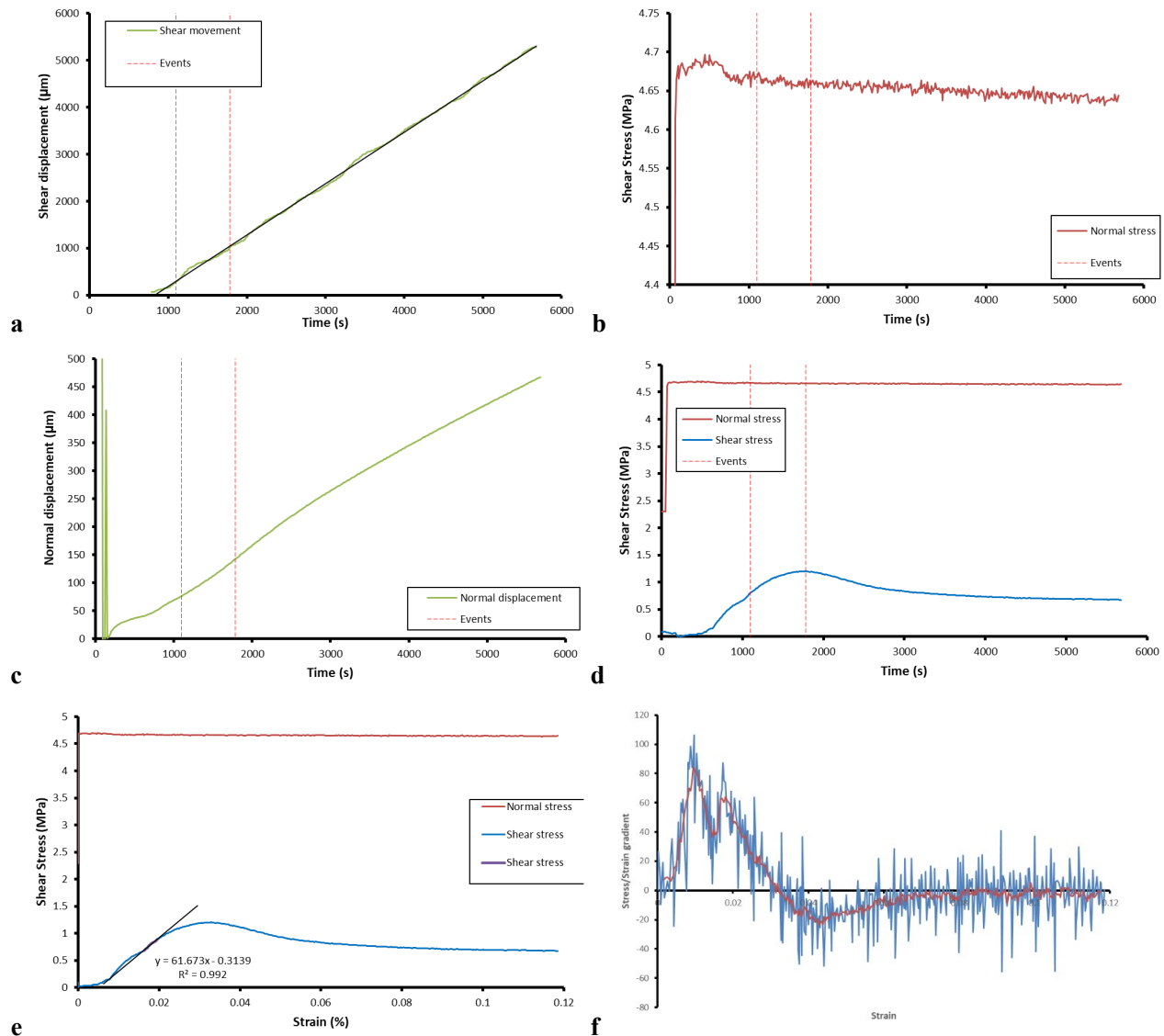


**Figure A-11.** Shear results for test FPR-24-238 (DH2:R9:200:825-BGS). a) Displacement with time; b) Normal load with time; c) Normal displacement with time; d) Normal and shear stress with time; e) Stress vs strain; f) Gradient of stress/strain (shear modulus).

# **FPR-24-238**

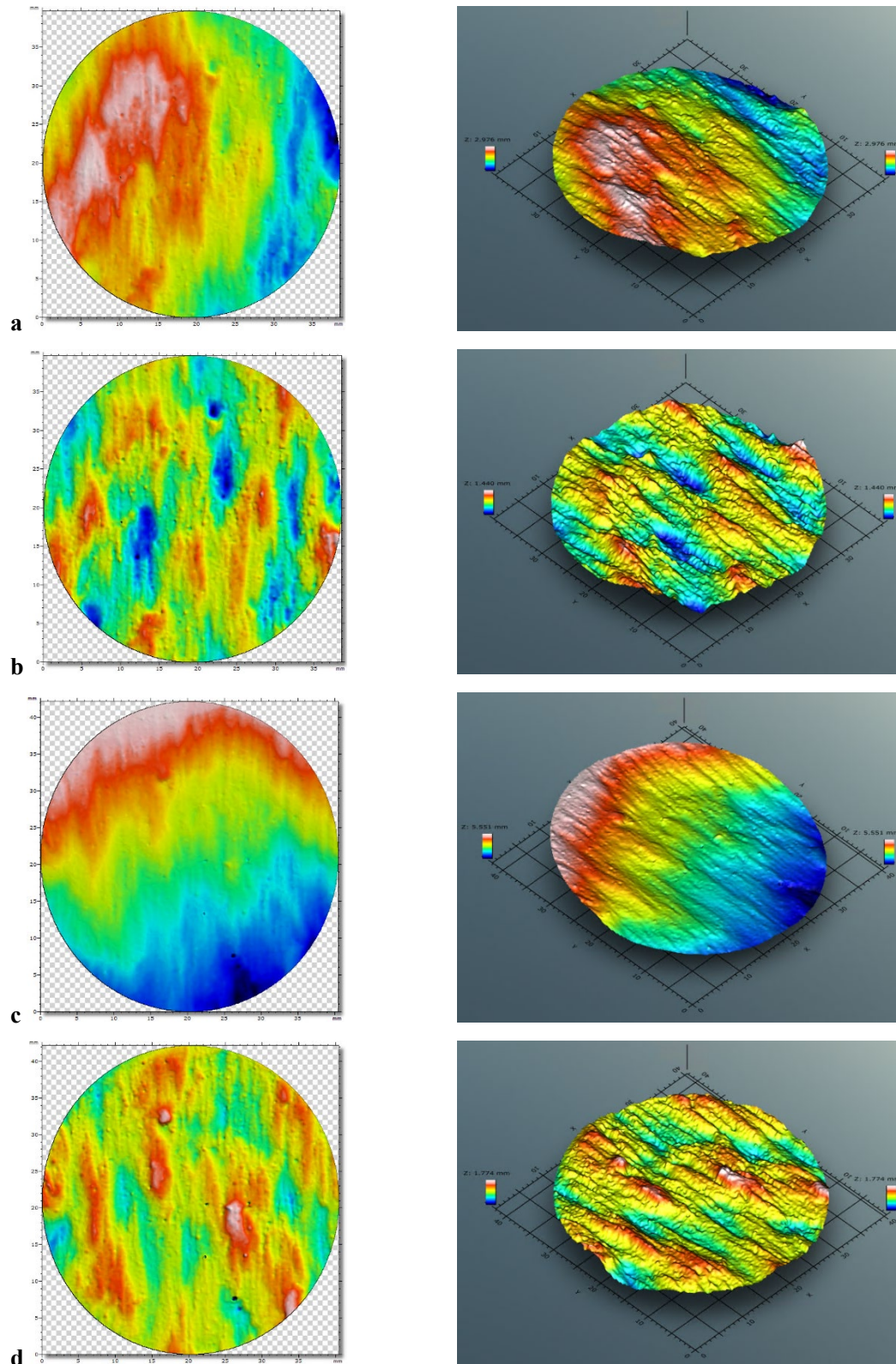


**Figure A-12.** Laser scan of shear fracture FPR-24-238 (DH2:R9:200:825-BGS). *a)* Bottom surface raw scan; *b)* Bottom surface with form removed; *c)* Top surface raw scan; *d)* Top surface with form removed. Shear direction is parallel with Y-axis, i.e. top-to-bottom in left.



**FPR-24-238****Table A-6. Results for test FPR-24-238 (DH2:R9:200:825-BGS)**

Parameter	Value	±	Units
SKB Sample name	DH2:R9:200:825-BGS		
BGS Sample name	FPR-24-238		
Normal load	4.684	0.001	MPa
Peak shear stress	1.204		MPa
Yield shear stress	0.808		MPa
Residual shear stress	0.695		MPa
Shear modulus	64.2		MPa
Displacement at peak	1548		µm
Maximum displacement	5573		µm
Displacement rate	1.032		µm/s
Sample diameter	47.00	0.08	mm
Sample height	52.69	0.03	mm
Sample weight	181.40		g
Bulk density	1.98		g/cm <sup>3</sup>
Sample colour	44.08,-6.42,7.42		L, a, b
Colour of bottom slip plane	37.40,-6.15,7.84		L, a, b
Weight of bottom sample	92.768		g
Weight after drying	72.824		g
Moisture content	21.5		%
Bottom: Raw: $s_a$	0.493		mm
Bottom: Raw: $s_q$	0.59		mm
Bottom: Raw: $s_t$	2.976		mm
Top: Raw: $s_a$	1.087		mm
Top: Raw: $s_q$	1.291		mm
Top: Raw: $s_t$	5.51		mm
Bottom: Surf: $s_a$	0.166		mm
Bottom: Surf: $s_q$	0.206		mm
Bottom: Surf: $s_t$	1.44		mm
Top: Surf: $s_a$	0.169		mm
Top: Surf: $s_q$	0.209		mm
Top: Surf: $s_t$	1.774		mm

# **FPR-24-242**

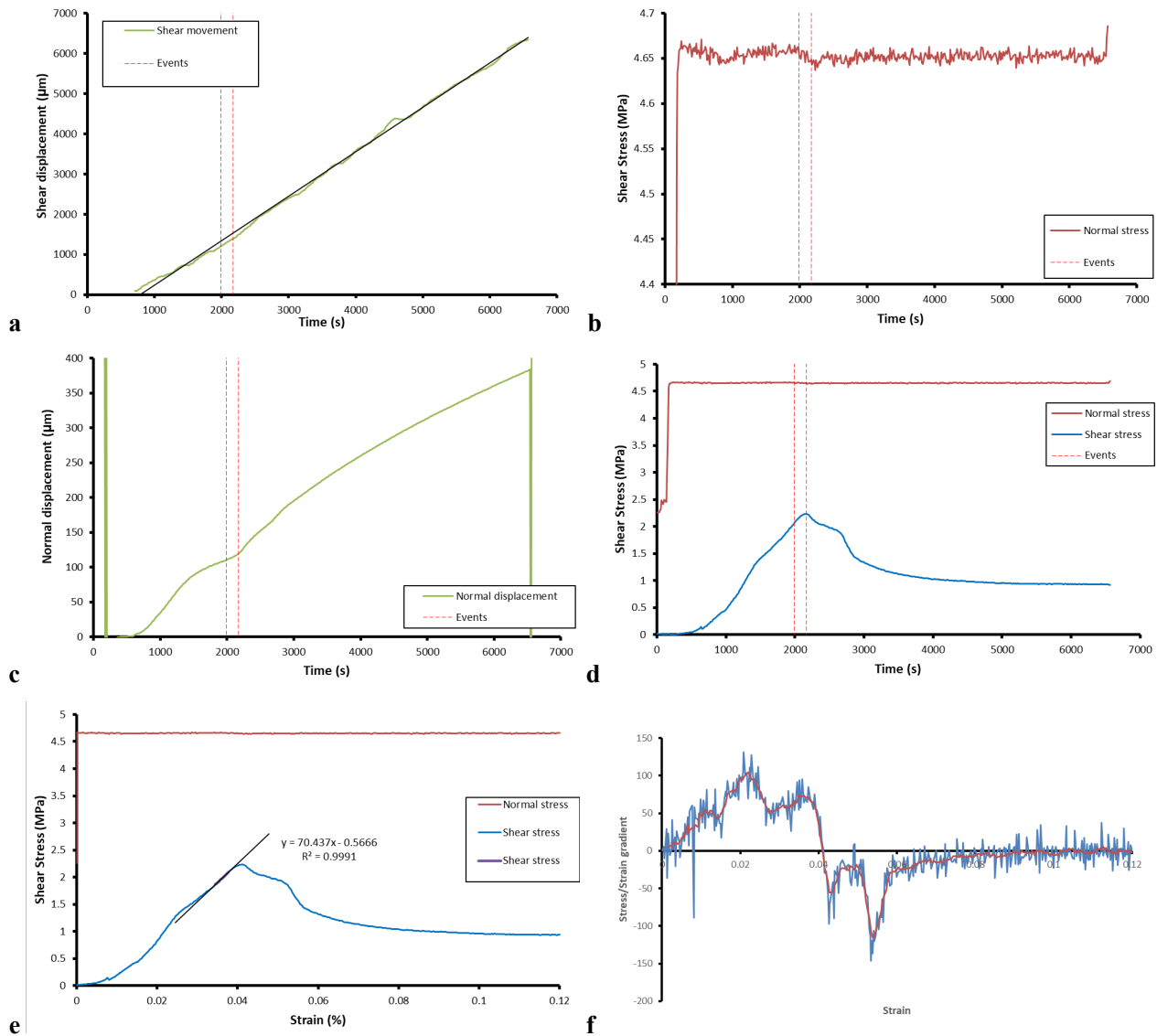


**Figure A-13.** Shear results for test FPR-24-242 (DH3:R9:200:575-BGS). a) Displacement with time; b) Normal load with time; c) Normal displacement with time; d) Normal and shear stress with time; e) Stress vs strain; f) Gradient of stress/strain (shear modulus).

# **FPR-24-242**

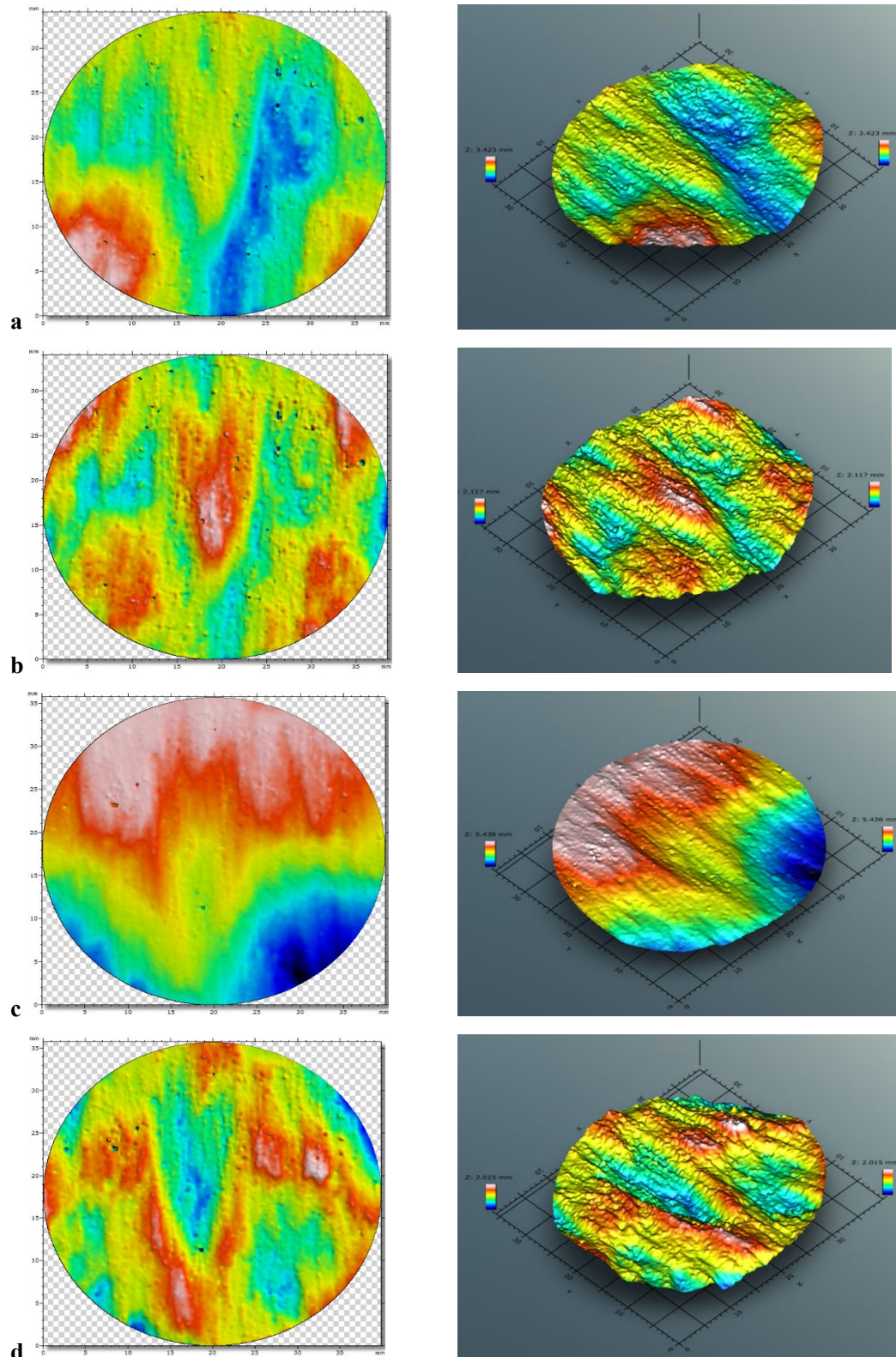


**Figure A-14.** Laser scan of shear fracture FPR-24-242 (DH3:R9:200:575-BGS). a) Bottom surface raw scan; b) Bottom surface with form removed; c) Top surface raw scan; d) Top surface with form removed. Shear direction is parallel with Y-axis, i.e. top-to-bottom in left.



**FPR-24-242****Table A-7. Results for test FPR-24-242 (DH3:R9:200:575-BGS)**

Parameter	Value	±	Units
SKB Sample name	DH3:R9:200:575-BGS		
BGS Sample name	FPR-24-242		
Normal load	4.681	0.000	MPa
Peak shear stress	2.234		MPa
Yield shear stress	2.064		MPa
Residual shear stress	0.959		MPa
Shear modulus	74.2		MPa
Displacement at peak	1940		µm
Maximum displacement	6481		µm
Displacement rate	1.032		µm/s
Sample diameter	47.15	0.12	mm
Sample height	51.85	0.07	mm
Sample weight	184.49		g
Bulk density	2.03		g/cm <sup>3</sup>
Sample colour	49.64,-5.42,7.93		L, a, b
Colour of bottom slip plane	40.58,-5.02,8.14		L, a, b
Weight of bottom sample	93.352		g
Weight after drying	75.472		g
Moisture content	19.2		%
Bottom: Raw: $s_a$	0.399		mm
Bottom: Raw: $s_q$	0.521		mm
Bottom: Raw: $s_t$	3.423		mm
Top: Raw: $s_a$	1.12		mm
Top: Raw: $s_q$	1.32		mm
Top: Raw: $s_t$	5.438		mm
Bottom: Surf: $s_a$	0.245		mm
Bottom: Surf: $s_q$	0.3		mm
Bottom: Surf: $s_t$	2.117		mm
Top: Surf: $s_a$	0.248		mm
Top: Surf: $s_q$	0.302		mm
Top: Surf: $s_t$	2.015		mm

**FPR-24-246**

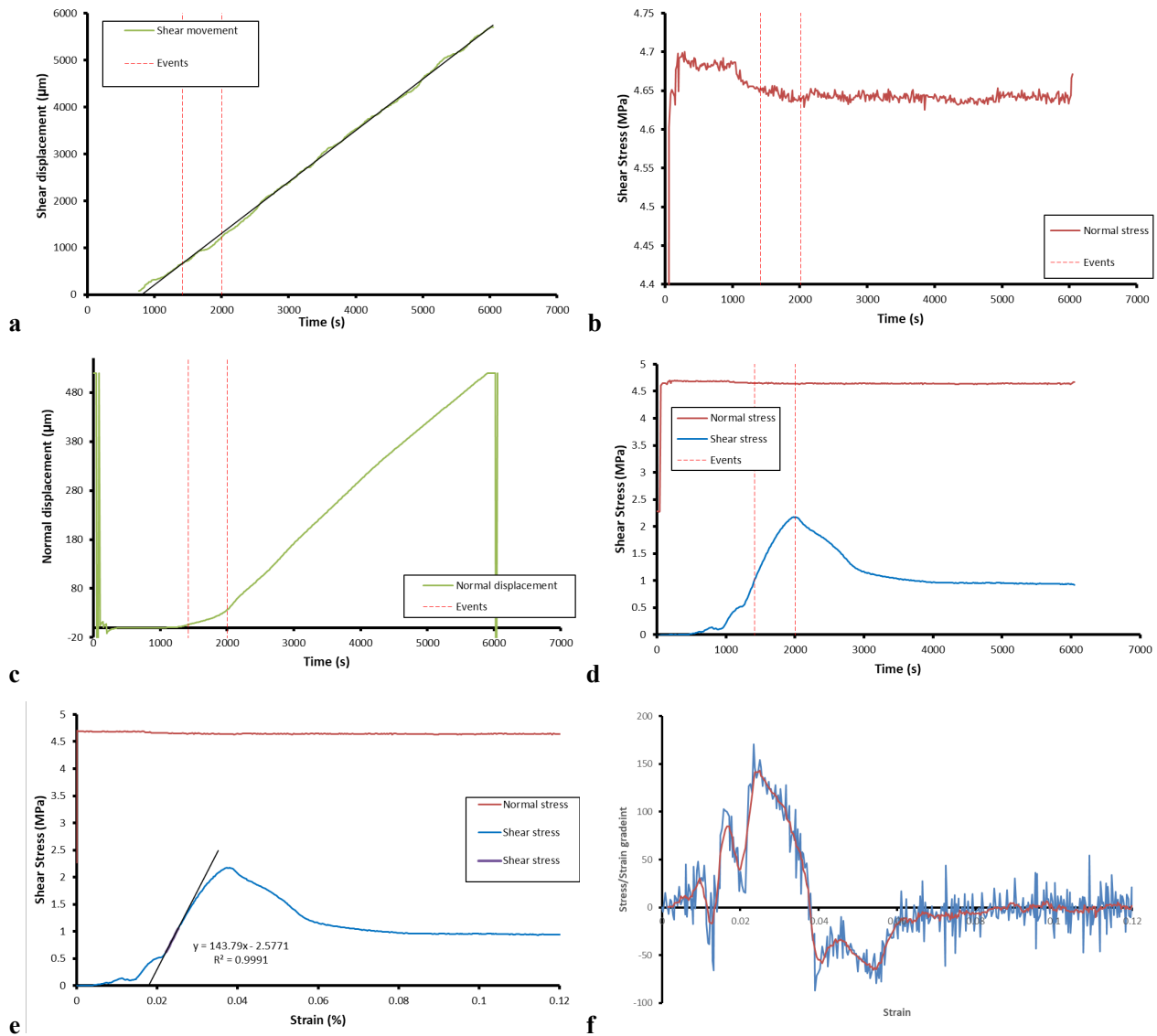


**Figure A-15.** Shear results for test FPR-24-246 (DH3:R9:200:625-BGS). a) Displacement with time; b) Normal load with time; c) Normal displacement with time; d) Normal and shear stress with time; e) Stress vs strain; f) Gradient of stress/strain (shear modulus).

# **FPR-24-246**

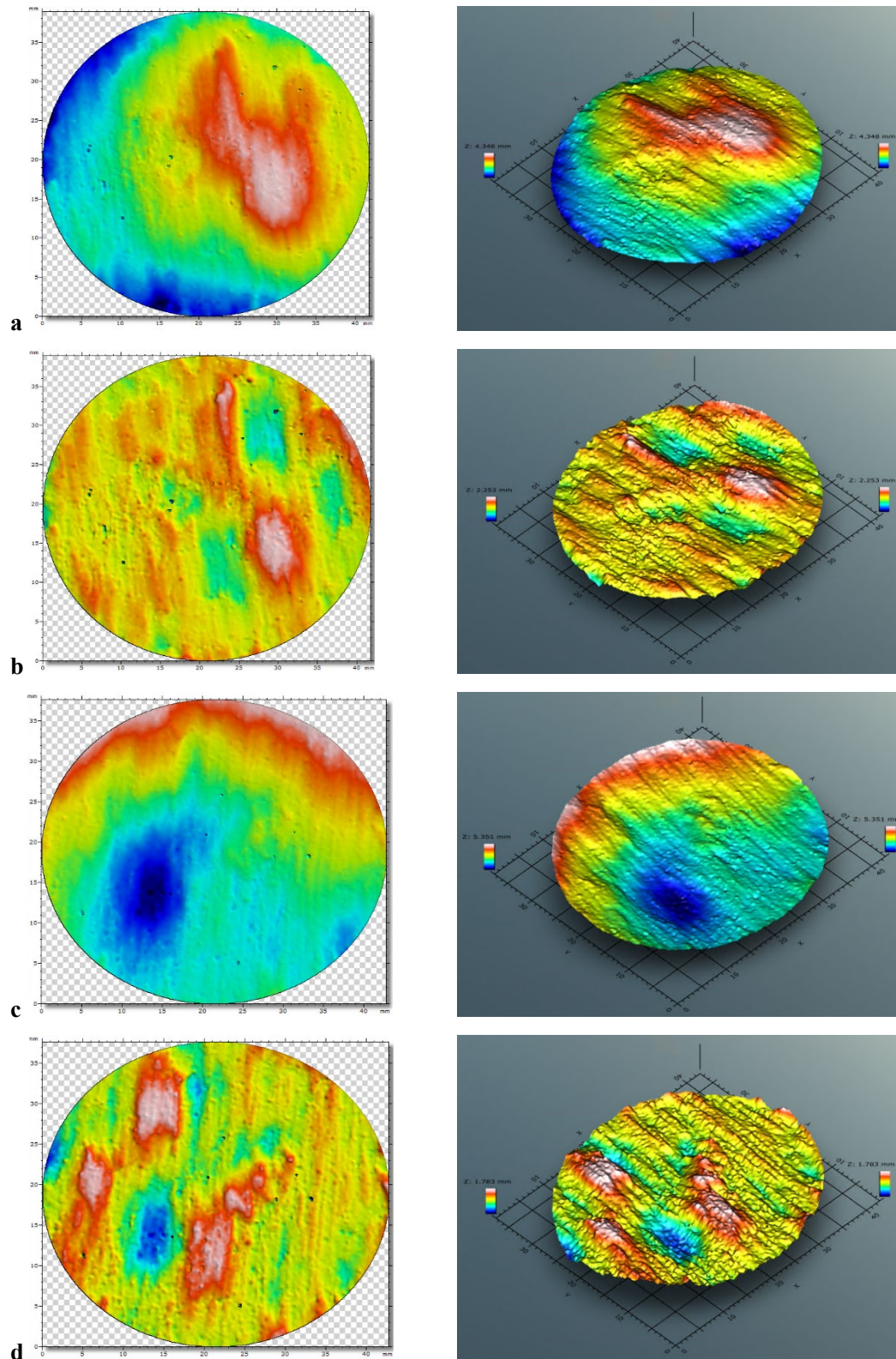


**Figure A-16.** Laser scan of shear fracture FPR-24-246 (DH3:R9:200:625-BGS). a) Bottom surface raw scan; b) Bottom surface with form removed; c) Top surface raw scan; d) Top surface with form removed. Shear direction is parallel with Y-axis, i.e. top-to-bottom in left.

**FPR-24-246****Table A-8. Results for test FPR-24-246 (DH3:R9:200:625-BGS)**

Parameter	Value	±	Units
SKB Sample name	DH3:R9:200:625-BGS		
BGS Sample name	FPR-24-246		
Normal load	4.677	0.001	MPa
Peak shear stress	2.176		MPa
Yield shear stress	1.024		MPa
Residual shear stress	0.959		MPa
Shear modulus	143.4		MPa
Displacement at peak	1785		µm
Maximum displacement	5955		µm
Displacement rate	1.032		µm/s
Sample diameter	47.22	0.09	mm
Sample height	52.52	0.00	mm
Sample weight	188.19		g
Bulk density	2.05		g/cm <sup>3</sup>
Sample colour	48.32,-5.81,7.79		L, a, b
Colour of bottom slip plane	37.76,-5.48,8.08		L, a, b
Weight of bottom sample	102.079		g
Weight after drying	82.451		g
Moisture content	19.2		%
Bottom: Raw: $s_a$	0.746		mm
Bottom: Raw: $s_q$	0.898		mm
Bottom: Raw: $s_t$	4.348		mm
Top: Raw: $s_a$	0.842		mm
Top: Raw: $s_q$	1.053		mm
Top: Raw: $s_t$	5.351		mm
Bottom: Surf: $s_a$	0.18		mm
Bottom: Surf: $s_q$	0.24		mm
Bottom: Surf: $s_t$	2.253		mm
Top: Surf: $s_a$	0.186		mm
Top: Surf: $s_q$	0.247		mm
Top: Surf: $s_t$	1.783		mm

# **FPR-24-250**

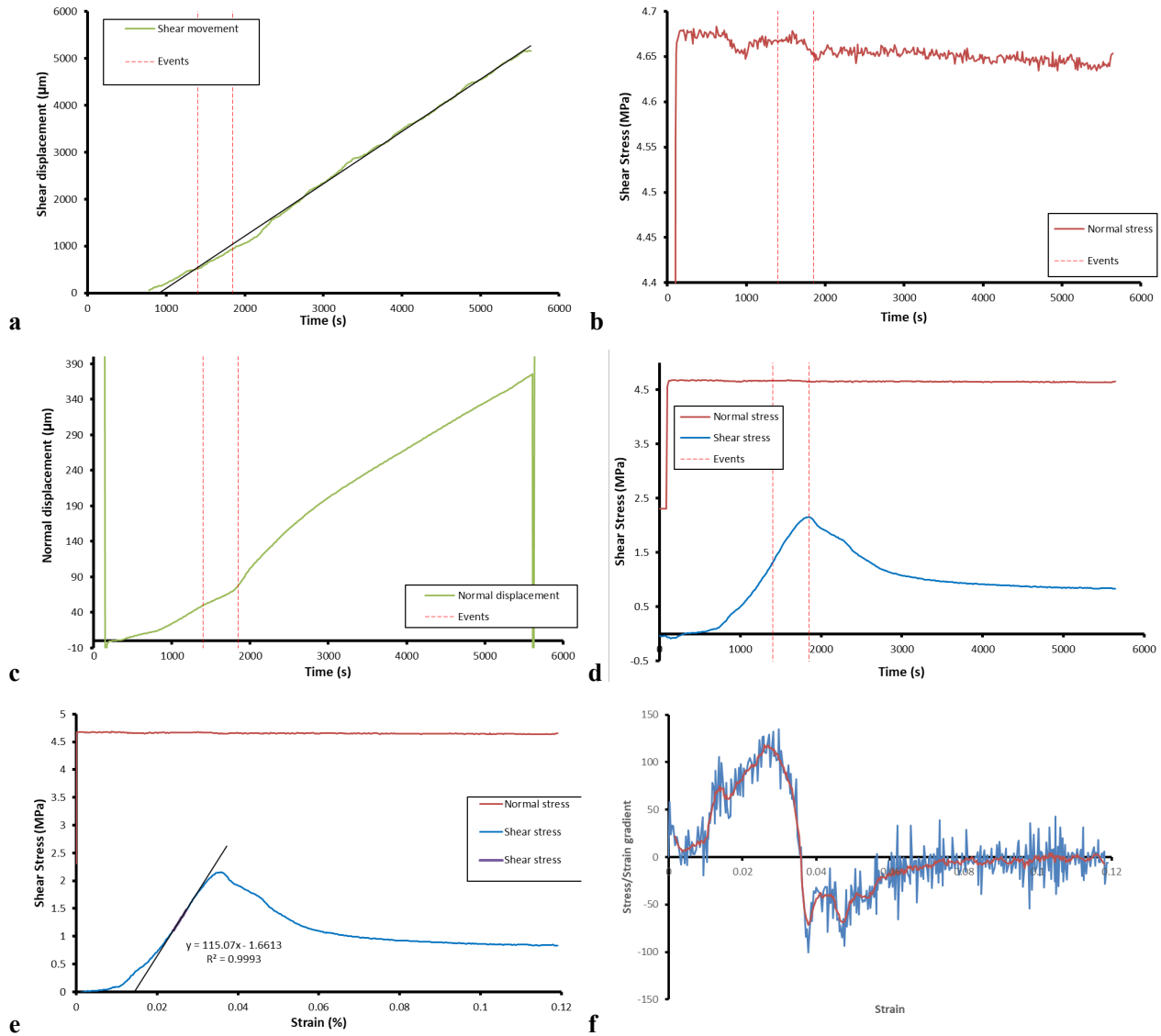


**Figure A-17.** Shear results for test FPR-24-250 (DH3:R9:200:675-BGS). a) Displacement with time; b) Normal load with time; c) Normal displacement with time; d) Normal and shear stress with time; e) Stress vs strain; f) Gradient of stress/strain (shear modulus).



# **FPR-24-250**

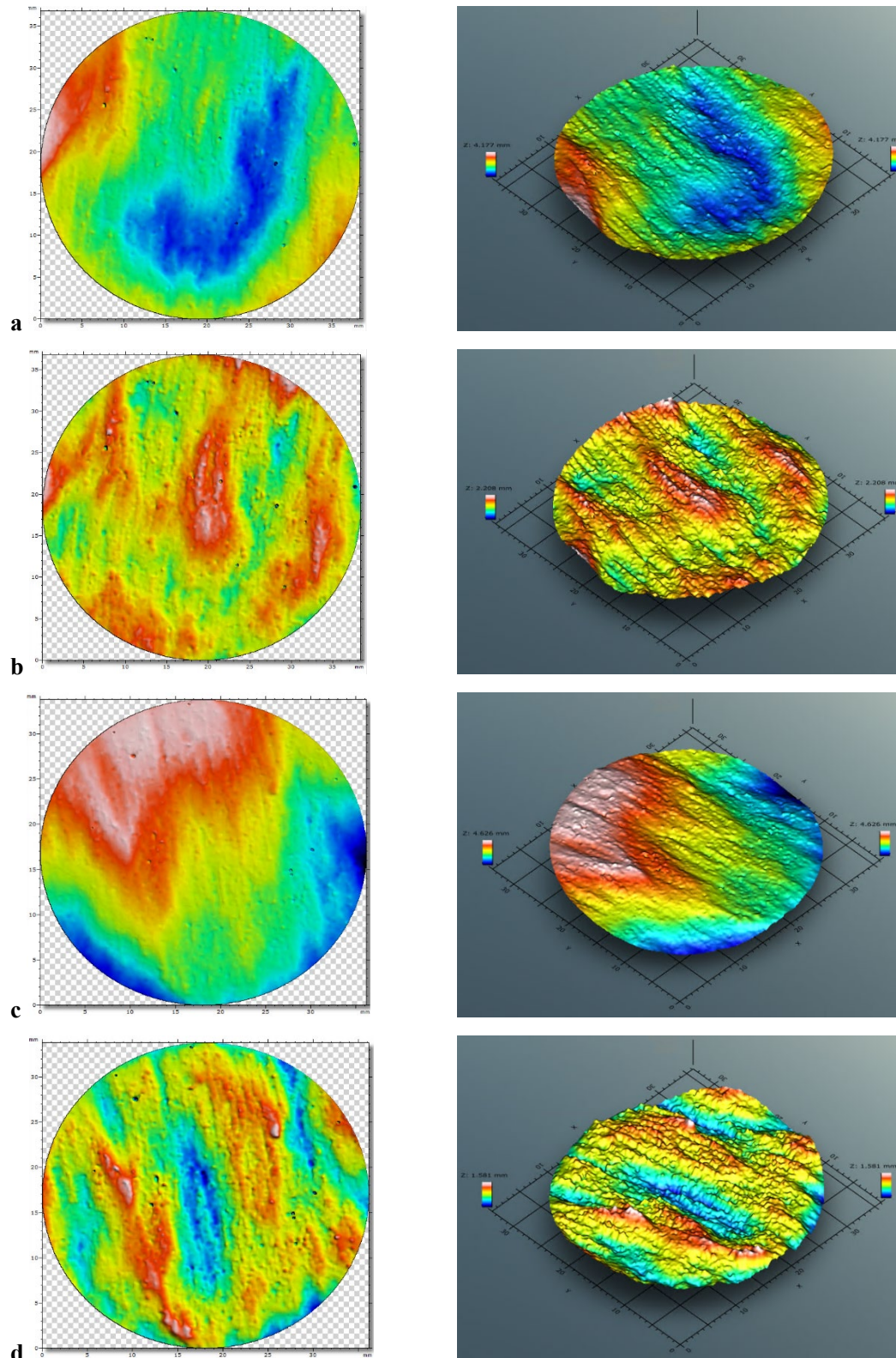


**Figure A-18.** Laser scan of shear fracture FPR-24-250 (DH3:R9:200:675-BGS). a) Bottom surface raw scan; b) Bottom surface with form removed; c) Top surface raw scan; d) Top surface with form removed. Shear direction is parallel with Y-axis, i.e. top-to-bottom in left.

**FPR-24-250****Table A-9. Results for test FPR-24-250 (DH3:R9:200:675-BGS)**

Parameter	Value	±	Units
SKB Sample name	DH3:R9:200:675-BGS		
BGS Sample name	FPR-24-250		
Normal load	4.684	0.001	MPa
Peak shear stress	2.153		MPa
Yield shear stress	1.320		MPa
Residual shear stress	0.859		MPa
Shear modulus	118.3		MPa
Displacement at peak	1682		µm
Maximum displacement	5594		µm
Displacement rate	1.032		µm/s
Sample diameter	47.24	0.08	mm
Sample height	52.30	0.03	mm
Sample weight	187.13		g
Bulk density	2.04		g/cm <sup>3</sup>
Sample colour	48.80,-5.79,7.53		L, a, b
Colour of bottom slip plane	36.38,-5.55,7.70		L, a, b
Weight of bottom sample	94.239		g
Weight after drying	76.109		g
Moisture content	19.2		%
Bottom: Raw: $s_a$	0.53		mm
Bottom: Raw: $s_q$	0.685		mm
Bottom: Raw: $s_t$	4.177		mm
Top: Raw: $s_a$	0.892		mm
Top: Raw: $s_q$	1.038		mm
Top: Raw: $s_t$	4.626		mm
Bottom: Surf: $s_a$	0.207		mm
Bottom: Surf: $s_q$	0.252		mm
Bottom: Surf: $s_t$	2.208		mm
Top: Surf: $s_a$	0.189		mm
Top: Surf: $s_q$	0.232		mm
Top: Surf: $s_t$	1.581		mm



# **FPR-24-251**

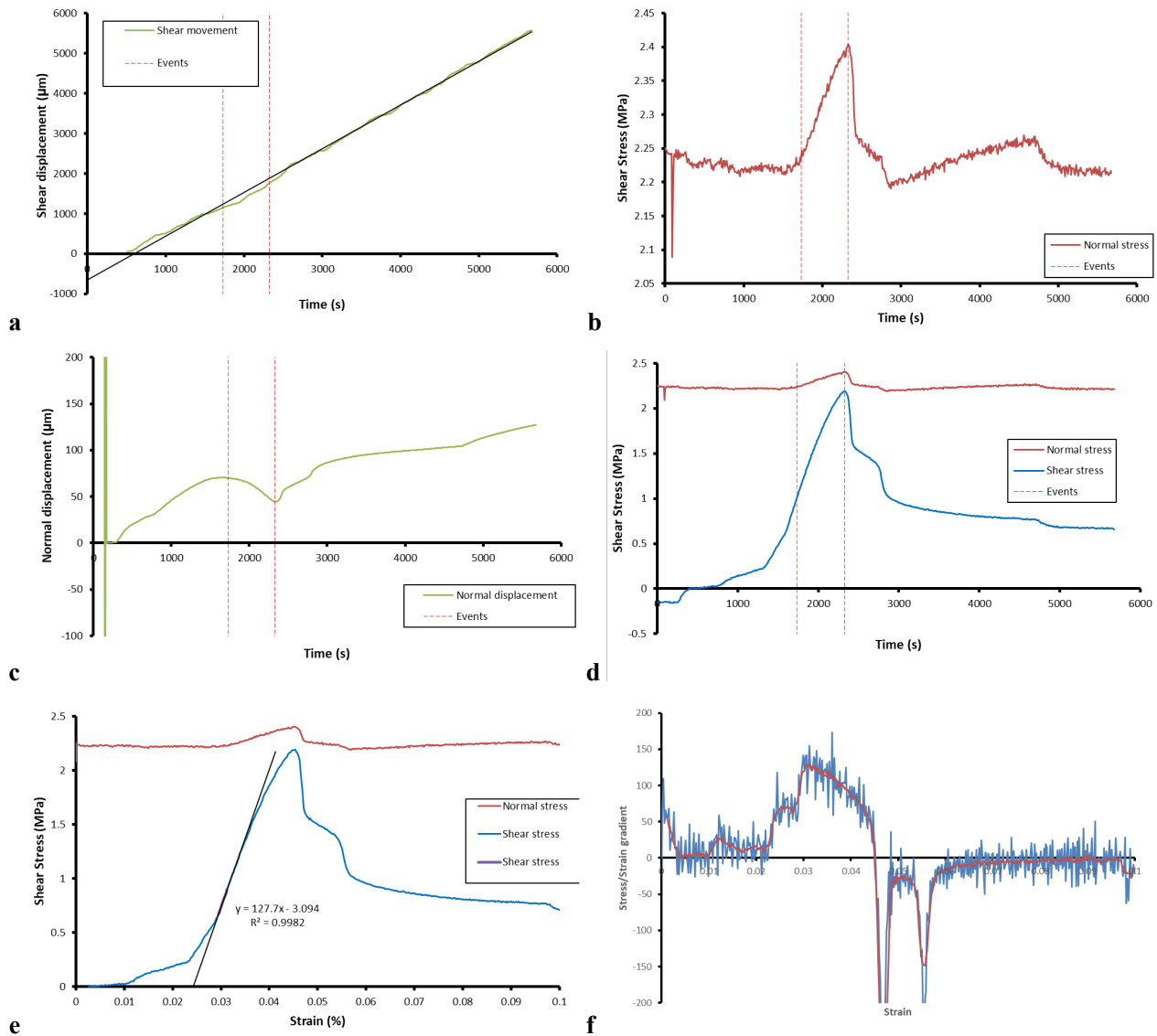


**Figure A-19.** Shear results for test FPR-24-251 (DH3:R9:200:675-BGS). a) Displacement with time; b) Normal load with time; c) Normal displacement with time; d) Normal and shear stress with time; e) Stress vs strain; f) Gradient of stress/strain (shear modulus).

# **FPR-24-251**

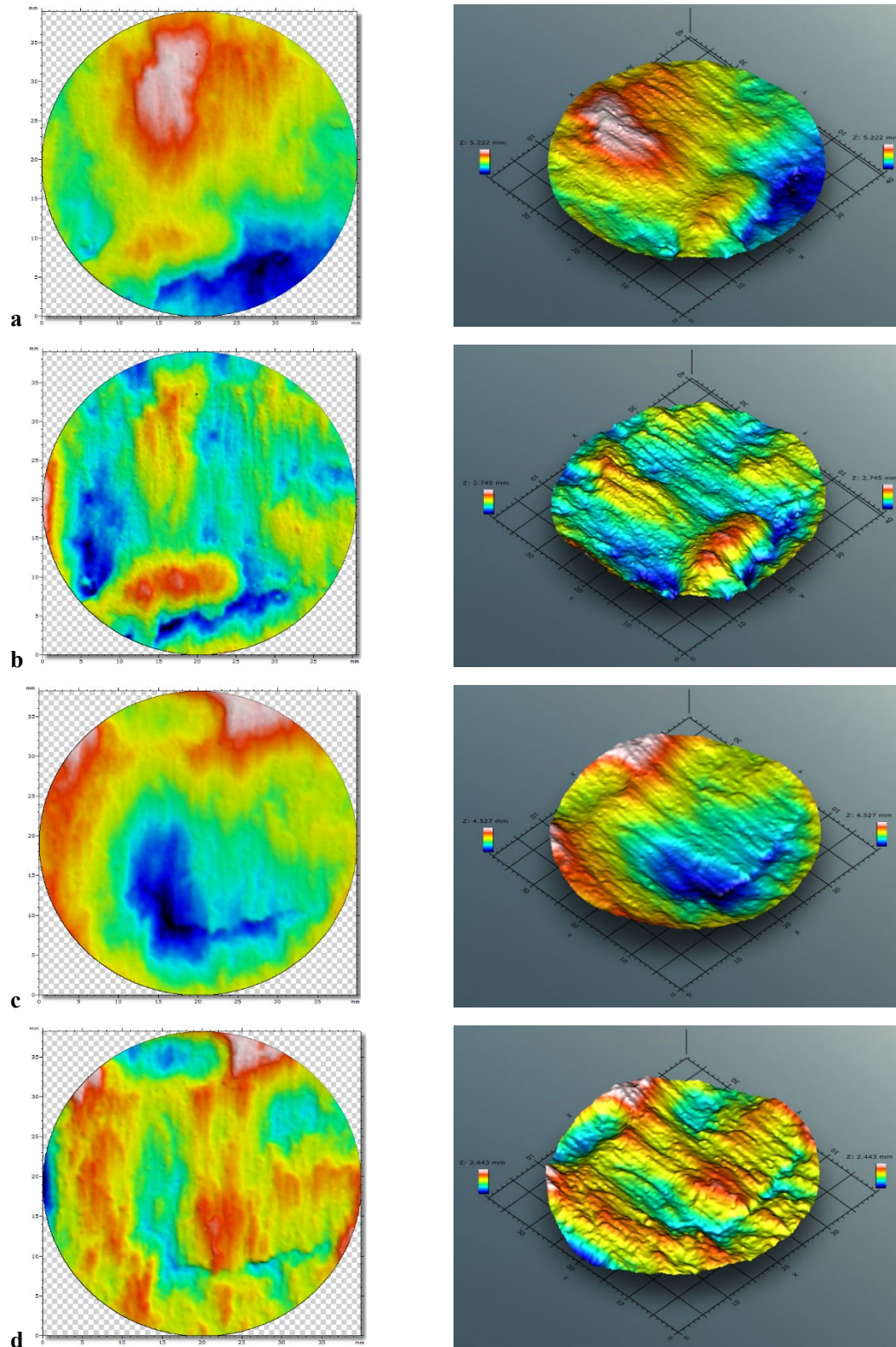


**Figure A-20.** Laser scan of shear fracture FPR-24-251 (DH3:R9:200:675-BGS). a) Bottom surface raw scan; b) Bottom surface with form removed; c) Top surface raw scan; d) Top surface with form removed. Shear direction is parallel with Y-axis, i.e. top-to-bottom in left.

**FPR-24-251****Table A-10. Results for test FPR-24-251 (DH3:R9:200:675-BGS)**

Parameter	Value	±	Units
SKB Sample name	DH3:R9:200:675-BGS		
BGS Sample name	FPR-24-251		
Normal load	2.255	0.002	MPa
Peak shear stress	2.192		MPa
Yield shear stress	1.011		MPa
Residual shear stress	0.712		MPa
Shear modulus	128.6		MPa
Displacement at peak	2131		µm
Maximum displacement	5587		µm
Displacement rate	1.032		µm/s
Sample diameter	47.30	0.08	mm
Sample height	52.80	0.00	mm
Sample weight	189.43		g
Bulk density	2.04		g/cm <sup>3</sup>
Sample colour	49.03,-5.55,7.70		L, a, b
Colour of bottom slip plane	39.17,-5.54,8.40		L, a, b
Weight of bottom sample	97.963		g
Weight after drying	79.078		g
Moisture content	19.3		%
Bottom: Raw: $s_a$	0.824		mm
Bottom: Raw: $s_q$	1.041		mm
Bottom: Raw: $s_t$	5.222		mm
Top: Raw: $s_a$	0.693		mm
Top: Raw: $s_q$	0.866		mm
Top: Raw: $s_t$	4.527		mm
Bottom: Surf: $s_a$	0.312		mm
Bottom: Surf: $s_q$	0.398		mm
Bottom: Surf: $s_t$	2.745		mm
Top: Surf: $s_a$	0.272		mm
Top: Surf: $s_q$	0.341		mm
Top: Surf: $s_t$	2.443		mm

# **FPR-24-254**

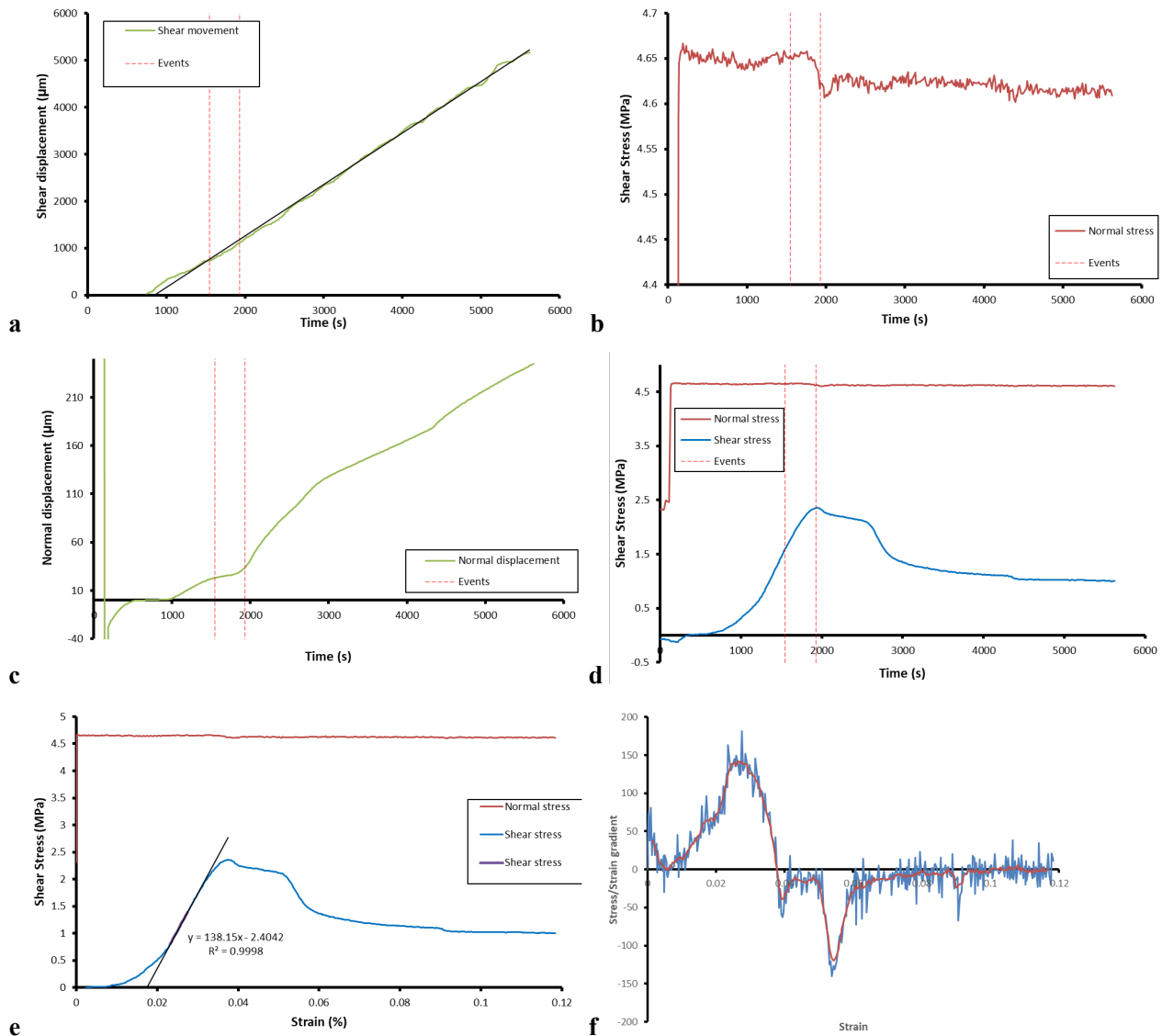


**Figure A-21.** Shear results for test FPR-24-254 (DH3:R9:200:725-BGS). a) Displacement with time; b) Normal load with time; c) Normal displacement with time; d) Normal and shear stress with time; e) Stress vs strain; f) Gradient of stress/strain (shear modulus).



# **FPR-24-254**

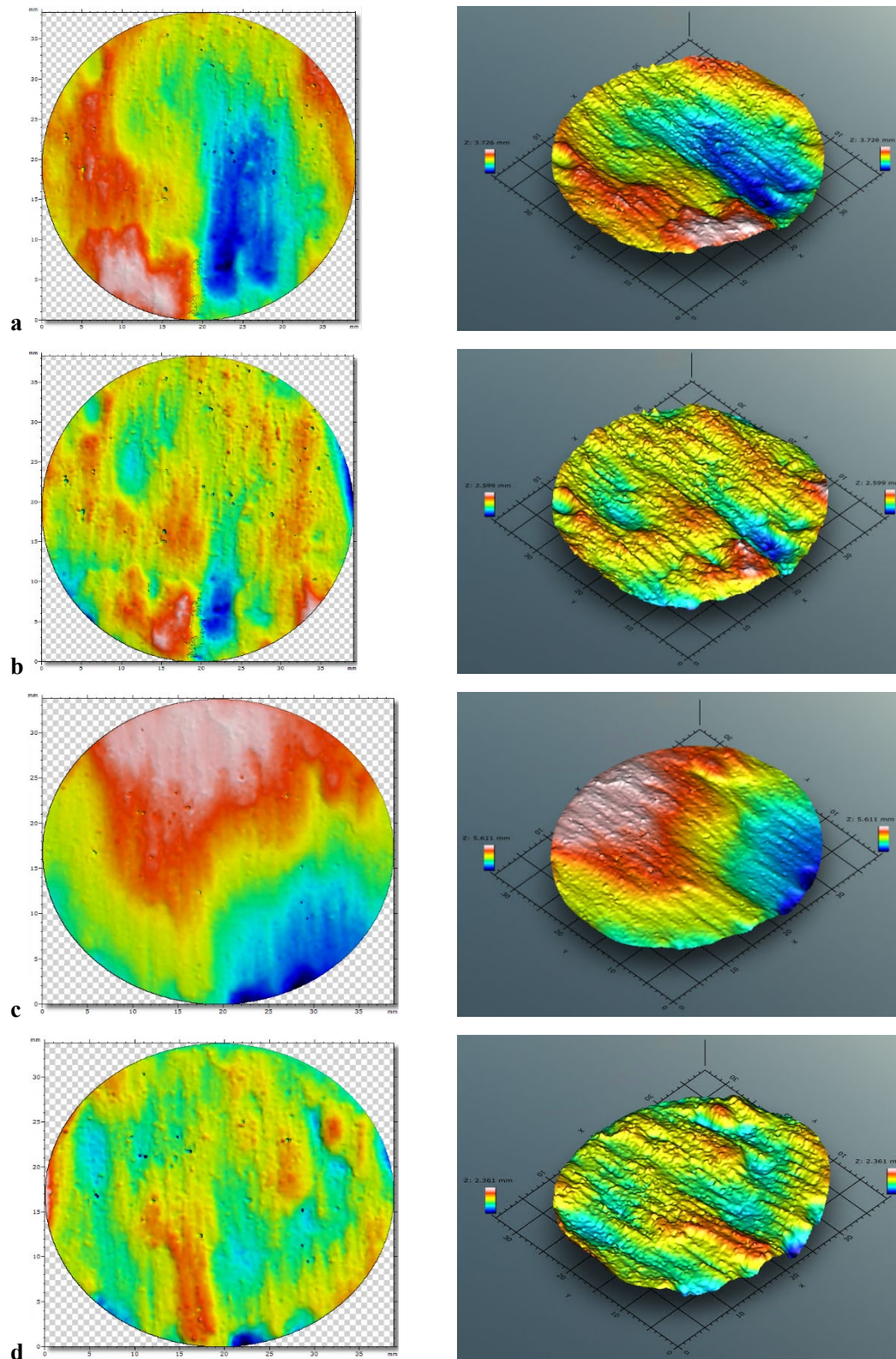


**Figure A-22.** Laser scan of shear fracture FPR-24-254 (DH3:R9:200:725-BGS). a) Bottom surface raw scan; b) Bottom surface with form removed; c) Top surface raw scan; d) Top surface with form removed. Shear direction is parallel with Y-axis, i.e. top-to-bottom in left.

**FPR-24-254****Table A-11. Results for test FPR-24-254 (DH3:R9:200:725-BGS)**

Parameter	Value	±	Units
SKB Sample name	DH3:R9:200:725-BGS		
BGS Sample name	FPR-24-254		
Normal load	4.657	0.001	MPa
Peak shear stress	2.361		MPa
Yield shear stress	1.602		MPa
Residual shear stress	1.024		MPa
Shear modulus	141.9		MPa
Displacement at peak	1754		µm
Maximum displacement	5563		µm
Displacement rate	1.032		µm/s
Sample diameter	47.15	0.06	mm
Sample height	53.28	0.02	mm
Sample weight	190.41		g
Bulk density	2.05		g/cm <sup>3</sup>
Sample colour	48.01,-5.77,7.66		L, a, b
Colour of bottom slip plane	41.95,-5.42,8.34		L, a, b
Weight of bottom sample	93.659		g
Weight after drying	75.864		g
Moisture content	19.0		%
Bottom: Raw: $s_a$	0.626		mm
Bottom: Raw: $s_q$	0.758		mm
Bottom: Raw: $s_t$	3.726		mm
Top: Raw: $s_a$	1.067		mm
Top: Raw: $s_q$	1.251		mm
Top: Raw: $s_t$	5.611		mm
Bottom: Surf: $s_a$	0.253		mm
Bottom: Surf: $s_q$	0.328		mm
Bottom: Surf: $s_t$	2.599		mm
Top: Surf: $s_a$	0.207		mm
Top: Surf: $s_q$	0.26		mm
Top: Surf: $s_t$	2.361		mm



# **FPR-24-258**

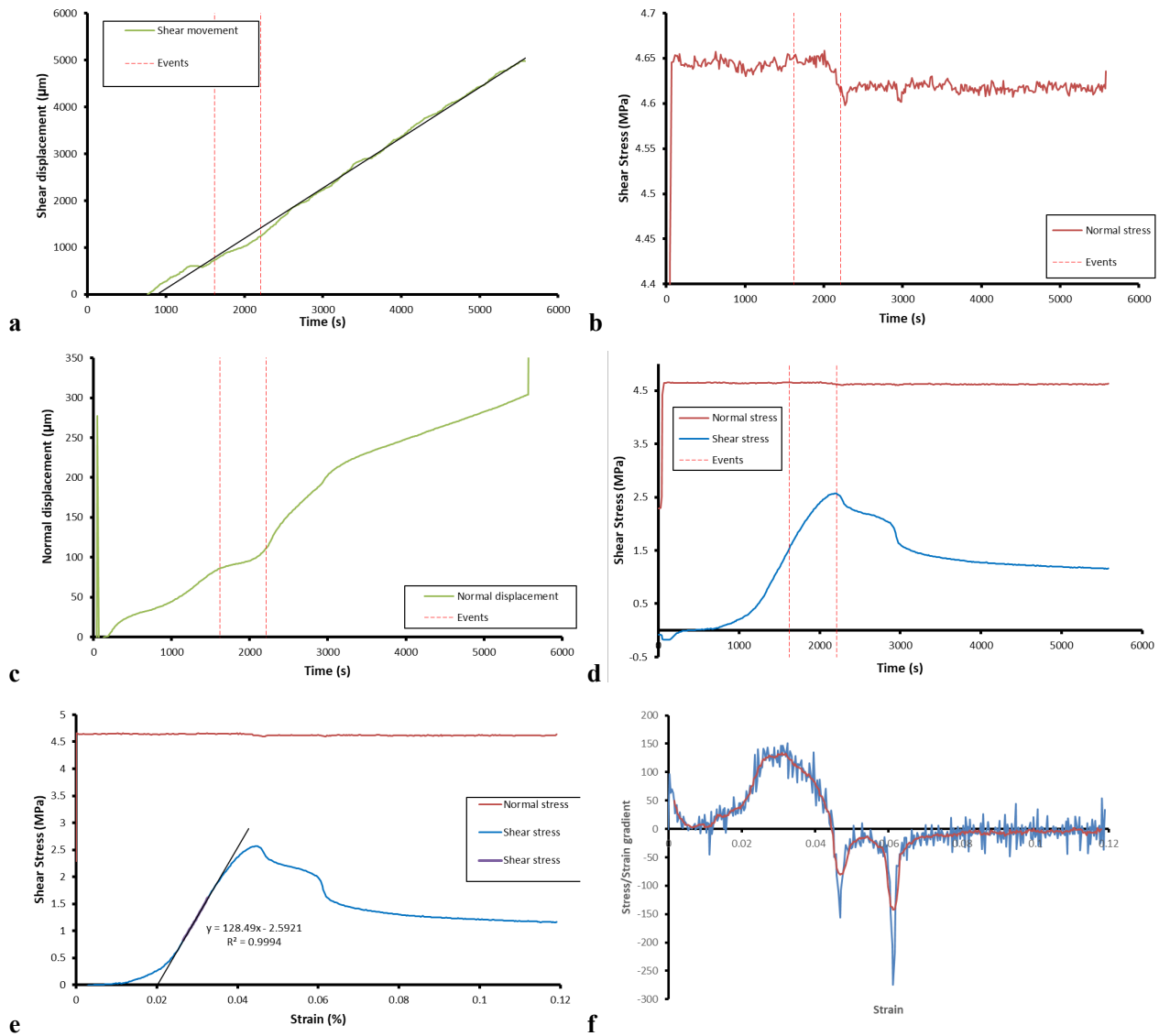


**Figure A-23.** Shear results for test FPR-24-258 (DH3:R9:200:775-BGS). a) Displacement with time; b) Normal load with time; c) Normal displacement with time; d) Normal and shear stress with time; e) Stress vs strain; f) Gradient of stress/strain (shear modulus).

**FPR-24-258**

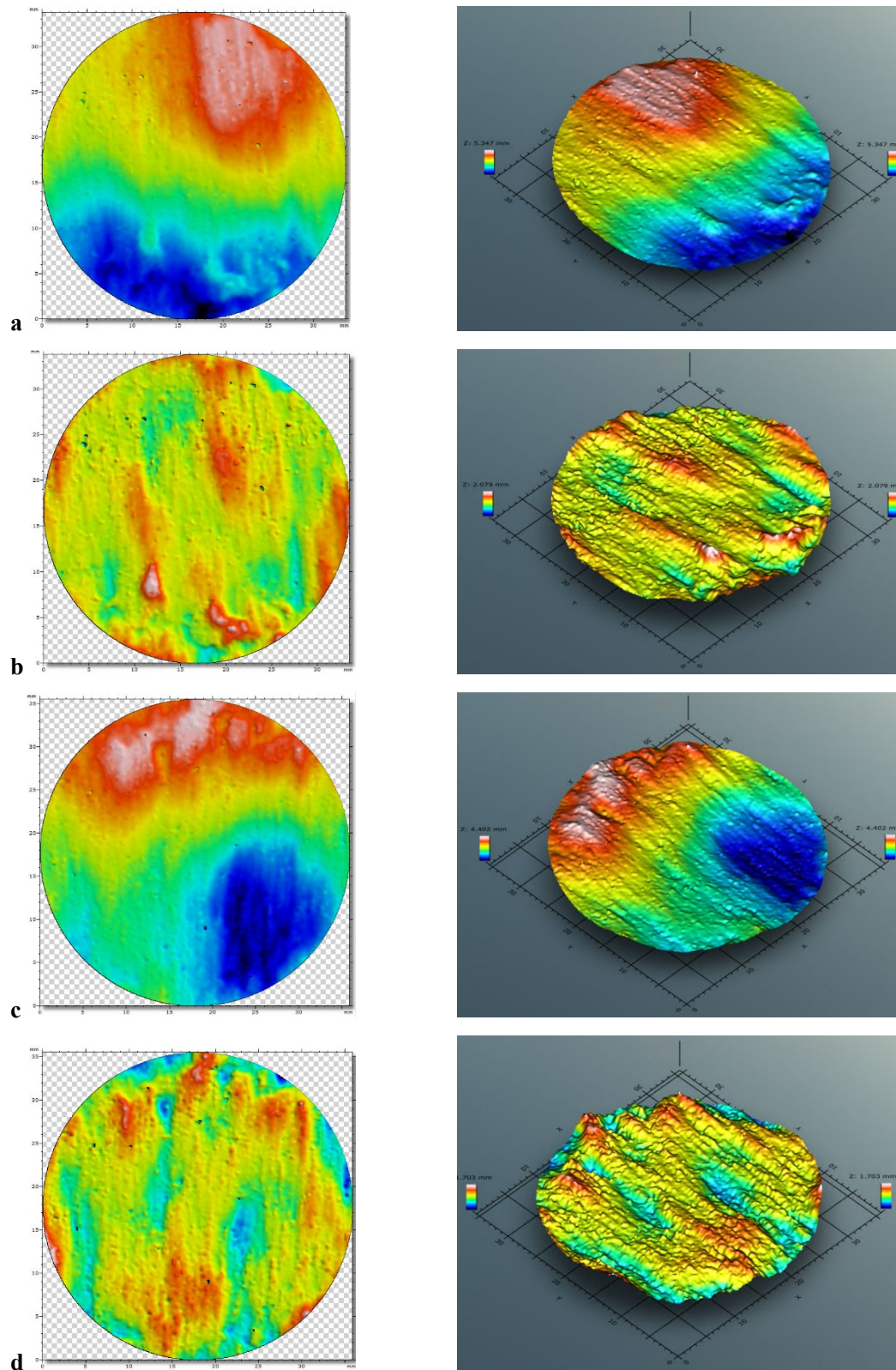


**Figure A-24.** Laser scan of shear fracture FPR-24-258 (DH3:R9:200:775-BGS). a) Bottom surface raw scan; b) Bottom surface with form removed; c) Top surface raw scan; d) Top surface with form removed. Shear direction is parallel with Y-axis, i.e. top-to-bottom in left.

**FPR-24-258****Table A-12. Results for test FPR-24-258 (DH3:R9:200:775-BGS)**

Parameter	Value	±	Units
SKB Sample name	DH3:R9:200:775-BGS		
BGS Sample name	FPR-24-258		
Normal load	4.656	0.001	MPa
Peak shear stress	2.572		MPa
Yield shear stress	1.530		MPa
Residual shear stress	1.213		MPa
Shear modulus	133.7		MPa
Displacement at peak	2116		µm
Maximum displacement	5594		µm
Displacement rate	1.032		µm/s
Sample diameter	47.06	0.03	mm
Sample height	53.38	0.01	mm
Sample weight	189.84		g
Bulk density	2.05		g/cm <sup>3</sup>
Sample colour	50.76,-5.47,7.81		L, a, b
Colour of bottom slip plane	39.60,-5.32,7.92		L, a, b
Weight of bottom sample	97.009		g
Weight after drying	78.795		g
Moisture content	18.8		%
Bottom: Raw: $s_a$	1.059		mm
Bottom: Raw: $s_q$	1.242		mm
Bottom: Raw: $s_t$	5.347		mm
Top: Raw: $s_a$	0.866		mm
Top: Raw: $s_q$	1.035		mm
Top: Raw: $s_t$	4.402		mm
Bottom: Surf: $s_a$	0.157		mm
Bottom: Surf: $s_q$	0.2		mm
Bottom: Surf: $s_t$	2.079		mm
Top: Surf: $s_a$	0.165		mm
Top: Surf: $s_q$	0.207		mm
Top: Surf: $s_t$	1.703		mm

# **FPR-24-262**

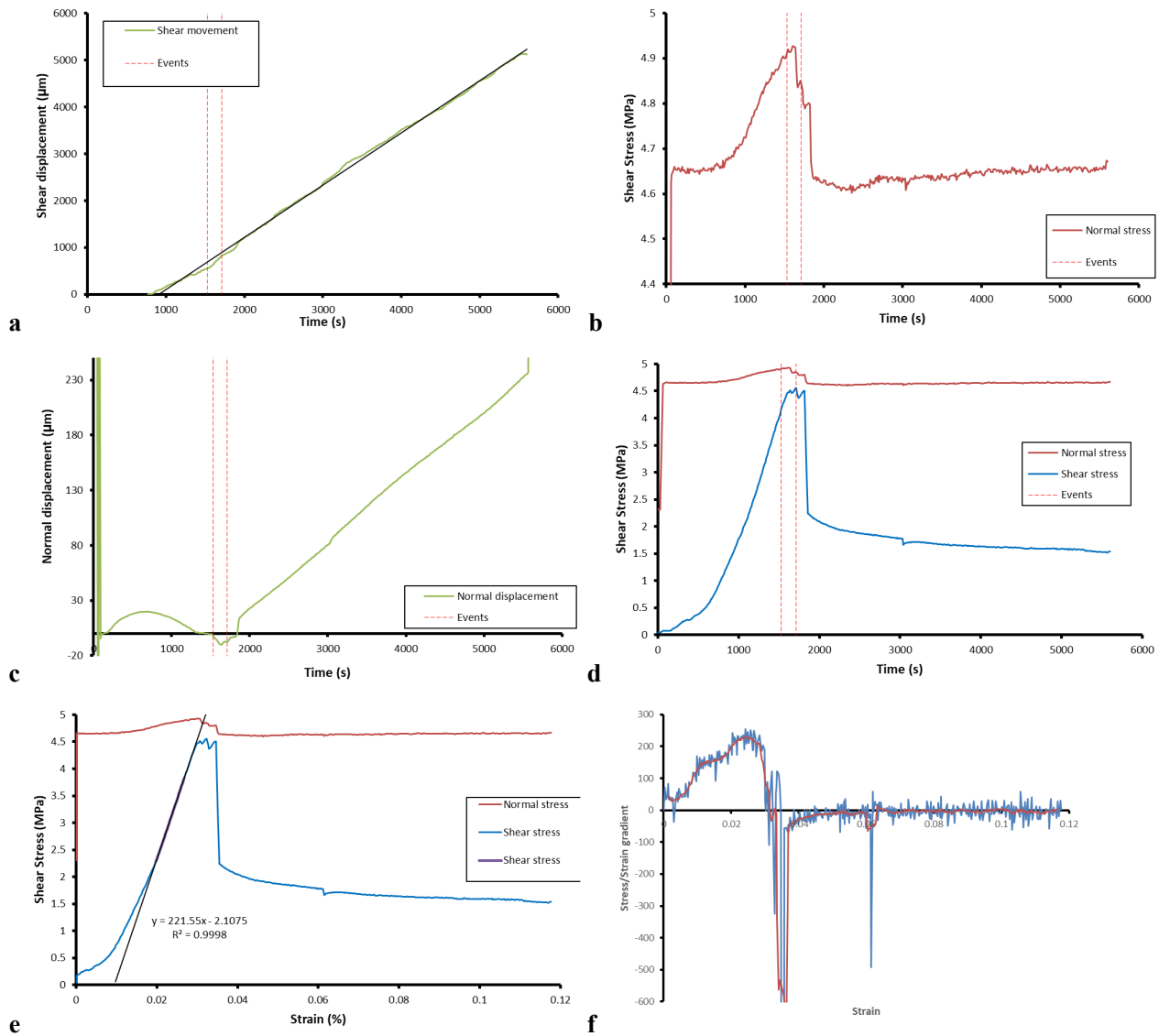


**Figure A-25.** Shear results for test FPR-24-262 (DH4;R2:290:575-BGS). a) Displacement with time; b) Normal load with time; c) Normal displacement with time; d) Normal and shear stress with time; e) Stress vs strain; f) Gradient of stress/strain (shear modulus).



# **FPR-24-262**

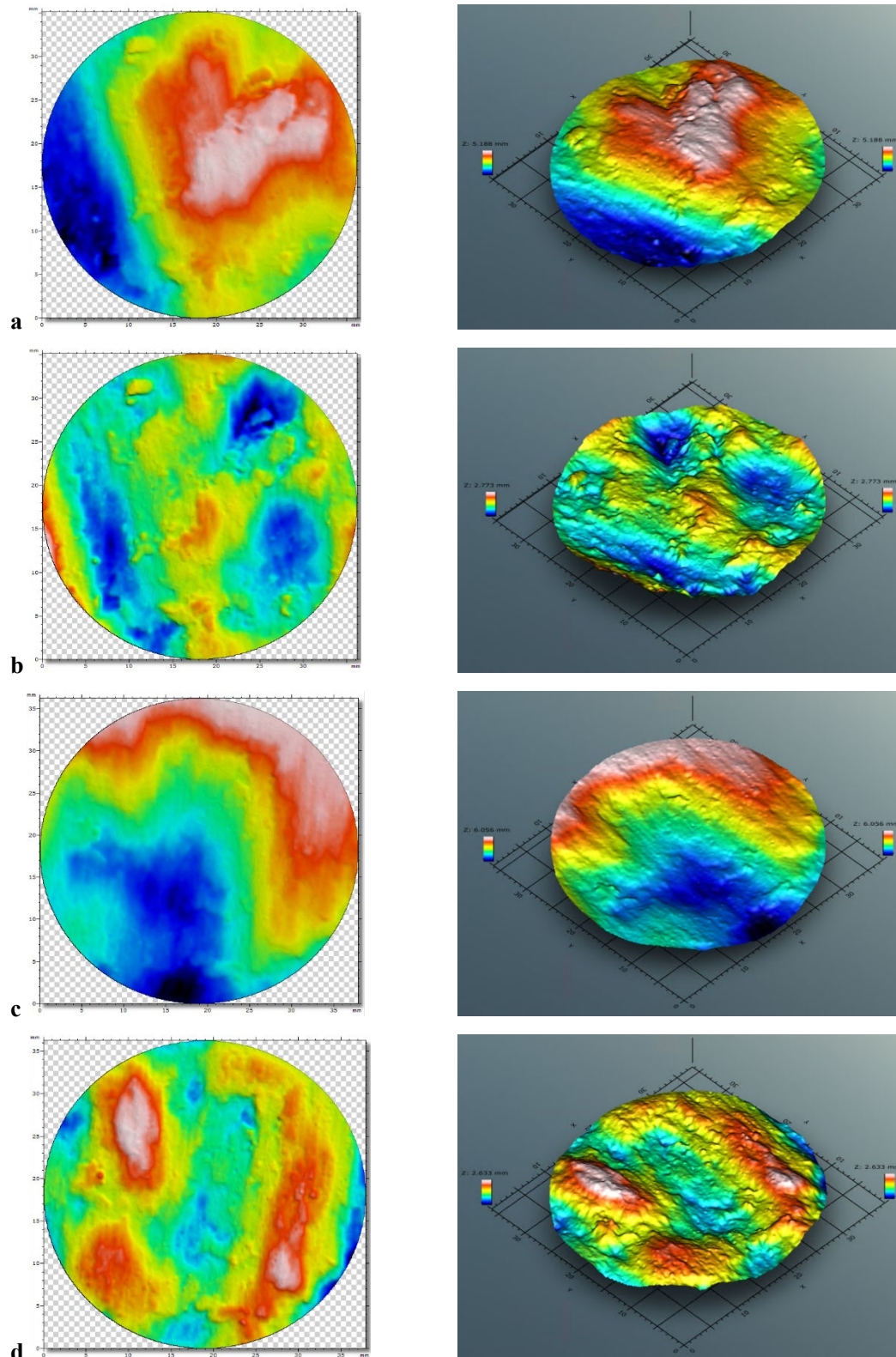


**Figure A-26.** Laser scan of shear fracture FPR-24-262 (DH4:R2:290:575-BGS). a) Bottom surface raw scan; b) Bottom surface with form removed; c) Top surface raw scan; d) Top surface with form removed. Shear direction is parallel with Y-axis, i.e. top-to-bottom in left.

**FPR-24-262****Table A-13. Results for test FPR-24-262 (DH4:R2:290:575-BGS)**

Parameter	Value	±	Units
SKB Sample name	DH4:R2:290:575-BGS		
BGS Sample name	FPR-24-262		
Normal load	4.704	0.004	MPa
Peak shear stress	4.553		MPa
Yield shear stress	4.165		MPa
Residual shear stress	1.591		MPa
Shear modulus	229.6		MPa
Displacement at peak	1517		µm
Maximum displacement	5532		µm
Displacement rate	1.032		µm/s
Sample diameter	47.25	0.02	mm
Sample height	53.10	0.02	mm
Sample weight	194.11		g
Bulk density	2.08		g/cm <sup>3</sup>
Sample colour	67.41,-5.73,6.51		L, a, b
Colour of bottom slip plane	68.07,-4.72,7.25		L, a, b
Weight of bottom sample	100.925		g
Weight after drying	87.924		g
Moisture content	12.9		%
Bottom: Raw: $s_a$	1.075		mm
Bottom: Raw: $s_q$	1.314		mm
Bottom: Raw: $s_t$	5.188		mm
Top: Raw: $s_a$	1.344		mm
Top: Raw: $s_q$	1.551		mm
Top: Raw: $s_t$	6.056		mm
Bottom: Surf: $s_a$	0.325		mm
Bottom: Surf: $s_q$	0.4		mm
Bottom: Surf: $s_t$	2.773		mm
Top: Surf: $s_a$	0.375		mm
Top: Surf: $s_q$	0.452		mm
Top: Surf: $s_t$	2.633		mm



# **FPR-24-266**

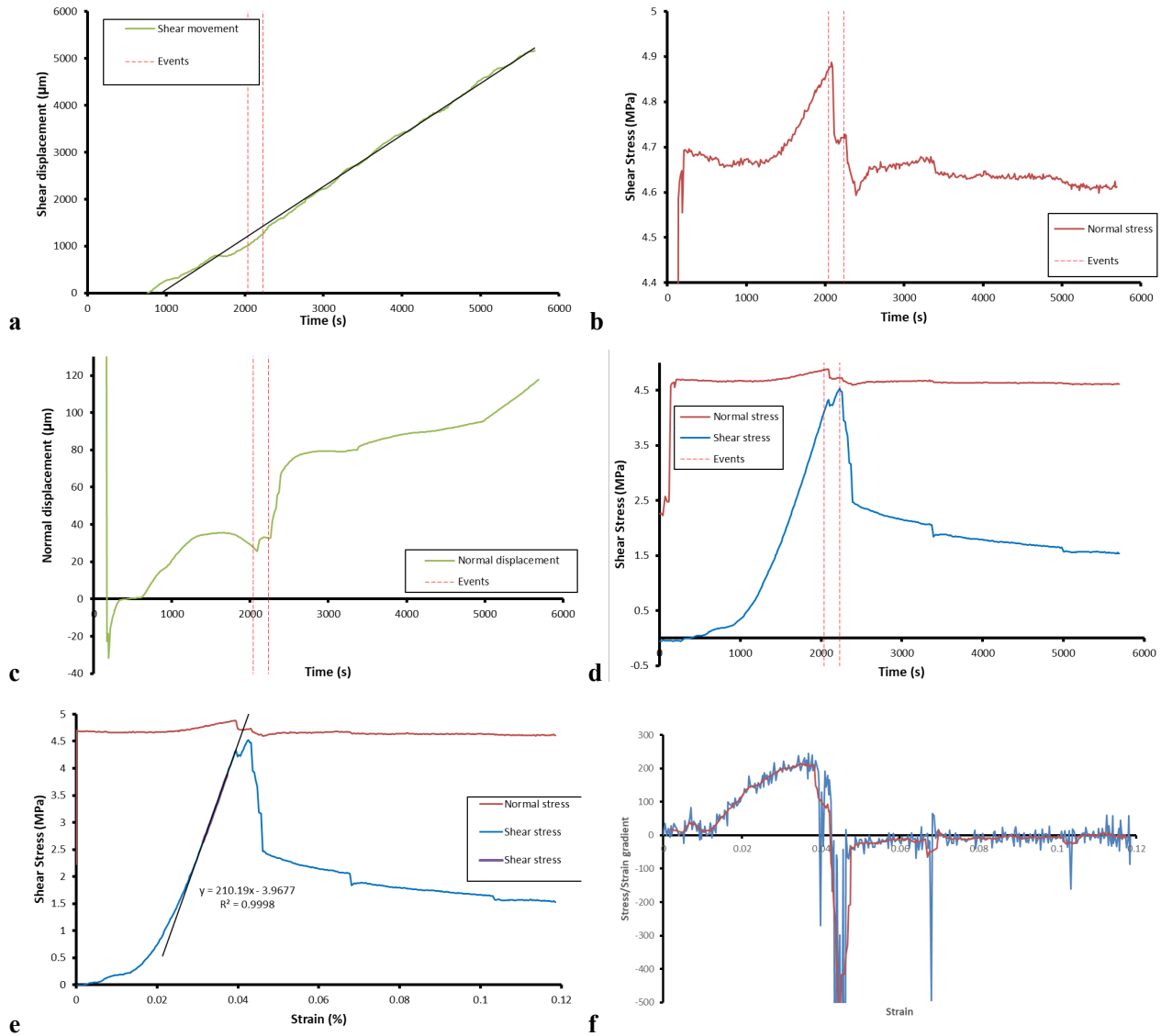


**Figure A-27.** Shear results for test FPR-24-266 (DH4;R2:290:625-BGS). a) Displacement with time; b) Normal load with time; c) Normal displacement with time; d) Normal and shear stress with time; e) Stress vs strain; f) Gradient of stress/strain (shear modulus).

**FPR-24-266**

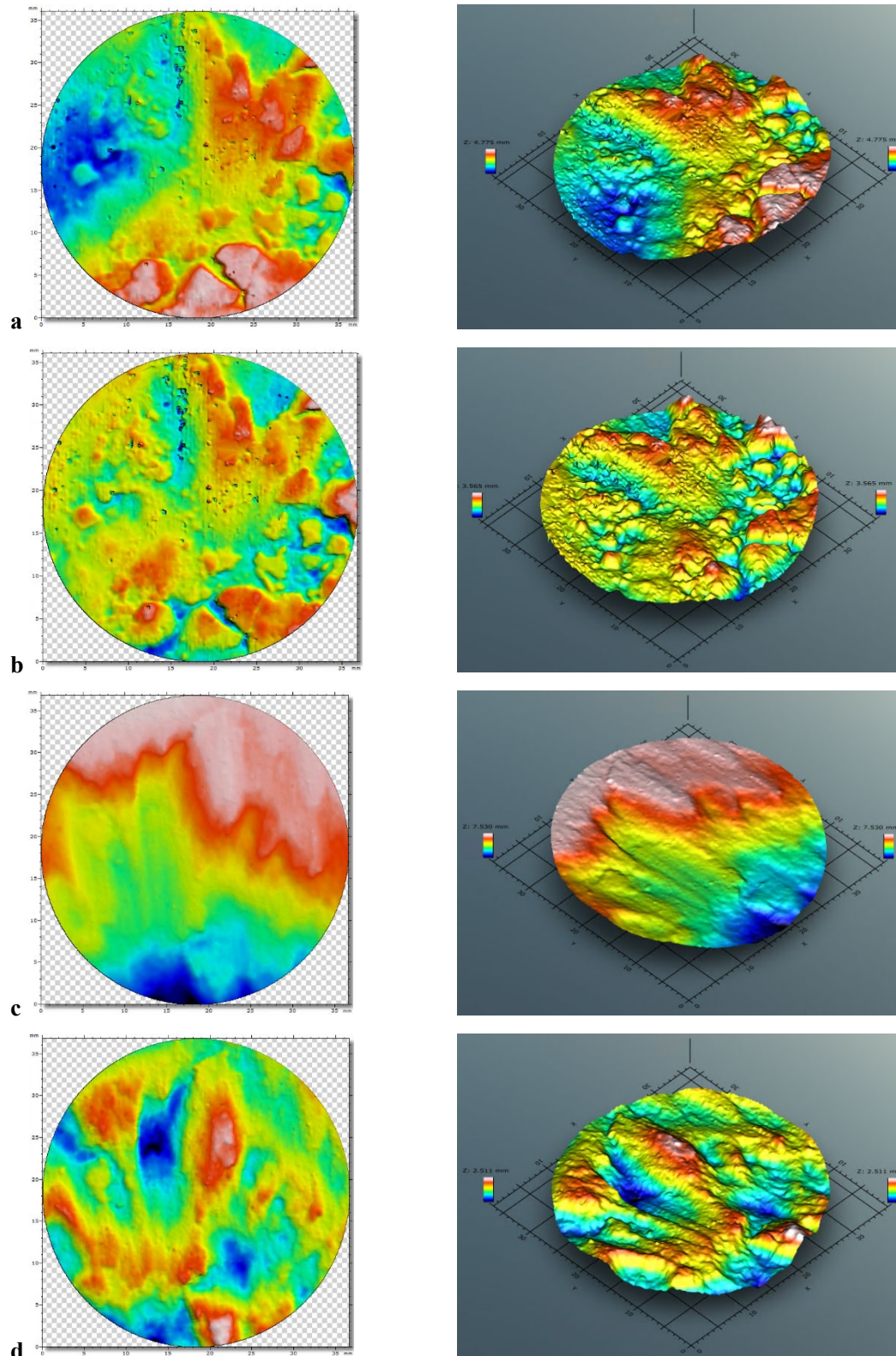


**Figure A-28.** Laser scan of shear fracture FPR-24-266 (DH4:R2:290:625-BGS). a) Bottom surface raw scan; b) Bottom surface with form removed; c) Top surface raw scan; d) Top surface with form removed. Shear direction is parallel with Y-axis, i.e. top-to-bottom in left.

**FPR-24-266****Table A-14. Results for test FPR-24-266 (DH4:R2:290:625-BGS)**

Parameter	Value	±	Units
SKB Sample name	DH4:R2:290:625-BGS		
BGS Sample name	FPR-24-266		
Normal load	4.695	0.003	MPa
Peak shear stress	4.530		MPa
Yield shear stress	4.116		MPa
Residual shear stress	1.660		MPa
Shear modulus	214.7		MPa
Displacement at peak	2002		µm
Maximum displacement	5573		µm
Displacement rate	1.032		µm/s
Sample diameter	47.24	0.02	mm
Sample height	52.88	0.01	mm
Sample weight	193.45		g
Bulk density	2.09		g/cm <sup>3</sup>
Sample colour	67.12,-5.56,7.08		L, a, b
Colour of bottom slip plane	61.69,-4.69,7.30		L, a, b
Weight of bottom sample	96.473		g
Weight after drying	83.839		g
Moisture content	13.1		%
Bottom: Raw: $s_a$	0.814		mm
Bottom: Raw: $s_q$	0.967		mm
Bottom: Raw: $s_t$	4.775		mm
Top: Raw: $s_a$	1.516		mm
Top: Raw: $s_q$	1.751		mm
Top: Raw: $s_t$	7.53		mm
Bottom: Surf: $s_a$	0.392		mm
Bottom: Surf: $s_q$	0.49		mm
Bottom: Surf: $s_t$	3.565		mm
Top: Surf: $s_a$	0.33		mm
Top: Surf: $s_q$	0.411		mm
Top: Surf: $s_t$	2.511		mm

# **FPR-24-267**

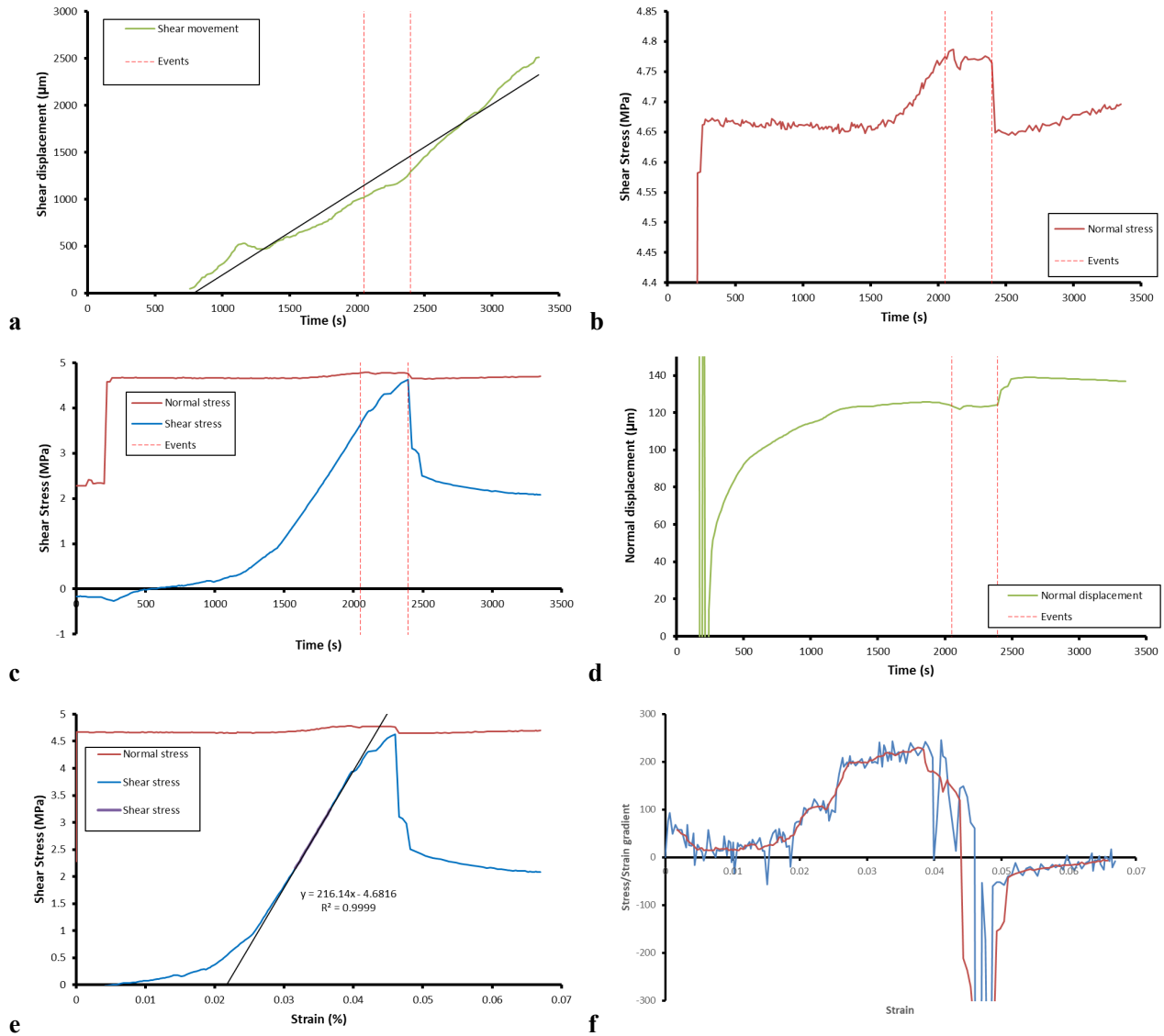


**Figure A-29.** Shear results for test FPR-24-267 (DH4;R2:290:625-BGS). a) Displacement with time; b) Normal load with time; c) Normal displacement with time; d) Normal and shear stress with time; e) Stress vs strain; f) Gradient of stress/strain (shear modulus).



# **FPR-24-267**

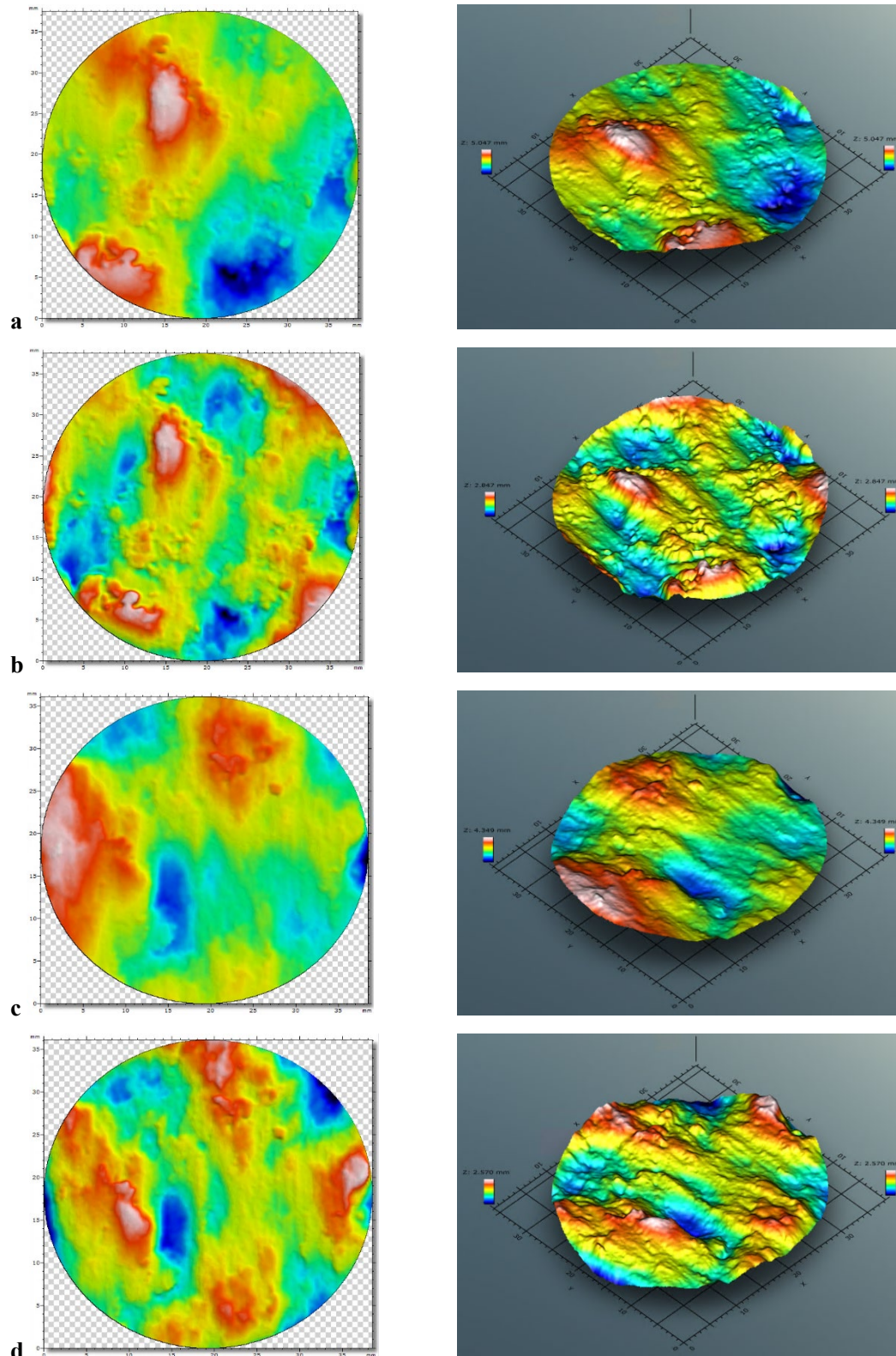


**Figure A-30.** Laser scan of shear fracture FPR-24-267 (DH4:R2:290:625-BGS). a) Bottom surface raw scan; b) Bottom surface with form removed; c) Top surface raw scan; d) Top surface with form removed. Shear direction is parallel with Y-axis, i.e. top-to-bottom in left.

**FPR-24-267****Table A-15. Results for test FPR-24-267 (DH4:R2:290:625-BGS)**

Parameter	Value	±	Units
SKB Sample name	DH4:R2:290:625-BGS		
BGS Sample name	FPR-24-267		
Normal load	4.711	0.003	MPa
Peak shear stress	4.629		MPa
Yield shear stress	3.644		MPa
Residual shear stress	2.082		MPa
Shear modulus	230.0		MPa
Displacement at peak	2162		µm
Maximum displacement	3147		µm
Displacement rate	1.032		µm/s
Sample diameter	47.27	0.02	mm
Sample height	52.82	0.03	mm
Sample weight	192.91		g
Bulk density	2.08		g/cm <sup>3</sup>
Sample colour	67.41,-5.76,6.58		L, a, b
Colour of bottom slip plane	60.22,-4.66,6.80		L, a, b
Weight of bottom sample	95.157		g
Weight after drying	82.749		g
Moisture content	13.0		%
Bottom: Raw: $s_a$	0.715		mm
Bottom: Raw: $s_q$	0.91		mm
Bottom: Raw: $s_t$	5.047		mm
Top: Raw: $s_a$	0.6		mm
Top: Raw: $s_q$	0.743		mm
Top: Raw: $s_t$	4.349		mm
Bottom: Surf: $s_a$	0.374		mm
Bottom: Surf: $s_q$	0.468		mm
Bottom: Surf: $s_t$	2.847		mm
Top: Surf: $s_a$	0.342		mm
Top: Surf: $s_q$	0.424		mm
Top: Surf: $s_t$	2.57		mm



# **FPR-24-271**

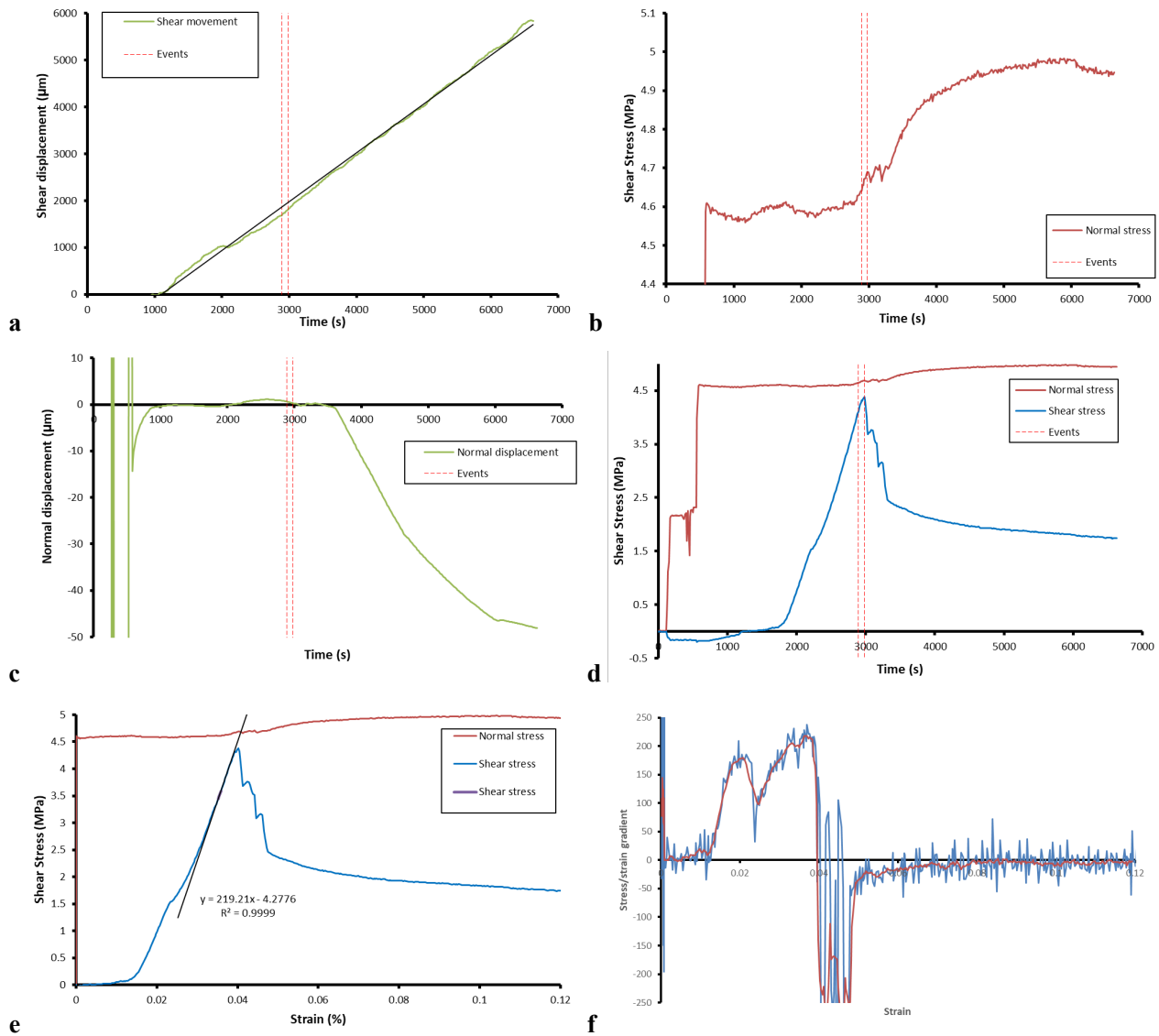


**Figure A-31.** Shear results for test FPR-24-271 (DH4;R2:290:675-BGS). a) Displacement with time; b) Normal load with time; c) Normal displacement with time; d) Normal and shear stress with time; e) Stress vs strain; f) Gradient of stress/strain (shear modulus).

**FPR-24-271**

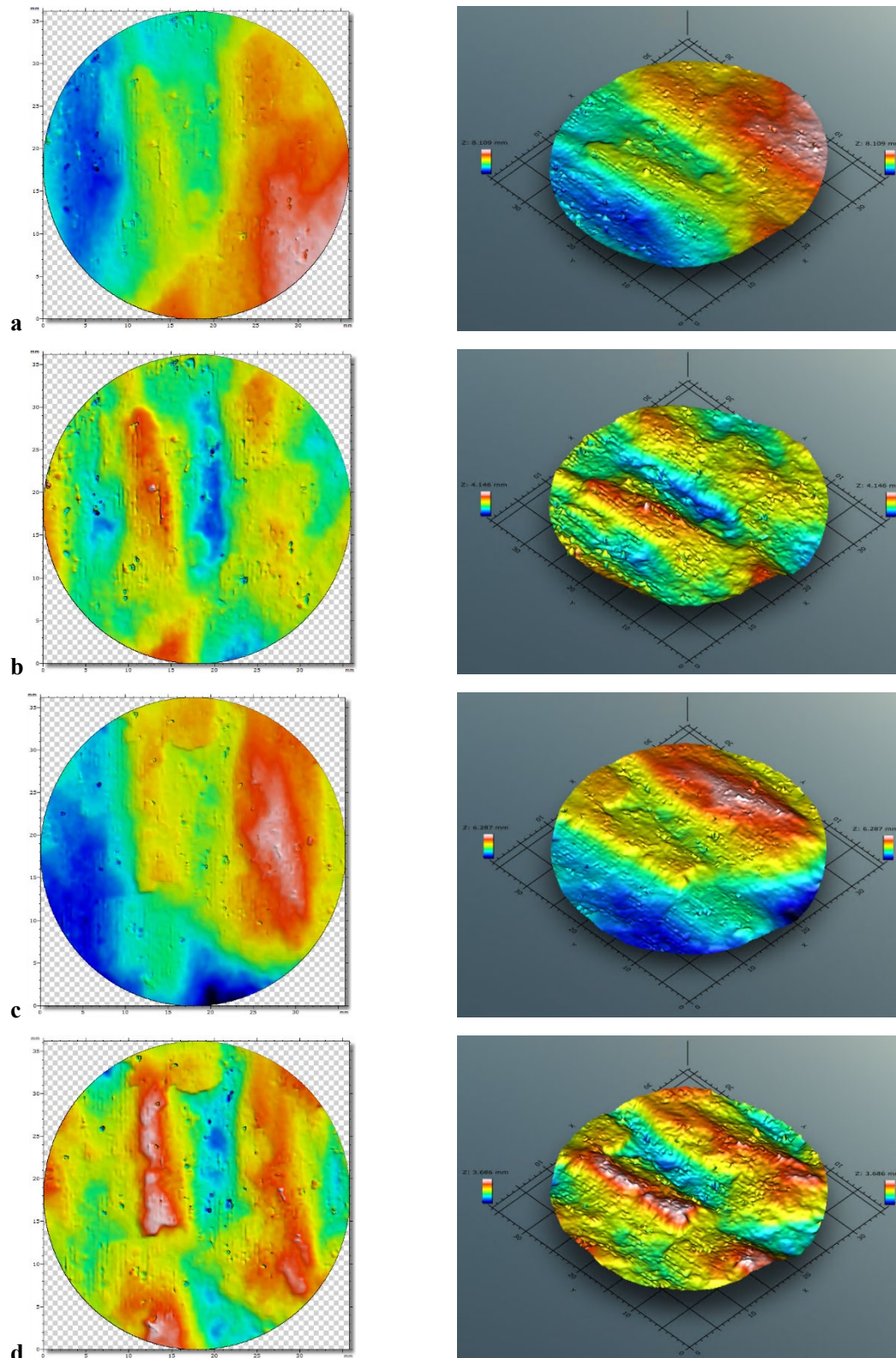


**Figure A-32.** Laser scan of shear fracture FPR-24-271 (DH4:R2:290:675-BGS). a) Bottom surface raw scan; b) Bottom surface with form removed; c) Top surface raw scan; d) Top surface with form removed. Shear direction is parallel with Y-axis, i.e. top-to-bottom in left.

**FPR-24-271****Table A-16. Results for test FPR-24-271 (DH4:R2:290:675-BGS)**

Parameter	Value	±	Units
SKB Sample name	DH4:R2:290:675-BGS		
BGS Sample name	FPR-24-271		
Normal load	4.809	0.008	MPa
Peak shear stress	4.382		MPa
Yield shear stress	4.105		MPa
Residual shear stress	1.838		MPa
Shear modulus	217.8		MPa
Displacement at peak	1892		µm
Maximum displacement	5659		µm
Displacement rate	1.032		µm/s
Sample diameter	47.18	0.01	mm
Sample height	49.96	0.03	mm
Sample weight	182.59		g
Bulk density	2.09		g/cm <sup>3</sup>
Sample colour	65.91,-5.62,6.90		L, a, b
Colour of bottom slip plane	57.36,-5.11,7.12		L, a, b
Weight of bottom sample	93.577		g
Weight after drying	81.197		g
Moisture content	13.2		%
Bottom: Raw: $s_a$	1.438		mm
Bottom: Raw: $s_q$	1.671		mm
Bottom: Raw: $s_t$	8.109		mm
Top: Raw: $s_a$	1.178		mm
Top: Raw: $s_q$	1.37		mm
Top: Raw: $s_t$	6.287		mm
Bottom: Surf: $s_a$	0.42		mm
Bottom: Surf: $s_q$	0.52		mm
Bottom: Surf: $s_t$	4.146		mm
Top: Surf: $s_a$	0.458		mm
Top: Surf: $s_q$	0.557		mm
Top: Surf: $s_t$	3.686		mm

# **FPR-24-274**

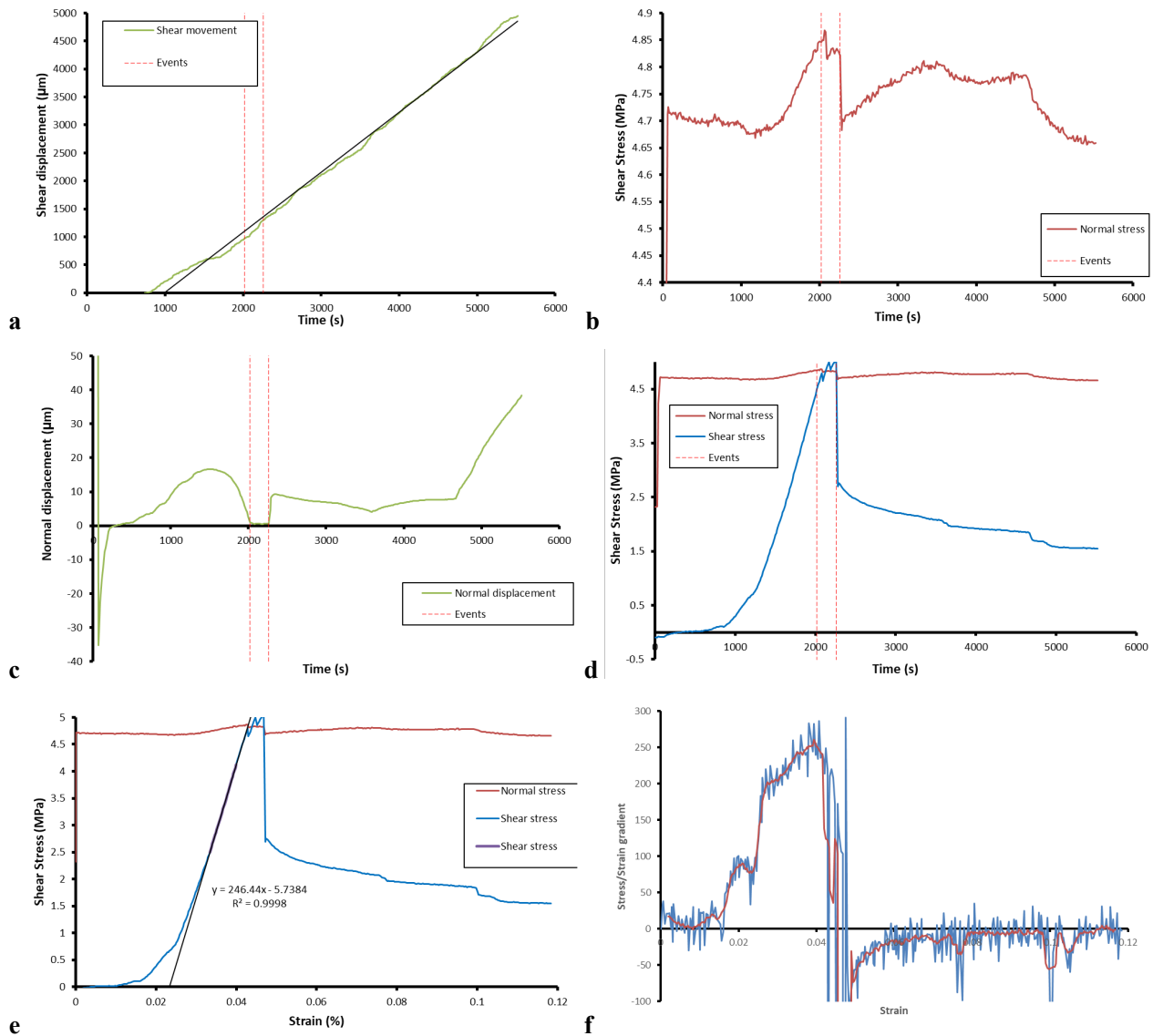


**Figure A-33.** Shear results for test FPR-24-274 (DH4:R2:290:725-BGS). a) Displacement with time; b) Normal load with time; c) Normal displacement with time; d) Normal and shear stress with time; e) Stress vs strain; f) Gradient of stress/strain (shear modulus).



# **FPR-24-274**

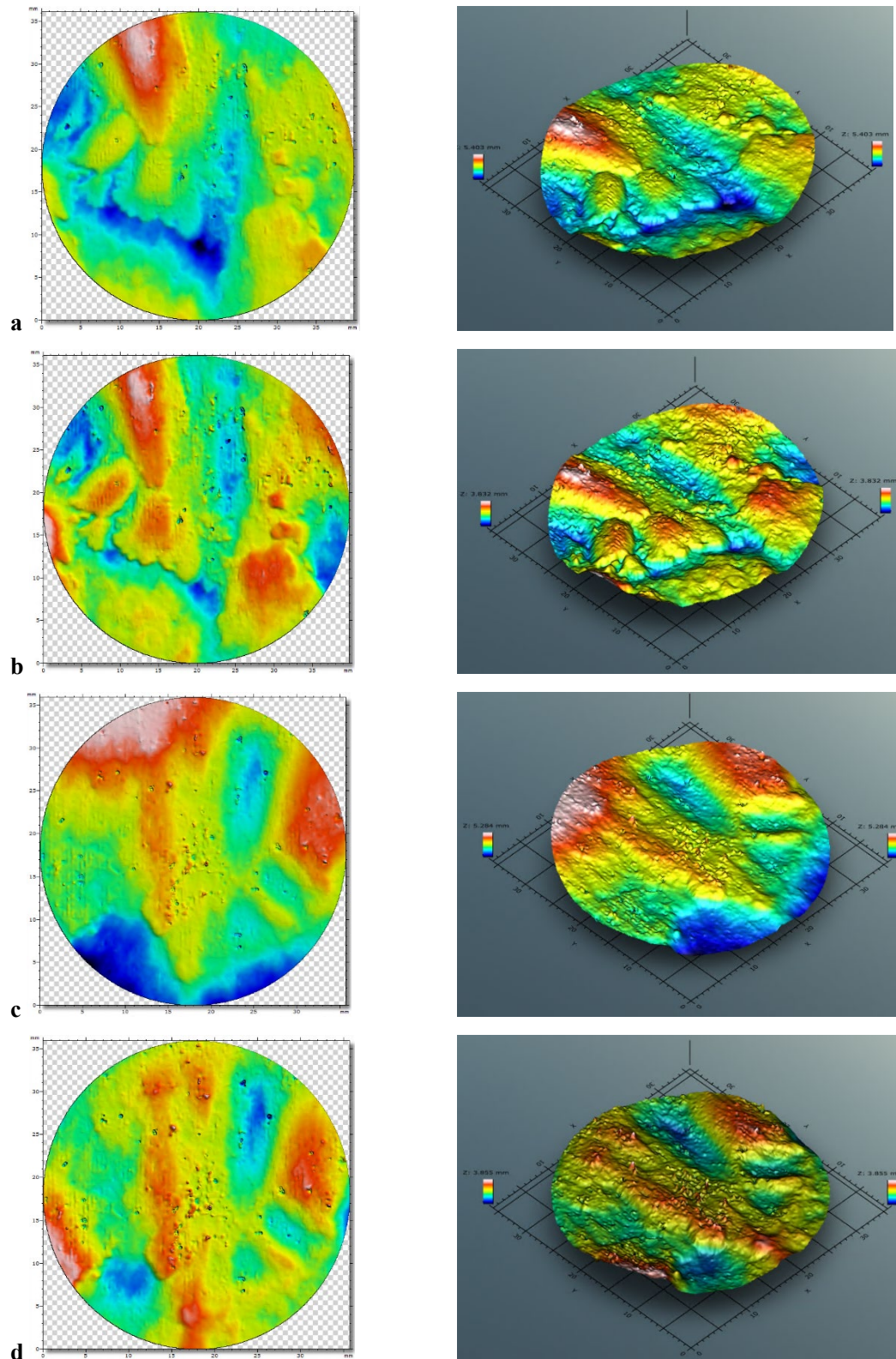


**Figure A-34.** Laser scan of shear fracture FPR-24-274 (DH4:R2:290:725-BGS). a) Bottom surface raw scan; b) Bottom surface with form removed; c) Top surface raw scan; d) Top surface with form removed. Shear direction is parallel with Y-axis, i.e. top-to-bottom in left.

**FPR-24-274****Table A-17. Results for test FPR-24-274 (DH4:R2:290:725-BGS)**

Parameter	Value	±	Units
SKB Sample name	DH4:R2:290:725-BGS		
BGS Sample name	FPR-24-274		
Normal load	4.771	0.003	MPa
Peak shear stress	5.047		MPa
Yield shear stress	4.495		MPa
Residual shear stress	1.756		MPa
Shear modulus	260.5		MPa
Displacement at peak	2198		µm
Maximum displacement	5563		µm
Displacement rate	1.032		µm/s
Sample diameter	47.21	0.01	mm
Sample height	52.74	0.05	mm
Sample weight	193.40		g
Bulk density	2.09		g/cm <sup>3</sup>
Sample colour	63.76,-5.54,7.04		L, a, b
Colour of bottom slip plane	59.96,-4.37,7.63		L, a, b
Weight of bottom sample	97.152		g
Weight after drying	83.951		g
Moisture content	13.6		%
Bottom: Raw: $s_a$	0.62		mm
Bottom: Raw: $s_q$	0.804		mm
Bottom: Raw: $s_t$	5.403		mm
Top: Raw: $s_a$	0.814		mm
Top: Raw: $s_q$	1.023		mm
Top: Raw: $s_t$	5.284		mm
Bottom: Surf: $s_a$	0.464		mm
Bottom: Surf: $s_q$	0.577		mm
Bottom: Surf: $s_t$	3.832		mm
Top: Surf: $s_a$	0.431		mm
Top: Surf: $s_q$	0.532		mm
Top: Surf: $s_t$	3.855		mm



# **FPR-24-277**

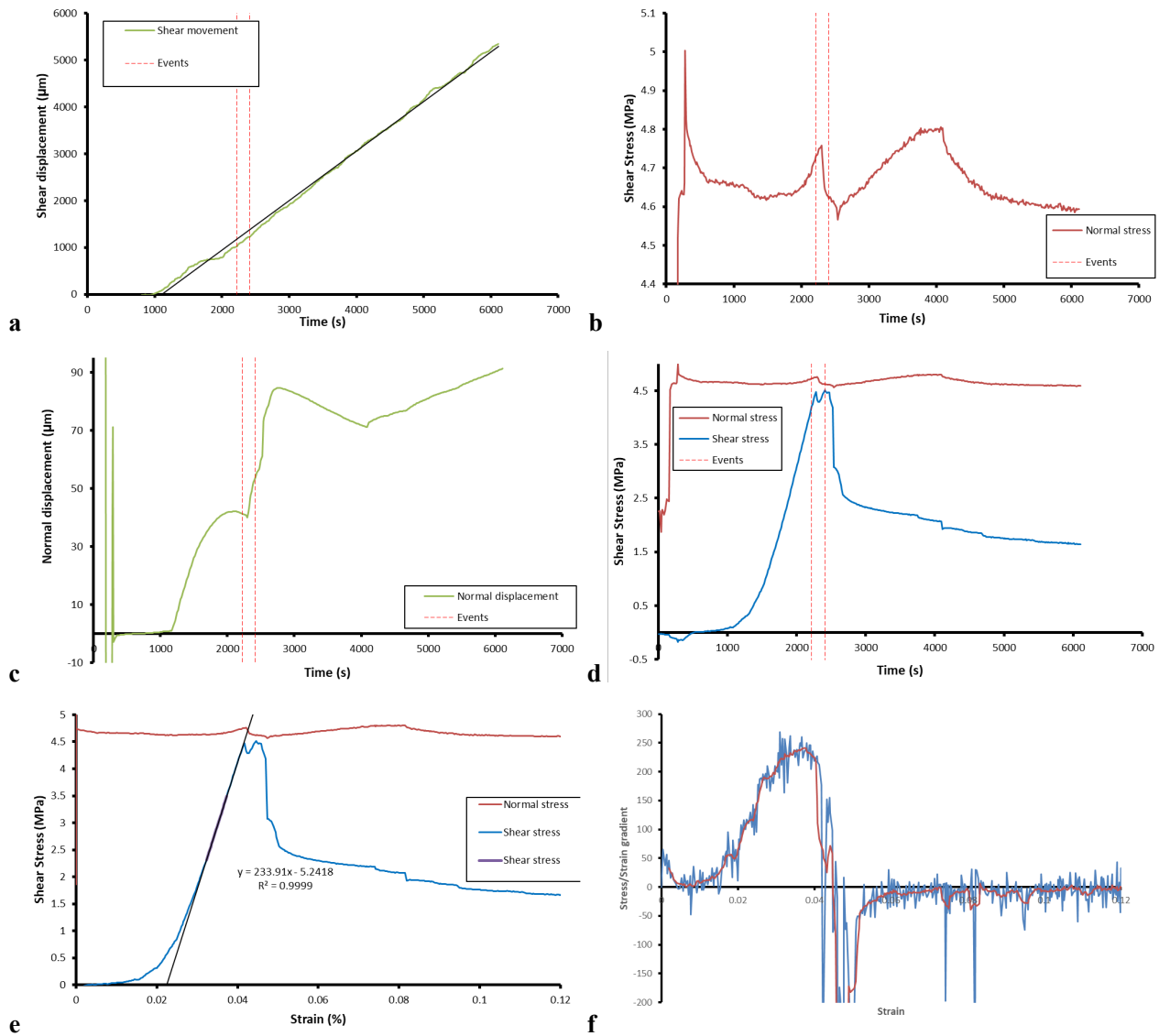


**Figure A-35.** Shear results for test FPR-24-277 (DH4;R2:290:775-BGS). a) Displacement with time; b) Normal load with time; c) Normal displacement with time; d) Normal and shear stress with time; e) Stress vs strain; f) Gradient of stress/strain (shear modulus).

# **FPR-24-277**

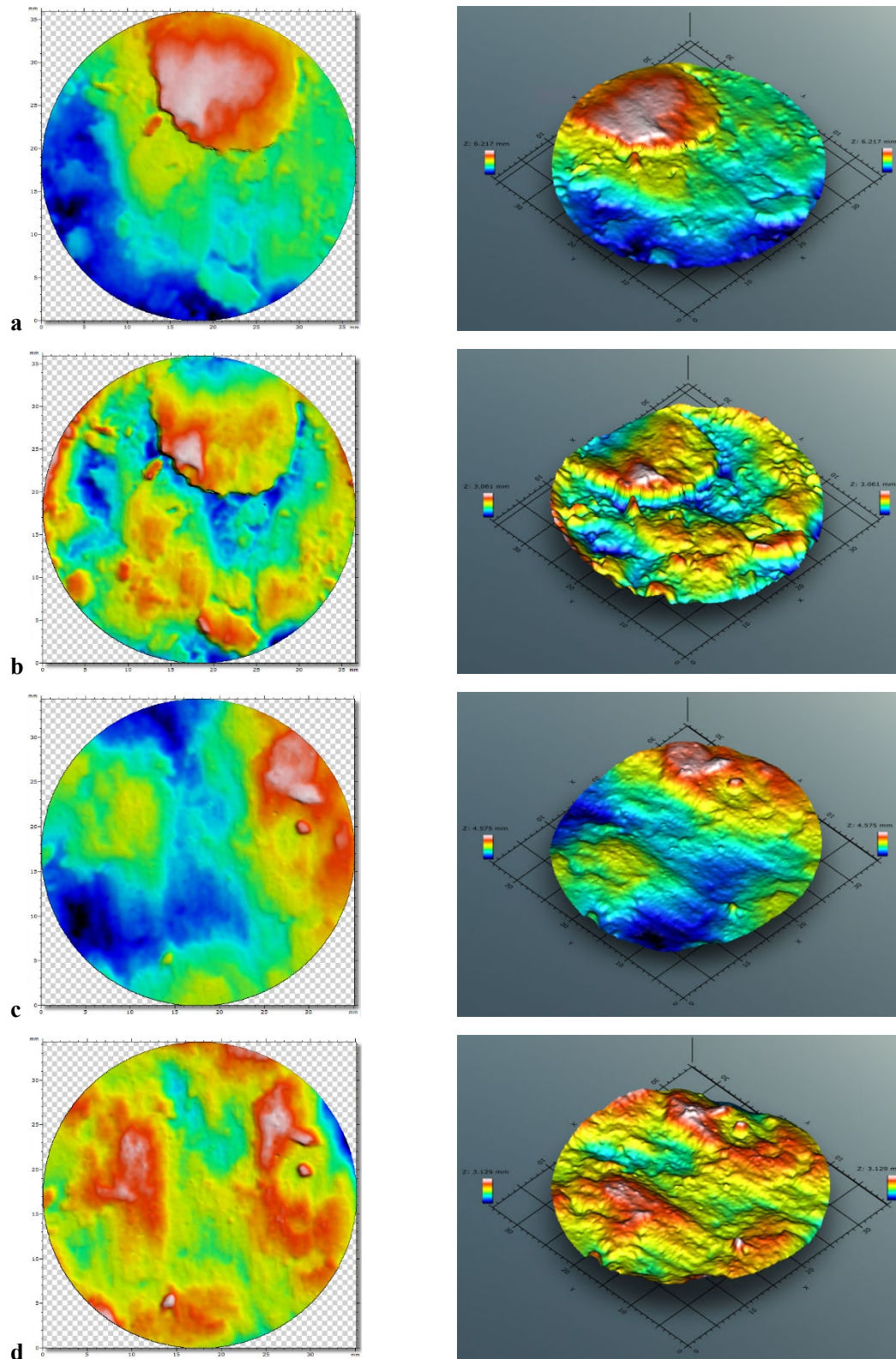


**Figure A-36.** Laser scan of shear fracture FPR-24-277 (DH4:R2:290:775-BGS). a) Bottom surface raw scan; b) Bottom surface with form removed; c) Top surface raw scan; d) Top surface with form removed. Shear direction is parallel with Y-axis, i.e. top-to-bottom in left.

**FPR-24-277****Table A-18. Results for test FPR-24-277 (DH4:R2:290:775-BGS)**

Parameter	Value	±	Units
SKB Sample name	DH4:R2:290:775-BGS		
BGS Sample name	FPR-24-277		
Normal load	4.695	0.003	MPa
Peak shear stress	4.510		MPa
Yield shear stress	4.206		MPa
Residual shear stress	1.762		MPa
Shear modulus	240.9		MPa
Displacement at peak	2095		µm
Maximum displacement	5913		µm
Displacement rate	1.032		µm/s
Sample diameter	47.23	0.01	mm
Sample height	53.14	0.01	mm
Sample weight	195.24		g
Bulk density	2.10		g/cm <sup>3</sup>
Sample colour	64.49,-5.52,7.14		L, a, b
Colour of bottom slip plane	61.44,-4.63,7.79		L, a, b
Weight of bottom sample	97.306		g
Weight after drying	83.932		g
Moisture content	13.7		%
Bottom: Raw: $s_a$	1.138		mm
Bottom: Raw: $s_q$	1.434		mm
Bottom: Raw: $s_t$	6.217		mm
Top: Raw: $s_a$	0.741		mm
Top: Raw: $s_q$	0.924		mm
Top: Raw: $s_t$	4.575		mm
Bottom: Surf: $s_a$	0.413		mm
Bottom: Surf: $s_q$	0.5		mm
Bottom: Surf: $s_t$	3.061		mm
Top: Surf: $s_a$	0.338		mm
Top: Surf: $s_q$	0.414		mm
Top: Surf: $s_t$	3.129		mm

# **FPR-24-282**

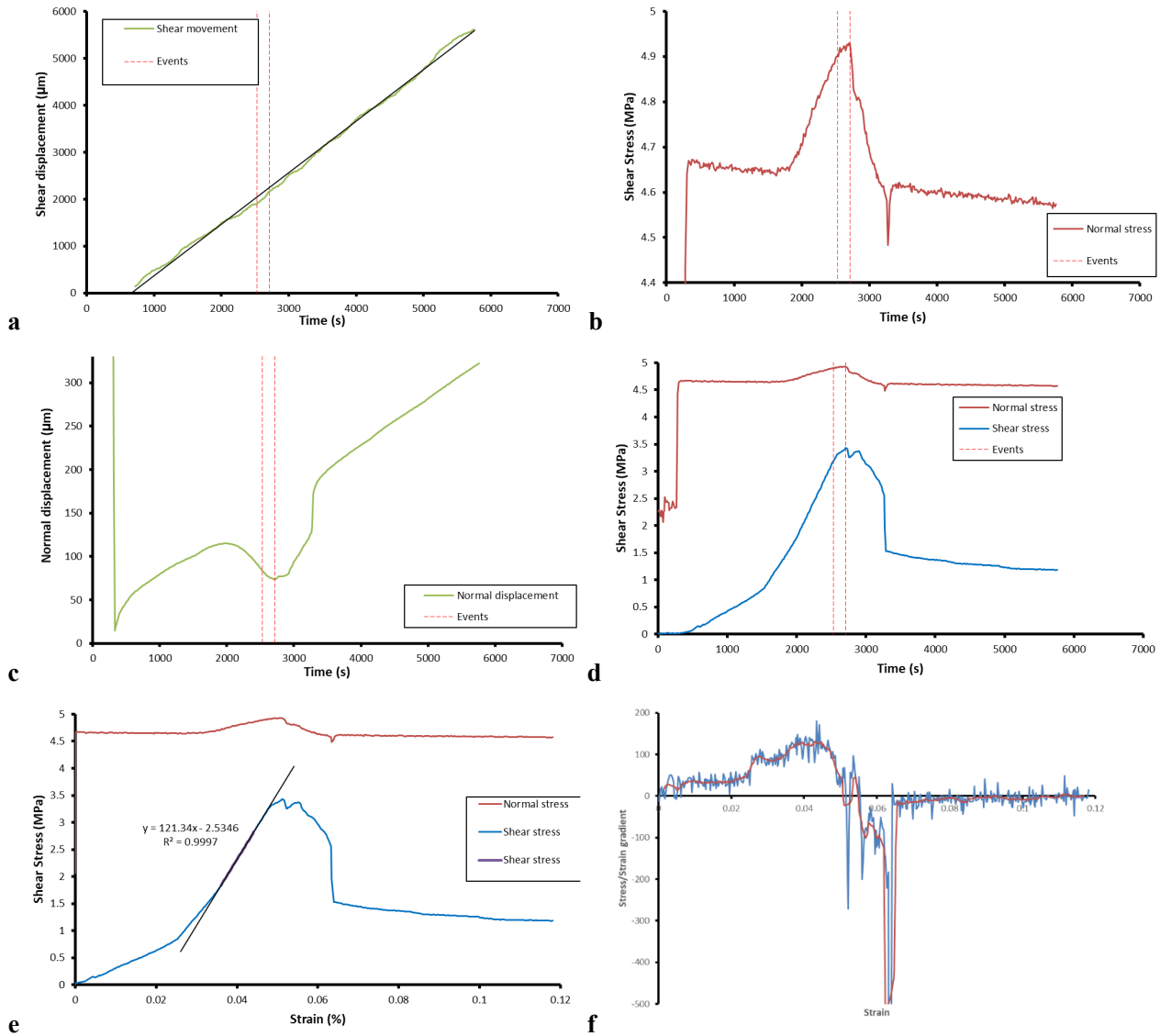


**Figure A-37.** Shear results for test FPR-24-282 (DH4;R6:290:575-BGS). a) Displacement with time; b) Normal load with time; c) Normal displacement with time; d) Normal and shear stress with time; e) Stress vs strain; f) Gradient of stress/strain (shear modulus).



# **FPR-24-282**

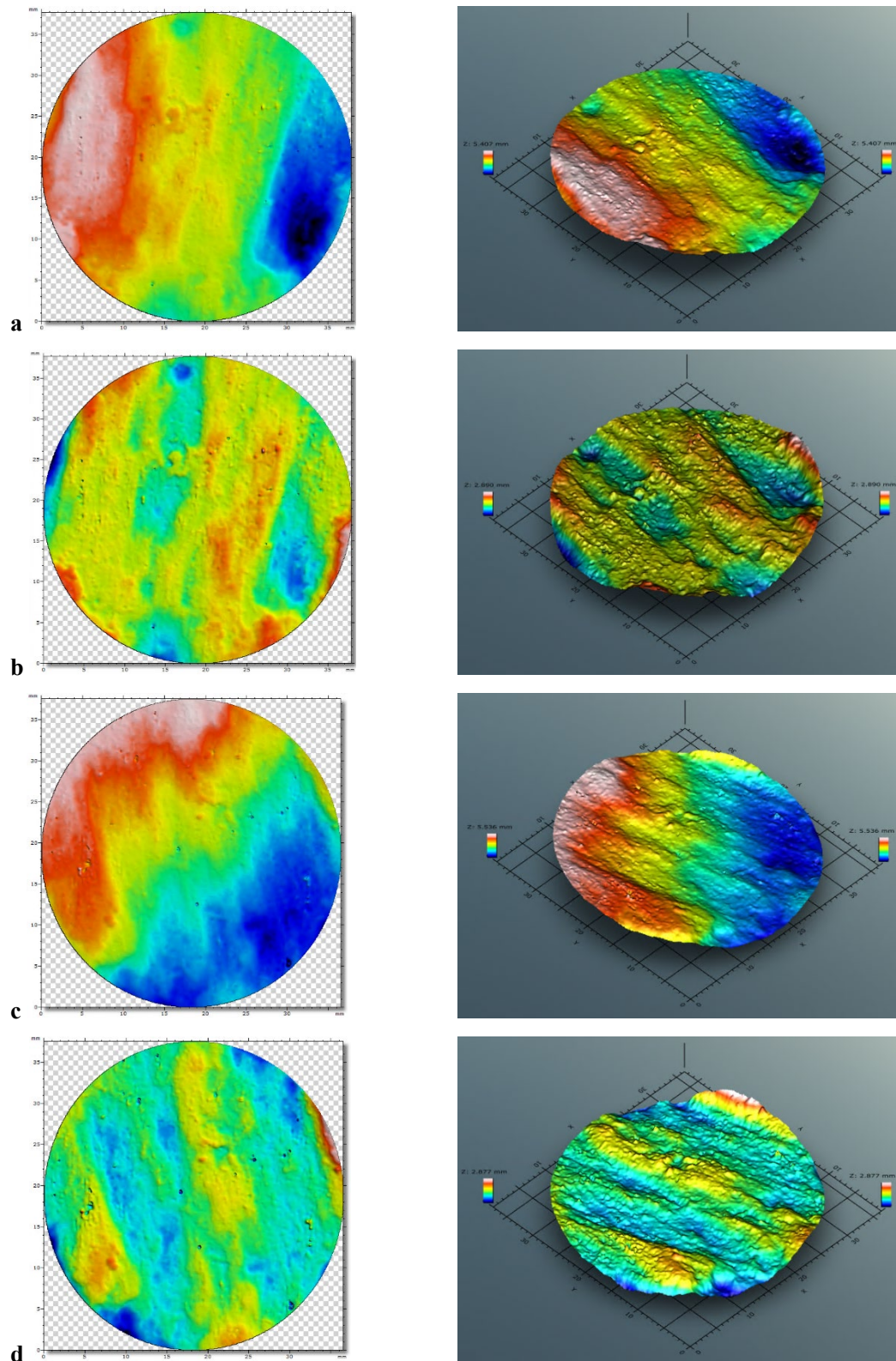


**Figure A-38.** Laser scan of shear fracture FPR-24-282 (DH4:R6:290:575-BGS). a) Bottom surface raw scan; b) Bottom surface with form removed; c) Top surface raw scan; d) Top surface with form removed. Shear direction is parallel with Y-axis, i.e. top-to-bottom in left.



**FPR-24-282****Table A-19. Results for test FPR-24-282 (DH4:R6:290:575-BGS)**

Parameter	Value	±	Units
SKB Sample name	DH4:R6:290:575-BGS		
BGS Sample name	FPR-24-282		
Normal load	4.686	0.005	MPa
Peak shear stress	3.431		MPa
Yield shear stress	3.189		MPa
Residual shear stress	1.244		MPa
Shear modulus	132.0		MPa
Displacement at peak	2405		µm
Maximum displacement	5552		µm
Displacement rate	1.032		µm/s
Sample diameter	47.04	0.10	mm
Sample height	53.24	0.04	mm
Sample weight	192.28		g
Bulk density	2.07		g/cm <sup>3</sup>
Sample colour	56.42,-5.22,7.57		L, a, b
Colour of bottom slip plane	49.73,-4.56,8.37		L, a, b
Weight of bottom sample	97.340		g
Weight after drying	81.042		g
Moisture content	16.7		%
Bottom: Raw: $s_a$	0.992		mm
Bottom: Raw: $s_q$	1.239		mm
Bottom: Raw: $s_t$	5.407		mm
Top: Raw: $s_a$	1.241		mm
Top: Raw: $s_q$	1.409		mm
Top: Raw: $s_t$	5.536		mm
Bottom: Surf: $s_a$	0.271		mm
Bottom: Surf: $s_q$	0.35		mm
Bottom: Surf: $s_t$	2.89		mm
Top: Surf: $s_a$	0.252		mm
Top: Surf: $s_q$	0.321		mm
Top: Surf: $s_t$	2.877		mm

# **FPR-24-285**

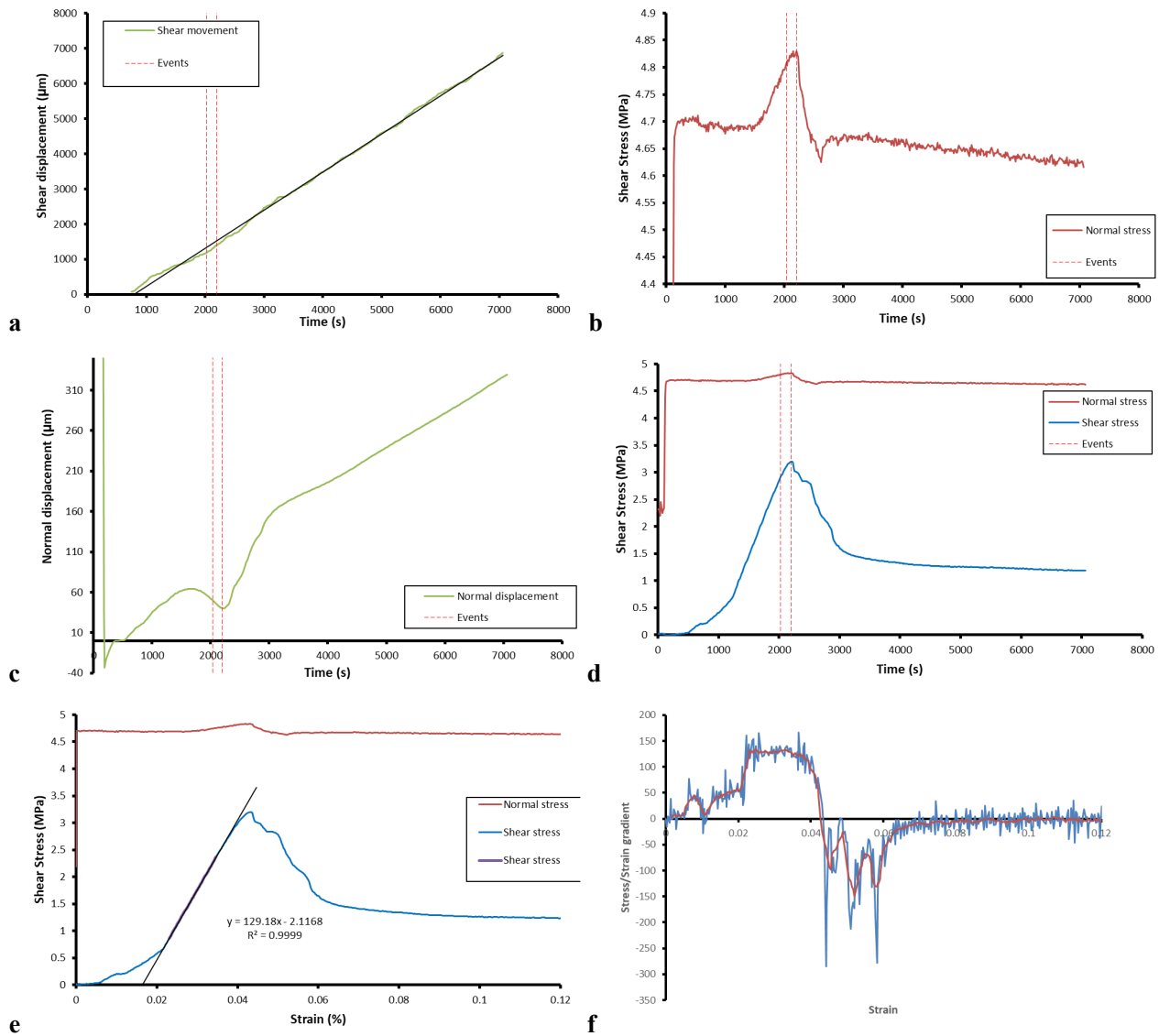


**Figure A-39.** Shear results for test FPR-24-285 (DH4;R6:290:625-BGS). a) Displacement with time; b) Normal load with time; c) Normal displacement with time; d) Normal and shear stress with time; e) Stress vs strain; f) Gradient of stress/strain (shear modulus).

# **FPR-24-285**

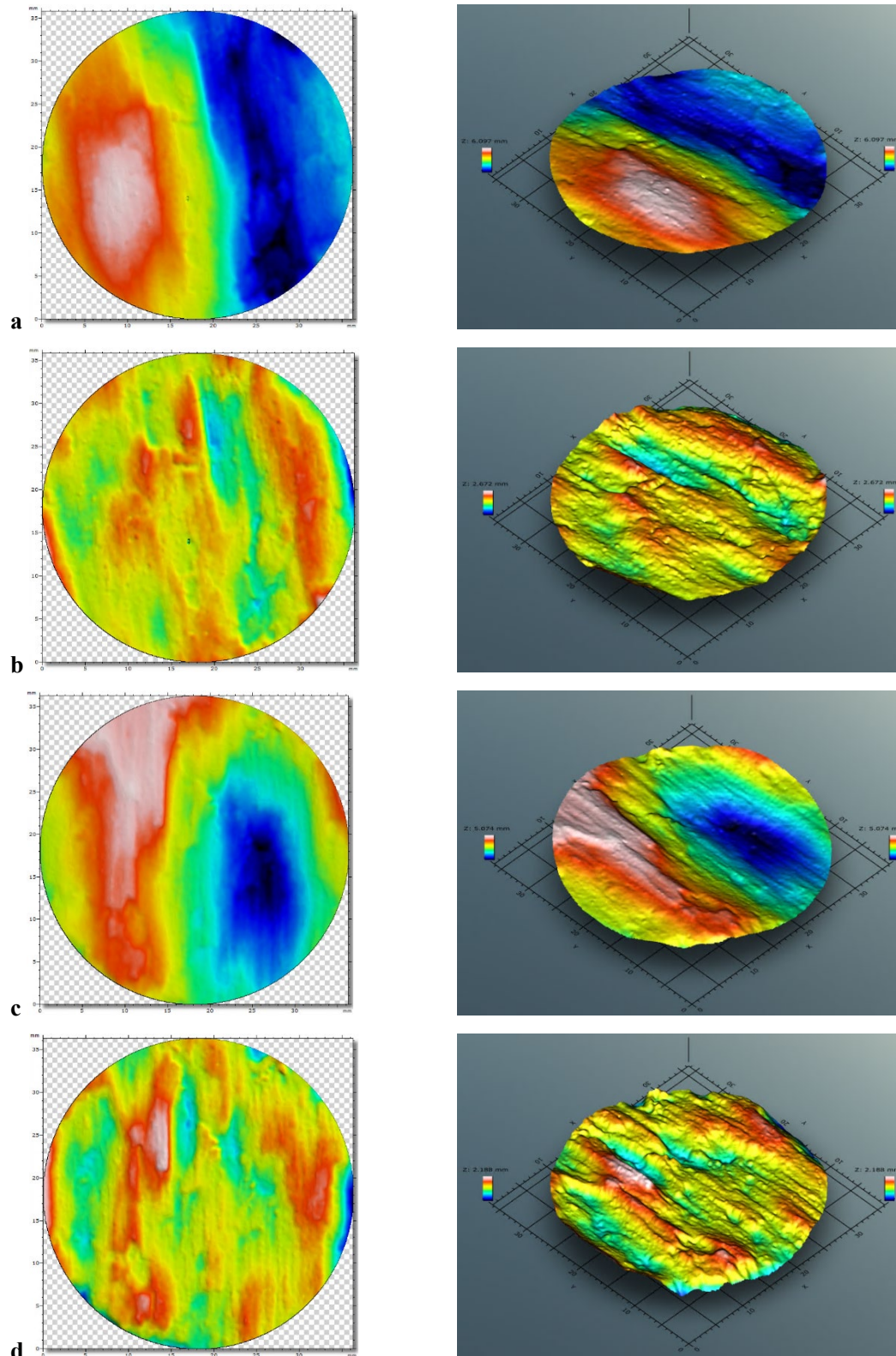


**Figure A-40.** Laser scan of shear fracture FPR-24-285 (DH4:R6:290:625-BGS). a) Bottom surface raw scan; b) Bottom surface with form removed; c) Top surface raw scan; d) Top surface with form removed. Shear direction is parallel with Y-axis, i.e. top-to-bottom in left.

**FPR-24-285****Table A-20. Results for test FPR-24-285 (DH4:R6:290:625-BGS)**

Parameter	Value	±	Units
SKB Sample name	DH4:R6:290:625-BGS		
BGS Sample name	FPR-24-285		
Normal load	4.700	0.002	MPa
Peak shear stress	3.200		MPa
Yield shear stress	2.918		MPa
Residual shear stress	1.266		MPa
Shear modulus	133.6		MPa
Displacement at peak	2023		µm
Maximum displacement	7038		µm
Displacement rate	1.032		µm/s
Sample diameter	47.11	0.09	mm
Sample height	51.90	0.02	mm
Sample weight	187.46		g
Bulk density	2.07		g/cm <sup>3</sup>
Sample colour	55.91,-5.23,8.04		L, a, b
Colour of bottom slip plane	48.24,-4.07,9.39		L, a, b
Weight of bottom sample	98.464		g
Weight after drying	81.305		g
Moisture content	17.4		%
Bottom: Raw: $s_a$	1.632		mm
Bottom: Raw: $s_q$	1.793		mm
Bottom: Raw: $s_t$	6.097		mm
Top: Raw: $s_a$	1.082		mm
Top: Raw: $s_q$	1.276		mm
Top: Raw: $s_t$	5.074		mm
Bottom: Surf: $s_a$	0.243		mm
Bottom: Surf: $s_q$	0.303		mm
Bottom: Surf: $s_t$	2.672		mm
Top: Surf: $s_a$	0.226		mm
Top: Surf: $s_q$	0.285		mm
Top: Surf: $s_t$	2.188		mm

# **FPR-24-290**

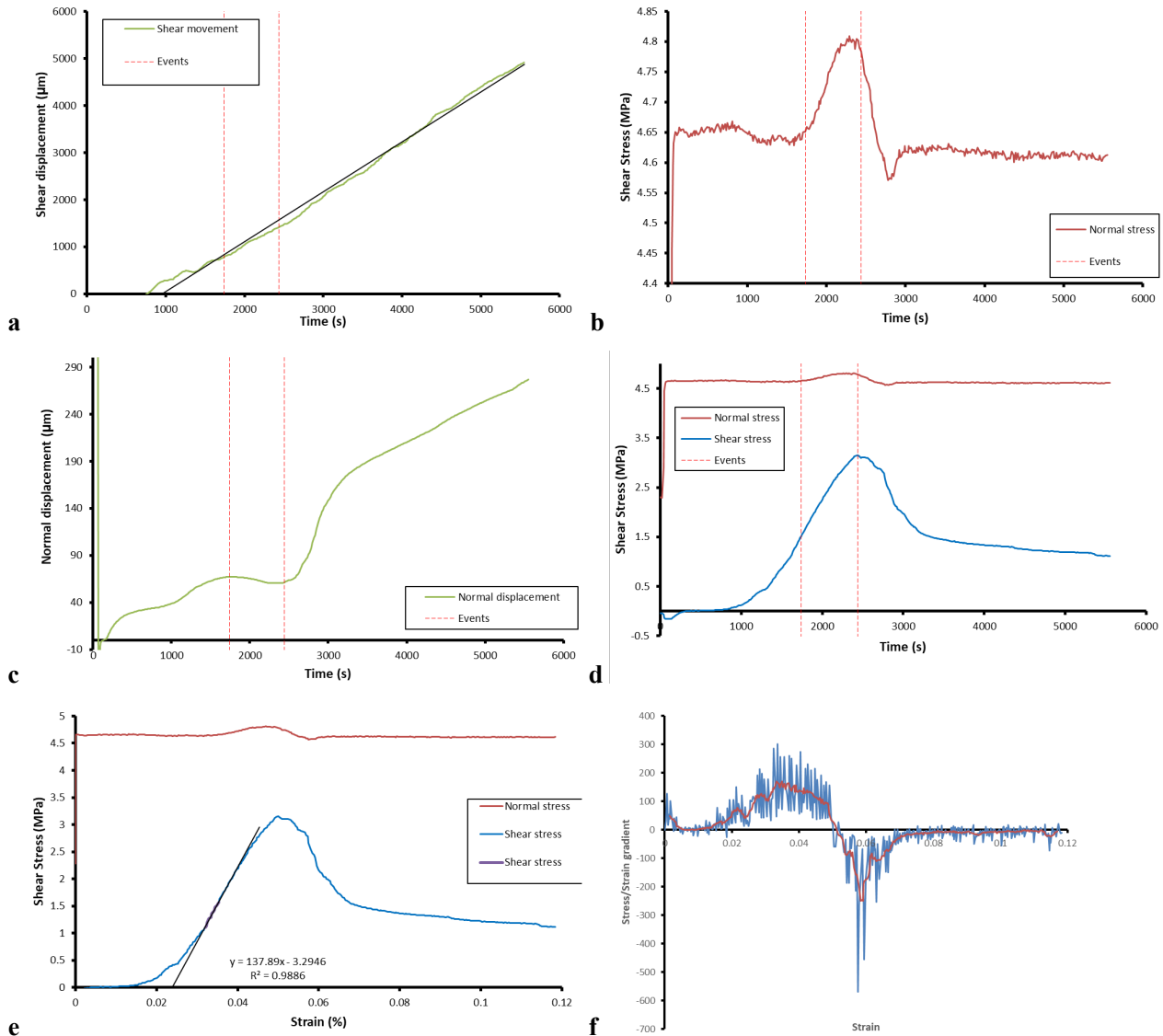


**Figure A-41.** Shear results for test FPR-24-290 (DH4;R6:290:675-BGS). a) Displacement with time; b) Normal load with time; c) Normal displacement with time; d) Normal and shear stress with time; e) Stress vs strain; f) Gradient of stress/strain (shear modulus).



# **FPR-24-290**

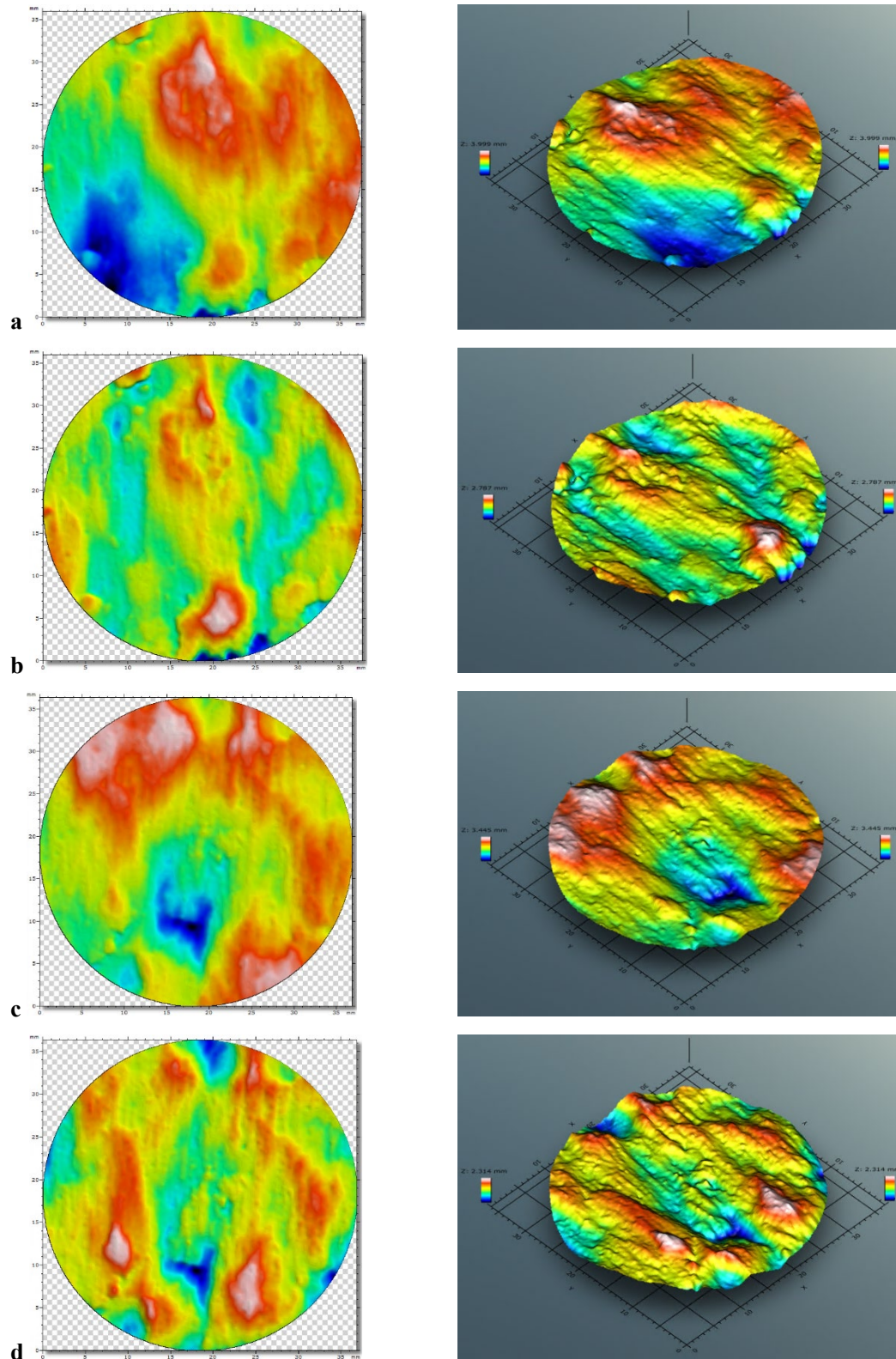


**Figure A-42.** Laser scan of shear fracture FPR-24-290 (DH4:R6:290:675-BGS). a) Bottom surface raw scan; b) Bottom surface with form removed; c) Top surface raw scan; d) Top surface with form removed. Shear direction is parallel with Y-axis, i.e. top-to-bottom in left.

**FPR-24-290****Table A-21. Results for test FPR-24-290 (DH4:R6:290:675-BGS)**

Parameter	Value	±	Units
SKB Sample name	DH4:R6:290:675-BGS		
BGS Sample name	FPR-24-290		
Normal load	4.673	0.003	MPa
Peak shear stress	3.152		MPa
Yield shear stress	1.513		MPa
Residual shear stress	1.224		MPa
Shear modulus	171.0		MPa
Displacement at peak	2353		µm
Maximum displacement	5563		µm
Displacement rate	1.032		µm/s
Sample diameter	47.07	0.07	mm
Sample height	53.17	0.01	mm
Sample weight	191.73		g
Bulk density	2.07		g/cm <sup>3</sup>
Sample colour	53.19,-5.35,8.10		L, a, b
Colour of bottom slip plane	47.08,-4.41,9.12		L, a, b
Weight of bottom sample	96.422		g
Weight after drying	79.628		g
Moisture content	17.4		%
Bottom: Raw: $s_a$	0.667		mm
Bottom: Raw: $s_q$	0.799		mm
Bottom: Raw: $s_t$	3.99		mm
Top: Raw: $s_a$	0.481		mm
Top: Raw: $s_q$	0.591		mm
Top: Raw: $s_t$	3.445		mm
Bottom: Surf: $s_a$	0.282		mm
Bottom: Surf: $s_q$	0.357		mm
Bottom: Surf: $s_t$	2.787		mm
Top: Surf: $s_a$	0.266		mm
Top: Surf: $s_q$	0.336		mm
Top: Surf: $s_t$	2.314		mm

# **FPR-24-294**

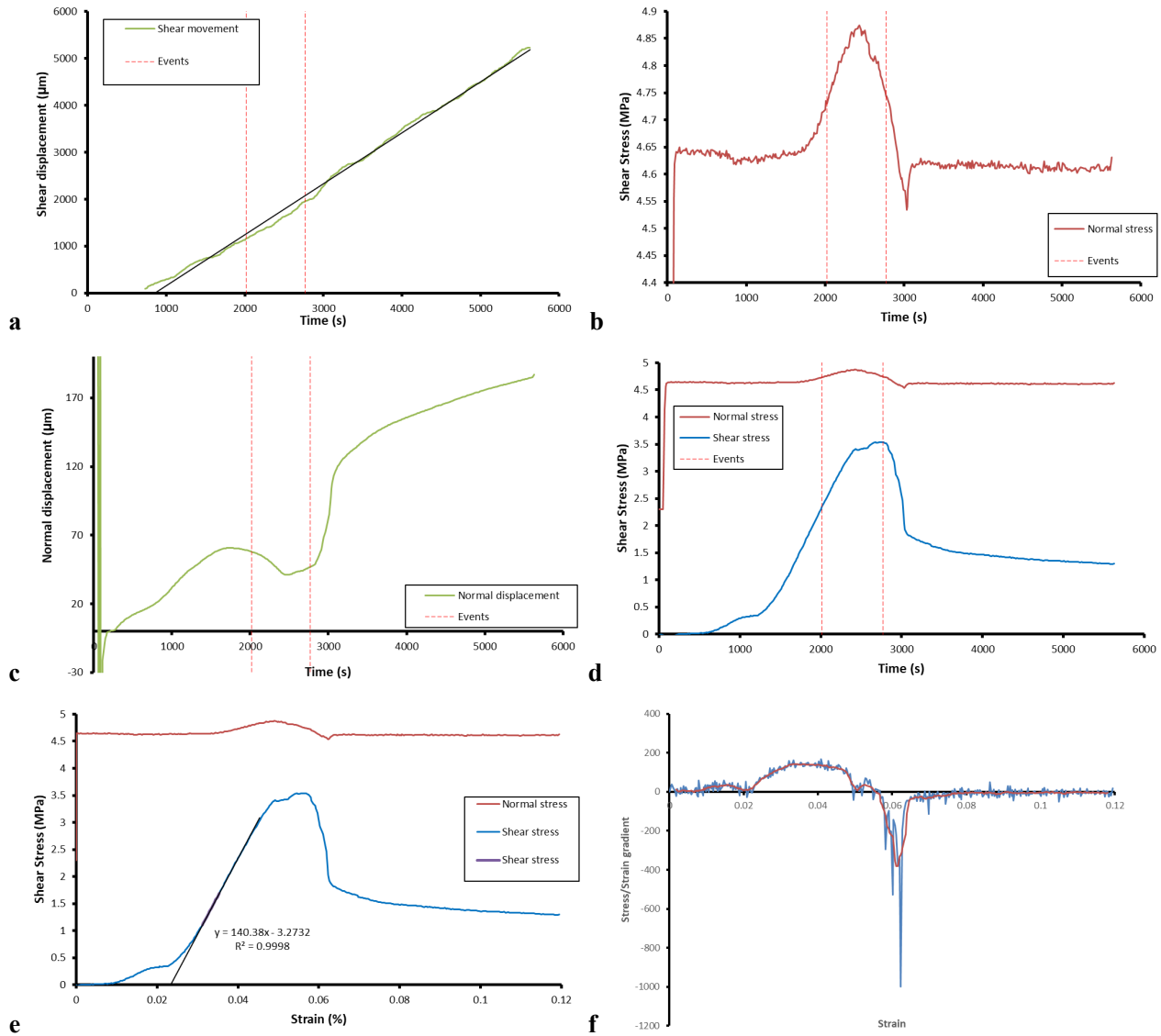


**Figure A-43.** Shear results for test FPR-24-294 (DH4;R6:290:725-BGS). a) Displacement with time; b) Normal load with time; c) Normal displacement with time; d) Normal and shear stress with time; e) Stress vs strain; f) Gradient of stress/strain (shear modulus).

**FPR-24-294**

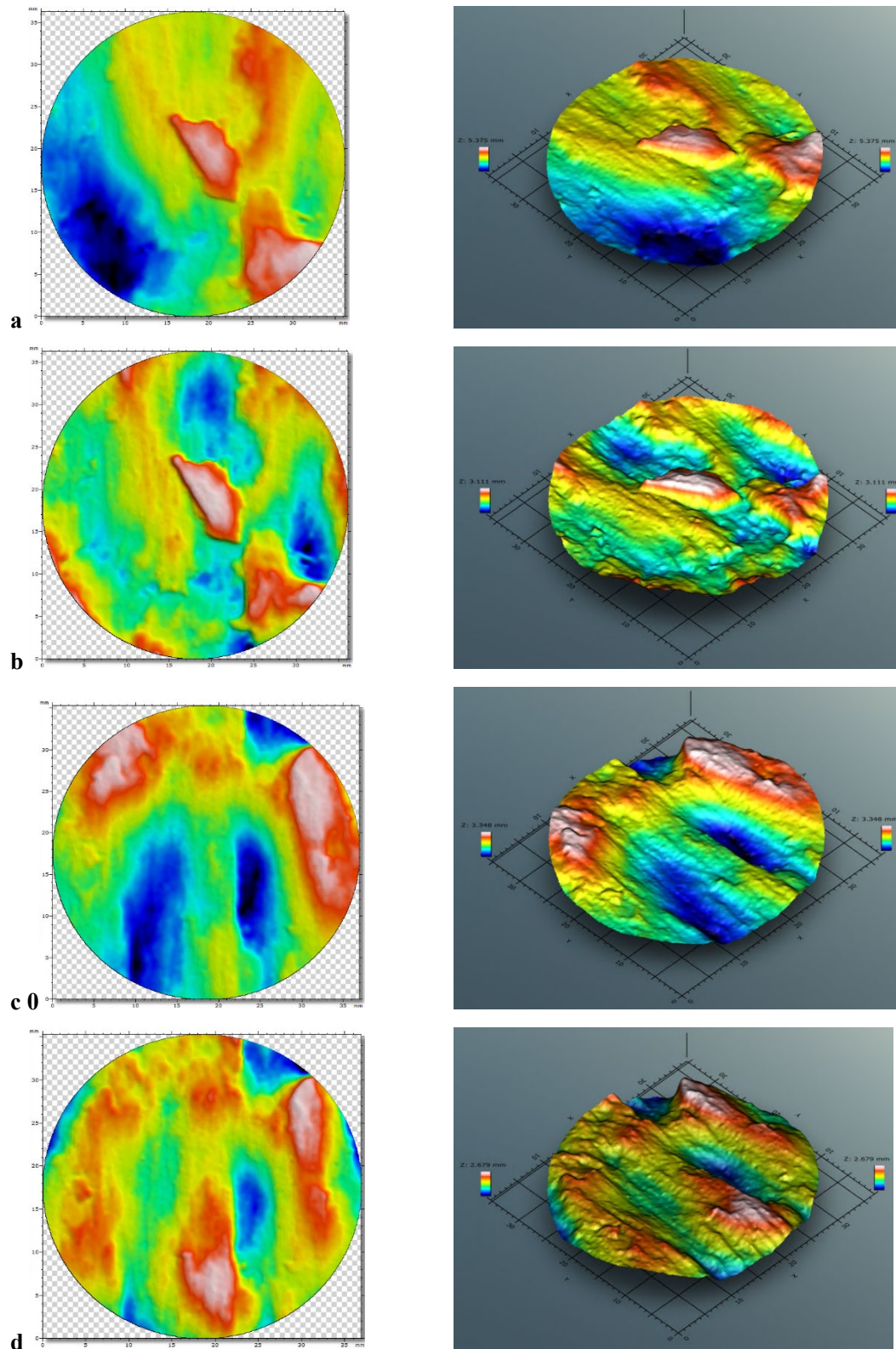


**Figure A-44.** Laser scan of shear fracture FPR-24-294 (DH4:R6:290:725-BGS). a) Bottom surface raw scan; b) Bottom surface with form removed; c) Top surface raw scan; d) Top surface with form removed. Shear direction is parallel with Y-axis, i.e. top-to-bottom in left.

**FPR-24-294****Table A-22. Results for test FPR-24-294 (DH4:R6:290:725-BGS)**

Parameter	Value	±	Units
SKB Sample name	DH4:R6:290:725-BGS		
BGS Sample name	FPR-24-294		
Normal load	4.682	0.004	MPa
Peak shear stress	3.540		MPa
Yield shear stress	2.362		MPa
Residual shear stress	1.357		MPa
Shear modulus	142.7		MPa
Displacement at peak	2663		µm
Maximum displacement	5614		µm
Displacement rate	1.032		µm/s
Sample diameter	46.97	0.05	mm
Sample height	52.91	0.01	mm
Sample weight	191.23		g
Bulk density	2.08		g/cm <sup>3</sup>
Sample colour	55.32,-5.14,8.08		L, a, b
Colour of bottom slip plane	49.43,-4.39,8.83		L, a, b
Weight of bottom sample	94.246		g
Weight after drying	78.393		g
Moisture content	16.8		%
Bottom: Raw: $s_a$	0.952		mm
Bottom: Raw: $s_q$	1.164		mm
Bottom: Raw: $s_t$	5.375		mm
Top: Raw: $s_a$	0.651		mm
Top: Raw: $s_q$	0.789		mm
Top: Raw: $s_t$	3.348		mm
Bottom: Surf: $s_a$	0.432		mm
Bottom: Surf: $s_q$	0.537		mm
Bottom: Surf: $s_t$	3.111		mm
Top: Surf: $s_a$	0.355		mm
Top: Surf: $s_q$	0.444		mm
Top: Surf: $s_t$	2.679		mm



**FPR-24-297**

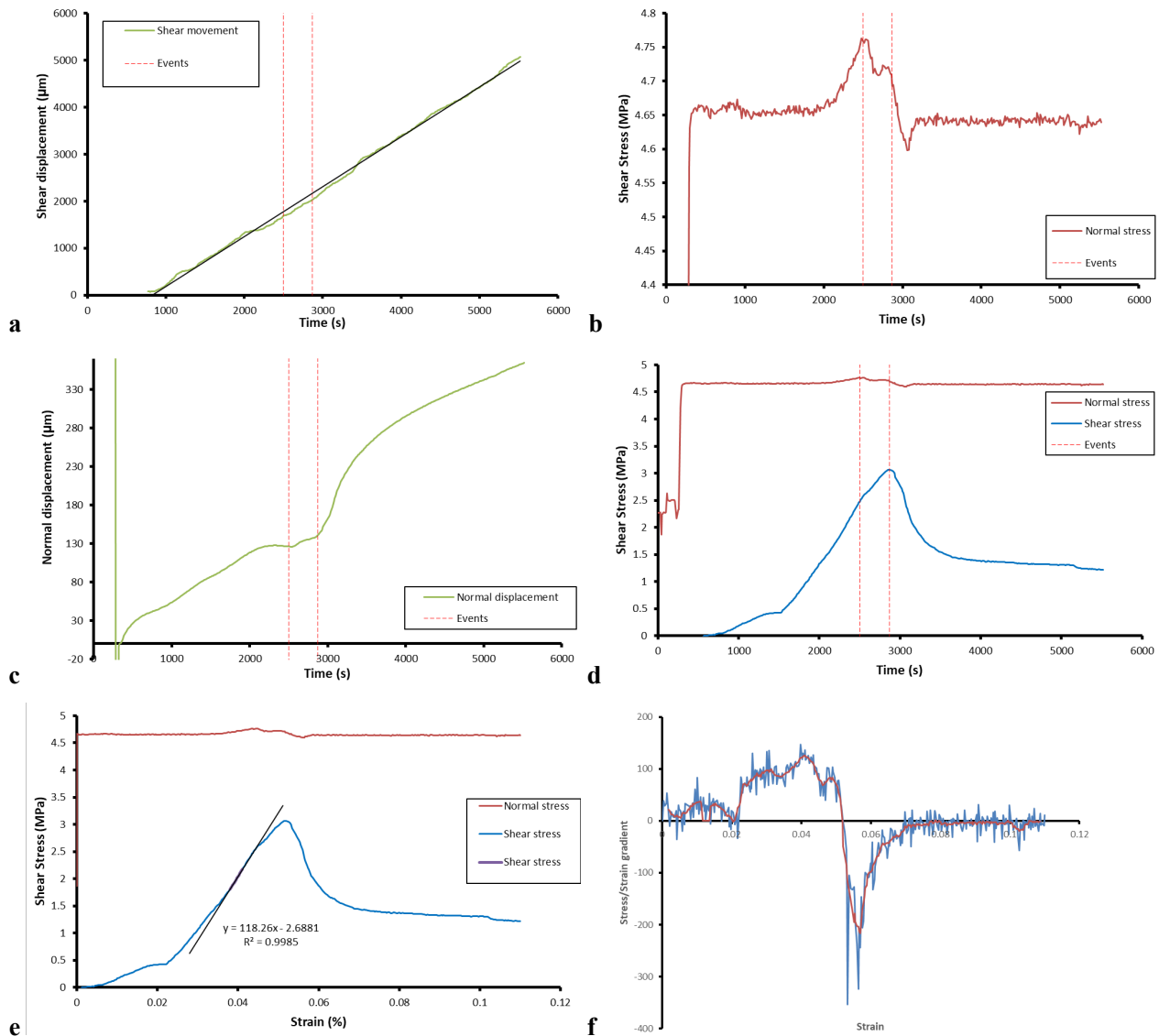


**Figure A-45.** Shear results for test FPR-24-297 (DH4:R6:290:775-BGS). a) Displacement with time; b) Normal load with time; c) Normal displacement with time; d) Normal and shear stress with time; e) Stress vs strain; f) Gradient of stress/strain (shear modulus).

**FPR-24-297**

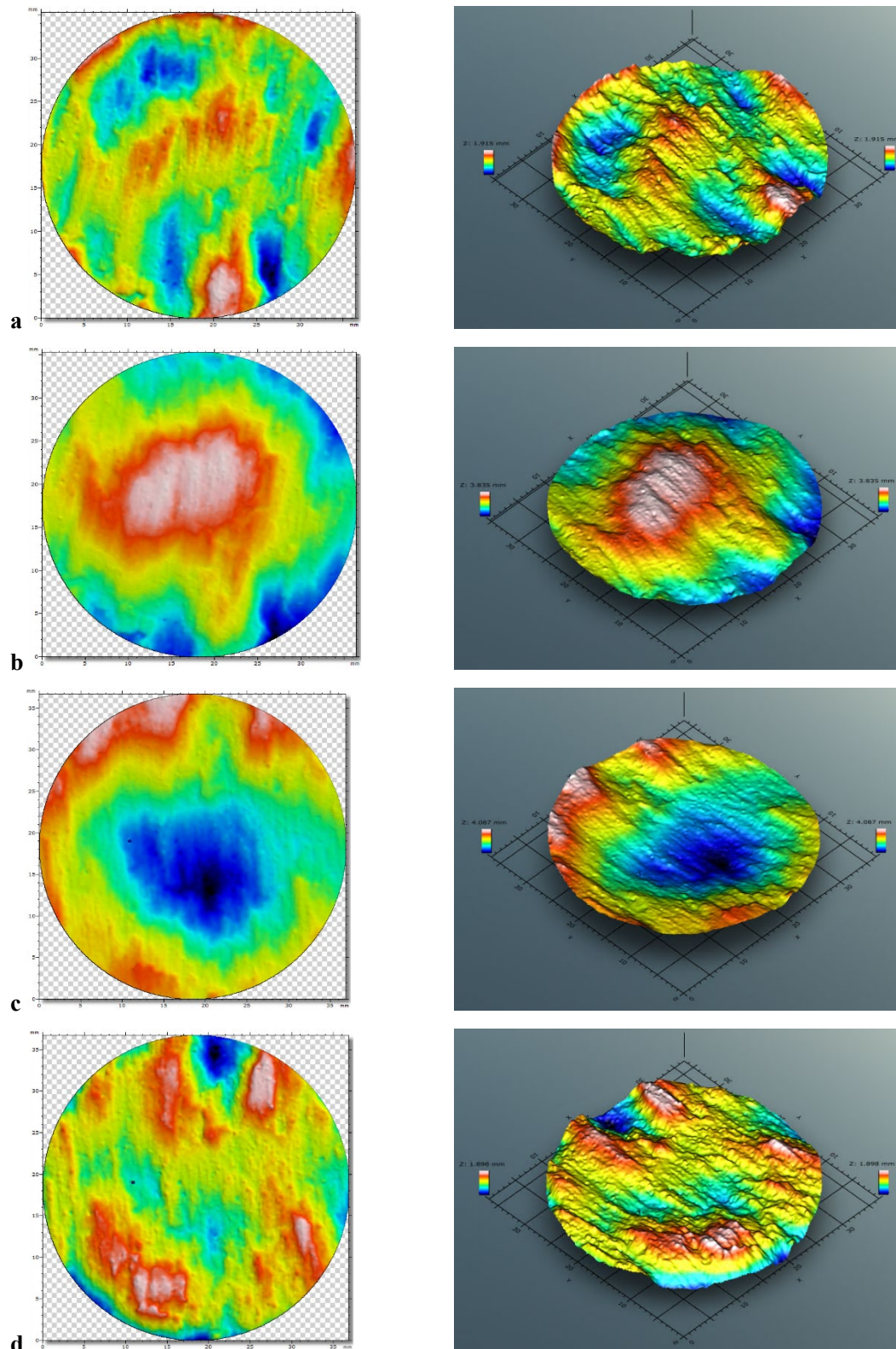


**Figure A-46.** Laser scan of shear fracture FPR-24-297 (DH4:R6:290:775-BGS). a) Bottom surface raw scan; b) Bottom surface with form removed; c) Top surface raw scan; d) Top surface with form removed. Shear direction is parallel with Y-axis, i.e. top-to-bottom in left.

**FPR-24-297****Table A-23. Results for test FPR-24-297 (DH4:R6:290:775-BGS)**

Parameter	Value	±	Units
SKB Sample name	DH4:R6:290:775-BGS		
BGS Sample name	FPR-24-297		
Normal load	4.686	0.002	MPa
Peak shear stress	3.067		MPa
Yield shear stress	2.480		MPa
Residual shear stress	1.308		MPa
Shear modulus	126.8		MPa
Displacement at peak	2436		µm
Maximum displacement	5170		µm
Displacement rate	1.032		µm/s
Sample diameter	46.89	0.06	mm
Sample height	52.81	0.01	mm
Sample weight	189.18		g
Bulk density	2.08		g/cm <sup>3</sup>
Sample colour	53.16,-5.48,7.65		L, a, b
Colour of bottom slip plane	45.81,-4.66,6.80		L, a, b
Weight of bottom sample	97.282		g
Weight after drying	80.201		g
Moisture content	17.6		%
Bottom: Raw: $s_a$	0.667		mm
Bottom: Raw: $s_q$	0.803		mm
Bottom: Raw: $s_t$	3.835		mm
Top: Raw: $s_a$	0.695		mm
Top: Raw: $s_q$	0.842		mm
Top: Raw: $s_t$	4.087		mm
Bottom: Surf: $s_a$	0.236		mm
Bottom: Surf: $s_q$	0.302		mm
Bottom: Surf: $s_t$	1.915		mm
Top: Surf: $s_a$	0.233		mm
Top: Surf: $s_q$	0.3		mm
Top: Surf: $s_t$	1.898		mm